Pedro Filipe Ribeiro da Costa

Development of mechanical, electrical and electromechanical properties of copolymer styrene-butadiene-styrene with carbon nanotubes composites

Outubro de 2013

Universidade do Minho
Escola de Engenharia

Pedro Filipe Ribeiro da Costa

Development of mechanical, electrical and electromechanical properties of copolymer styrene-butadiene-styrene with carbon nanotubes composites

Outubro de 2013

DECLARAÇÃO

Pedro Filipe Ribeiro da Costa

Endereço electrónico: pcosta@fisica.uminho.pt     Telefone: 936396162

Número do Bilhete de Identidade: 12040047

Título tese

**Development of mechanical, electrical and electromechanical properties of copolymer styrene-butadiene-styrene with carbon nanotubes composites**

Orientadores:

Professor Doutor Senentxu Lanceros-Mendéz

Professor Doutor Júlio César Machado Viana

Ano de conclusão: 2013

Designação do Ramo de Conhecimento do Doutoramento:

Programa Doutoral em Engenharia de Materiais

Nos exemplares das teses de doutoramento ou de mestrado ou de outros trabalhos entregues para prestação de provas públicas nas universidades ou outros estabelecimentos de ensino, e dos quais é obrigatoriamente enviado um exemplar para depósito legal na Biblioteca Nacional e, pelo menos outro para a biblioteca da universidade respectiva, deve constar uma das seguintes declarações:

> É AUTORIZADA A REPRODUÇÃO INTEGRAL DESTA TESE APENAS PARA EFEITOS DE INVESTIGAÇÃO, MEDIANTE DECLARAÇÃO ESCRITA DO INTERESSADO, QUE A TAL SE COMPROMETE.

Universidade do Minho, ____/____/_____

Assinatura: _____

# Acknowledgements

This PhD thesis could not be completed without the support of many people that supported me during the thesis. My thanks to all persons that helped me in several tasks during PhD thesis.

The good and motivating environment in Electroactive Smart Materials group turned the daily work much easier. I really appreciate everyone's help, either personally or professionally, in my work. I wish to give my special thanks, for this work and my scientific way, to Vítor and Carlos due to the help in the beginning of my work.

I want to thank my supervisor Senentxu Lanceros Mendez for giving me the opportunity, advices and knowledge before and during PhD thesis. It is a great pleasure to be your student.

Also, I'm grateful for the excellent welcome and help given by my co-supervisor Júlio Viana and his group during the several tasks I realized in his laboratories.

Thanks to María Teresa Martínez, Alejandro Ansón, Jose Miguel González and the remaining researchers of the Institute of Carbochemistry, CSIC (Zaragoza) for warm welcome and help.

Thanks to María José Abad and the remaining researchers of Labplast of University of Coruña for warm welcome and help.

Finally but most important, I want to thank my family for support and care. I owe you what I am today.

A lovely thank for my girlfriend Marta for her support over the last years.

**Abstract**

Composites are an important class of materials as they allow to reinforce or to include specific properties not typically found in nature. In this way, suitable electromechanical materials allow the measurement of large deformations by electrical means can be achieved by the development of composites. Research in electromechanical composites has been based in several polymer matrices with carbon nanoallotropes to increase the electrical conductivity of the composites. Successful development of electromechanical transducer materials has been accomplished, but reliable solutions for the development of large deformation sensors are still to be developed to meet the increasing industrial needs.

This work is focused on the study of the electromechanical response of carbon nanotubes/thermoplastic elastomers (CNT/TPE) composites with the main goal of maximizing sensitivity and deformation (> 30%) in order to improve the application range of the composites for sensor applications.

The composite materials used in these work are four different tri-block copolymers styrene-butadiene-styrene (SBS) (with reference C401, C411, C500 and C540) where the block copolymer structure is linear or radial and butadiene/styrene ratio ranged between 80/20 to 60/40. The composites materials are prepared by three different processing methods: solvent casting, extrusion and electrospinning. The amount of CNT included in the composites prepared by the different processing methods are 0, 1, 2, 4 and 8 weight percentage (wt%) for solvent casting, 0, 2, 4, 6, 8 and 10 wt% for extruded composites and 0, 0.05, 0.1 and 0.5 wt% for electrospun composites. It was important to find the electrical percolation threshold to obtain suitable electromechanical responses for sensors applications. Different types of CNT such as single walled CNT (SWCNT) and multi walled CNT (MWCNT) were used to study electrical and electromechanical properties of the composites. Chemical treatment of the CNT was also performed to understand the effect of functionalization on CNT dispersion and in the electromechanical response of the CNT/SBS composites. Covalent and non-covalent functionalization on MWCNT has been used for filler concentrations up to 8 wt%.

SBS shows maximum strain larger than 1000% both for pure SBS and the both composites prepared by solvent casting and extrusion. On the other hand, composites prepared by electrospinning show a maximum strain of 350%. The ratio of butadiene/styrene in the copolymer and the different copolymer architecture mainly

influences the mechanical properties. Initial modulus is larger for matrices with higher amounts of styrene and for CNT/SBS composites increases with increasing CNT content, independently of the composite processing method.

Mechanical hysteresis of the composite increases with applied strain (from 5% to 20%) and decreases with increasing the number of stress-strain cycles. Softer matrices (higher amount of butadiene) have lower mechanical hysteresis than harder matrices (higher amounts of styrene), demonstrating the influence of the butadiene/styrene ratio on the mechanical properties of the composites.

Morphological evaluation of the composites shows well dispersed clusters of CNT inside SBS matrices for pristine CNT and individual dispersion of functionalized CNT within the SBS matrices. The percolation theory concludes that hopping between nearest fillers is considered as the main mechanism for the composite electrical conduction, the overall composite conductivity is explained by the existence of a weak disorder regime.

The amount of pristine CNT inside the SBS matrix improves electrical properties of the composites, the electrical percolation threshold being lower than 1 wt% CNT for composites prepared by solvent casting and electrospinning processing methods, increasing up to 4-5 wt% CNT content for extruded composites. Composites with covalent and non-covalent functionalization, do not present electrical percolation threshold for filler contents up to 8 wt% CNT, where conductivity remains similar to pure SBS matrix.

The electromechanical properties of the composites depend on composite fillers content, CNT functionalization state and processing methods. Uniaxial strain and 4-point-bending measurements for solvent casting composites show larger electromechanical response for all matrices with maximized sensibility after initial pre-stress. The Gauge Factor (GF) for solvent casted composites with 4 wt% CNT filler content can reach values of GF~120 for C540 samples under uniaxial strain and GF~100 for C401 samples under 4-point-bending mechanical solicitation. For extruded composites with 8 wt% CNT, they reach a value of ~30 for C401 SBS under uniaxial strain. The maximum deformation with suitable electromechanical response can reach 50% of strain.

The proof of concept of the composites for sensor applications has been performed with the development of a glove with finger movement monitoring.

# Estudo das propriedades mecânicas, eléctricas e electromecânicas de compósitos copolímeros de estireno-butadieno-estireno com nanotubos de carbono

**Resumo**

Compósitos são atualmente uma importante classe em materiais e possibilitam obter propriedades únicas não presentes na natureza. Seguindo esta ideia, podem ser desenvolvidos materiais com propriedades electromecânicas para medir grandes deformações mecânicas através da resposta elétrica. A procura destes compósitos eletromecânicos é baseada em diversas matrizes poliméricas com o reforço dos diversos nanomateriais carbonáceos. O presente trabalho é focado no estudo da resposta eletromecânica de compósitos nanotubos de carbono/termoplásticos elastómeros tendo como objectivo principal maximizar a sensibilidade eletromecânica e a deformação (> 30%), alargando o leque de aplicações destes compósitos.

Os materiais utilizados neste trabalho são quatro diferentes copolímeros de estireno-butadieno-estireno (com a referencia C401, C411, C500 e C540), utilizados como matriz, tendo o copolímero estrutura linear ou radial e rácio butadieno/estireno varia entre 60/40 e 80/20. Como material de reforço são usados três diferentes tipos de nanotubos de carbono, de parede simples ou múltipla com a referência C150P, NC7000 e AP-SWNT.

Os compósitos foram preparados por três métodos: a partir da dissolução num solvente, por *electrospinning* e extrusão. A quantidade, em massa, de nanotubos de carbono presente nos compósitos foi de 0, 1, 2, 4 e 8% para o processamento a partir da solução, de 0, 2, 4, 6, 8 e 10% para o processamento por extrusão, e de 0, 0.05, 0.1 e 0.5% para os materiais processados por *electrospinning*. As várias concentrações foram utilizadas de forma a determinar o limite de percolação elétrico dos compósitos, de forma a otimizar a resposta eletromecânica destes. Os nanotubos de carbono também foram alvo de funcionalização, covalente e não-covalente, com o intuito de entender a evolução das propriedades dos compósitos com os diferentes nanotubos e funcionalizações destes. Compósitos até 8% em massa de nanotubos foram processados a partir de um solvente com nanotubos de carbono funcionalizados.

As matrizes poliméricas apresentam excelentes propriedades mecânicas com a deformação máxima a variar entre 350% para os materiais processados por

*electrospinning* e mais de 1000% para os compósitos preparados com os restantes tipos de processamento. O rácio butadieno/estireno influencia essencialmente as propriedades mecânicas e o módulo elástico aumenta com a quantidade de estireno e de nanotubos de carbono na matriz, independentemente do processamento utilizado. A histerese mecânica aumenta com a deformação e diminui com o número de ciclos tensão-deformação aplicados no compósito, sendo maior para as matrizes com maior quantidade de estireno no copolímero.

A morfologia dos compósitos é similar para os nanotubos de carbono sem tratamento, apresentando uma boa dispersão de agregados de nanotubos de carbono. Os compósitos com os nanotubos de carbono funcionalizados apresentam uma dispersão individual de nanotubos de carbono em vez de uma dispersão de agregados. A teoria da percolação mostra que o *hopping* entre os nanotubos vizinhos é considerado o principal mecanismo de condução elétrica no compósito, e a condutividade total do compósito pode ser explicada pela existência de um regime de fraca desordem.

O aumento de nanotubos de carbono não funcionalizados na matriz polimérica melhora as propriedades elétricas do compósito sendo o limite de percolação elétrico menor que 1% em massa para os compósitos processados a partir do solvente e por *electrospinning* e cerca de 4-5% para os compósitos processados por extrusão. Os compósitos usando nanotubos de carbono funcionalizados não apresentam percolação elétrica.

As propriedades eletromecânicas do compósito dependem da quantidade de nanotubos de carbono na matriz e do método de processamento. As medidas para a deformação unidireccional e a flexão de 4 pontas para compósitos processados a partir de solução no solvente apresentam uma boa resposta eletromecânica para as quatro matrizes poliméricas, tendo a sua sensibilidade maximizada após pré-deformação. O Factor de Gauge para os compósitos com 4%, em massa, de nanotubos de carbono é cerca de 120 e 100 para a matriz C540 medida pelo método de deformação unidireccional e de flexão de 4 pontas, respectivamente. Para compósitos processados por extrusão, com 8% em massa, o Factor de Gauge máximo é cerca de 30, para a matriz C401 medido na deformação unidireccional. A deformação máxima com uma boa resposta eletromecânica é de 50% nestes compósitos.

A prova de conceito da utilização destes compósitos para aplicações de sensores foi realizada através do desenvolvimento de uma luva com a monitorização do movimento dos dedos.

**List of Symblos and Abbreviatours**

## A

A       Area
ATR      Attenuated Total Reflectance

## C

C       Celsius Degrees
CB      Carbon Black
CF      Covalent Functionalization
cm      Centimeter
CNF      Carbon Nanofibers
CNT      Carbon Nanotubes

## D

d       Thickness
D       Diameter
DMF      $N,N$-dimethylformamide
DNA      Deoxyribonucleic Acid
DSC      Differential Scanning Calorimetric
DTG      Differential Thermal Gravimetric

## E

E       Initial modulus

## F

FTIR      Fourier Transformed Infrared Spectroscopy

## G

g       Gram
GPa      Gigapascal
GF      Gauge Factor

## H

h       Hour
Hz      Hertz

## I

I       Electrical current

## J

J       Joule

## K

K       Kelvin
Kg      Kilogram
kHz      KiloHertz

## L

l       Length

## M

| m | Meter |
|---|---|
| MC | Microcontroller |
| MCU | Microcontroller Unit |
| min | Minute |
| ml | Milliliter |
| mm | Millimeter |
| MWCNT | Multi Walled Carbon Nanotubes |

## N

| N | Newton |
|---|---|
| NCF | Non-Covalent Functionalization |
| nm | Nanometer |

## P

| Pa | Pascal |
|---|---|
| PANI | Polyaniline |
| PB | Polybutadiene |
| PC | Polycarbonate |
| PDMS | Polydimethylsiloxane |
| PEBA | Polyether block amide |
| PEN | Poly(ethylene 2,6-naphthalate) |
| PEO | Polyethylene |
| PET | Polyethylene terephthalate |
| PMMA | Poly(methyl methacrylate) |
| PP | Polypropylene |
| PS | Polystyrene |
| PSF | Polysulfone |
| PU | Polyurethane |

## R

| R | Electrical Resistance |
|---|---|
| RF | Radio Frequency |
| Rpm | Rotation per minute |

## S

| SB | Styrene-butadiene |
|---|---|
| SBS | Styrene-butadiene-styrene |
| SEBS | Styrene-ethylene/butadiene-styrene |
| SEM | Scanning electron microscopic |
| SPU | Synthesized polyurethane |
| SWCNT | Single-walled carbon nanotubes |

## T

| t | Universal critical exponent |
|---|---|
| TEM | Transmission electron microscopy |
| TF | Tecoflex |

**V**

| | |
|---|---|
| V | Volt |
| $V_e$ | Excluded volume |

**W**

| | |
|---|---|
| W | Watt |
| wt% | Weight percentage |

**Greek**

| | |
|---|---|
| ε | Mechanical strain |
| μm | micrometer |
| $\phi$ | Volume Fraction |
| ρ | Electrical Resistivity |
| $\upsilon$ | Poisson Coefficient |
| $\Phi_c$ | Critical Concentration |
| | Mechanical Stress |
| $\sigma$ | |

# Chapter 1.  Introduction

The introduction chapter has a summary state of art of composites with electromechanical properties, using several matrices and reinforcement materials, and then is presented the main objectives proposed for the work in this thesis.

Finally are presented the thesis structure for an overview of this work.

## 1.1 Introduction

The research and development of new sensing composite materials and the understanding of the electrical transport properties in conductor-insulator composites are important to design innovative functional composite materials with unique properties providing new application possibilities [1-3]. In recent years it has been make remarkable advances in the design, synthesis and processing of polymer nanocomposites with controllable structural, electrical and mechanical properties, among others, to combine the advantageous properties of insulating polymer matrices (flexibility, light weight, transparency, easy processing, etc.) with the excellent mechanical and electrical properties of the reinforcement nanofillers [1, 3, 4].

Composites from carbon nanoallotrope fillers within a polymer matrix have been gaining more interest, more specifically the polymer matrices ranging from thermoplastic or thermosetting [3] to elastomers.

Within the fillers, most of the attention has been devoted to carbon nanotubes (CNTs) as reinforcement material due their outstanding mechanical, electrical and thermal properties [5]. CNTs have demonstrated to be the most effective nanofillers for the production of electrically conductive polymer composites, when compared to metallic or carbon black particles, attributed both to the CNTs high aspect ratio and intrinsic conducting properties [3, 5]. The incorporating of CNTs into a polymer provides the composite with outstanding electrochemical and electromechanical properties, allowing the use of the composite as smart sensing material [6] in areas such as chemical, mechanical stress or strain, pressure, temperature, gas, bio-molecular and flow sensors [5].

A conductive CNT/polymer composite is typically formed when the concentration of the CNTs reaches a critical value, which is known as the electrical percolation threshold. At that concentration, there is an increase of the electrical conductivity in several orders of magnitude, being the variations above and below this concentration much lower [5, 7].

The percolation threshold strongly depends on the filler type, dispersion and/or functionalization, which in turn also depend on the composite preparation method.

In this way, the concentration at which the percolation threshold occurs depends on the carbon nanoallotrope, being 15-20 wt% for carbon black needs [8, 9], 4-6 wt% for

carbon nanofibers [10] and less than 1 wt% going down to less than 0.1 wt% for carbon nanotubes [3].

Other applications of CNT/polymer functional composites based on the unique properties of CNT include heat resistance, chemical sensing, electrical and thermal management, photoemission, electromagnetic absorption and energy storage [7]. To maximize the advantages of CNTs as effective filler, the CNTs should not form large aggregates and must be well dispersed to enhance the interfacial interaction with the matrix [3]. Several processing methods available for fabricating CNT/polymer composites applied in different matrices have been described [3], including solvent casting, in situ polymerization, melt blending, electrospinning and chemical modification processes [2, 3, 6].

Solvent casting is one of the most common processing methods for the preparation of CNT/polymer composites. First, the CNT dispersion is achieved in a chemical solvent of the polymer. Subsequently, the dispersed CNT are mixed with the polymer matrix and the composite is finally obtained by precipitating or casting the mixture. Melt blending is largely used too and has the major advantage of not making use of solvents, using high temperature and high shear forces to disperse CNTs in the polymer matrix. Equipment such as extruder and injection machines capable of operating at an elevated temperature and generating high shear forces are employed to disperse CNTs within the polymer melt [7]. When compared to solution mixing methods, this technique is generally less effective in dispersing CNTs in polymers, and its application is limited to low filler concentrations in thermoplastic matrices [7]. Electrospinning is also used to produce composite fibers of micro and nanometric diameter [11] from different polymer solutions [11]. Finally, to obtain CNT/polymer nanocomposites for specific applications, other methods have been developed including densification, layer-by-layer deposition and pulverization [7].

Incorporation of CNT into polymer matrices influences the mechanical, electrical and electromechanical properties of the composites and this effect is more pronounced when the polymer-nanotube interaction is stronger [12]. Several methods can be applied to maximize the interaction between the matrix and the reinforcement material [12].

Both, single walled carbon nanotubes (SWCNT) and multi walled carbon nanotubes (MWCNT) have been used as fillers for thermosetting polymers, such as epoxy, polyurethane or phenol-formaldehyde resins and thermoplastic polymers, including polyethylene, prolypropylene, polystyrene, nylon, etc [7].

Mechanical properties are particularly dependent on the dispersion state and aspect ratio of CNT, with large aspect ratio (ratio between length and diameter of nanotubes) maximizing the load transfer between CNT and matrix [7]. Initial modulus and tensile strength of the polymer can increase up to 35% and 25%, respectively, with 1 wt% of CNT [7]. With respect to the electrical properties, the insulator polymer matrix is transformed in a conducting composites for CNT contents often as low 0.5 wt% [7]. Most CNT/polymer composites show percolation thresholds below 5 wt% [7] and can be as low as 0.002 wt% for CNT/polymer composites depending on CNT type, functionalization, dispersion and process method [3, 7, 12, 13].

Composites containing dispersed conductive fillers in an insulator matrix have been studied for force sensor applications [14, 15]. The applications of strain sensors are mainly used in engineering fields for damage detection and characterization of structures. Some limitations of traditional sensors with respect to large area and large deformations applications as well as integrations problems can be overcome by the use of polymer composites. The matrices used for these composites materials can be from thermosets, thermoplastics as well thermoplastics elastomers or rubbers matrices. Further interest in CNT/polymer composites comes from their piezoresistive capability, which is strongly dependent on loading type (tension, compression), loading history and on the matrix mechanical behavior. These properties are being explored, for example, in reinforced polymer matrices or wearable textiles [16, 17].

Elastomeric matrices composites exhibit multifunctionality [18] and are suitable for the development of conductive polymer composites for flexible strain sensing applications [15, 19]. The matrices mostly studied are synthetic and natural rubbers, thermoplastic elastomers and silicone elastomers [20]. Thermoplastic elastomers are known for combining their elastomeric mechanical behavior with the processability of thermoplastics [21]. Recently, these composites materials have attracted large interest [15, 22] with applications as tensile or pressure sensors [23, 24], gas sensors [23], electronic skin [15] and capacitors [18], among others.

Linear electromechanical sensors have been developed and, when compared to conventional sensors, show high sensitivity [22]. Investigations of these composites as mechanical actuators, comparing their properties with natural muscles, started some years ago [25] and is continuously increasing [26-28].

Harder polymer matrices, such as thermosets and thermoplastics, have been more investigated than elastomeric matrices for strain sensor applications. CNT/polymer composites with strain sensing capabilities have been recently studied [21]. Traditional strain gages show gauge factors (sensitivity) between 0.6-2.2 [4, 22]. Wichmann et al. [29] found electromechanical properties in MWCNT/epoxy composites, where strain sensitive capabilities are found with at least 0.1 wt% CNT and the average gauge factor is between 3.4-4.3 for maximum strain of 6%. Measurements on unidirectional and multidirectional carbon fiber epoxy laminates show gauge factors of 1.75 and 2.7 for parallel and transverse current flow, respectively, for uniaxial strain measurements between 0-0.3% of strain [30]. CNF/epoxy composites show gauge factors varying between 1.5 to near 10 [31]. The dependence of piezoresistivity on CNT content in composites was studied with CNT/polyvinylidene fluoride (PVDF) composites with a maximum gauge factor of 6.2 measured close to the percolation threshold [31]. Results for other composites point out in the same directions with gauge factors between 1 and 15 for CNT/poly(methyl methacrylate) (PMMA) composites [32, 33], MWCNT/polycarbonate (PC) composites [34] and MWCNT/polysulfone (PSF) [24, 35], most of them for deformations up to 1%.

For larger strain or pressure sensor applications, mechanical properties of the matrix are fundamental, being the most used materials like thermoplastic elastomers, natural rubber and silicone matrices.

Silicone rubber with SWCNT composites can be highly stretchable until 200% and retained their high conductivity (18 S.cm$^{-1}$) for 20 loading/unloading cycles [36]. Silicone elastomers with carbon black (9 wt%) composites also presents good linearity between deformation and electrical resistance variation up to 50% deformation [20].

MWCNT/thermoplastic polyurethane (TPU) non-woven electrospinning composites also show linear increasing gauge factors up to 70 with strains up to 400% [4]. It has been also reported that MWCNT/TPU can sense strain deformations up to 80% with 0.35 wt% CNT and up to 10% strains for 2 wt% CNT content [37].

Composites of SWCNT with PDMS were studied for small (2%) and large (20-30%) deformations and gauge factors around 5 were reported [38] with negligible dependence on the film thickness for small strains but not for large strains [38].

Different segments of elastomeric PU with CNT composites show electrical percolation around 1 wt% and high electromechanical sensitivity, reaching values of $\Delta R / R_0 \approx 30$ for 25% strain [21]. The maximum measured strain was larger than 100% [21].

In this way, the large potential of CNT/elastomer composites has still to be explored to determine the best materials for applications as well as their application range. Further, thermoplastic elastomer styrene-butadiene-styrene with carbon nanotubes show interesting physic-chemical properties and have not been yet explored for large area sensor applications.

## 1.2 Objectives

Electromechanical polymer based on composite materials has attracted more attention for strain sensing applications. The main goal of this work is the development of electromechanical composites for large deformation sensor applications, using a TPE as matrix and CNT as reinforcement material.

Linear relation between electrical resistance variations with strain in the composites at suitable resistance values is essential for these applications. Mechanical properties of matrices and electrical properties of fillers are important for tailoring the electromechanical response of the composites.

The main objectives of the present work are thus:

- to prepare polymer composites for large strain sensor applications, with optimized electromechanical sensitivity in order to increase their application range. In this way, elastomeric matrices will be selected with large deformation and mechanical recovery to the initial state under stress-strain solicitation. Polymer matrices should be submitted to repeat stress-strain cycles without losses of the mechanical properties. CNT will be included in the polymer matrix to increase electrical conductivity as well as its variability with strain. The electrical percolation threshold and maximum conductivity are of critical importance for the electromechanical properties of the composites. In this way, one of the main objective is to maximize the electromechanical sensibility of the composites for increasing their application range;

- to apply suitable theoretical models to understand the electrical behavior of the composites;
- to explore the preparation of the composites with different techniques ranging from lab-scale processing to industrial up-scalable processes;
- to develop a proof of concept of the suitability of the materials for applications.

## 1.3 Structure of the thesis

The results of the research were divided into different publishable works with focus on different aspects on materials processing, the theoretical interpretation of the electrical behavior and their applicability.

Previous to these works, chapter 1 provides a short introduction, as the state of the art is written specifically in each chapter, the main objectives and the structure of the thesis. Chapter 2 presents the materials and experimental methods.

In chapters 3 to 6 are presented the main properties of the composites, including morphological, electrical, mechanical and electromechanical properties. In chapter 3 the composites processed by solvent casting are studied and the main properties of composites addressed. The electromechanical properties are evaluated thoroughly in chapter 4 to discuss maximum deformation and sensitivity of the electromechanical response. Chapter 5 shows the effect of the carbon nanotube characteristics on the electromechanical response, including different carbon nanotubes and functionalization procedure. In chapter 6 are reported different processing methods of the composites, extrusion and electrospinning, and the main advantages and limitations of these methods on the mechanical and electrical properties of the prepared composites.

In the following chapter, an application is reported in chapter 7, monitoring the deformation of the fingers with the developed composites.

The final chapter is focused on the main conclusions of this work and the future research needs and possible applications of these composites.

**References**

[1]     Nigro B, Grimaldi C, Miller M A, Ryser P and Schilling T 2012 Tunneling conductivity in composites of attractive colloids *J Chem Phys* 136 164903

[2]     Roy N, Sengupta R and Bhowmick A K 2012 Modifications of carbon for polymer composites and nanocomposites *Progress in Polymer Science* 37 781-819

[3]     Spitalsky Z, Tasis D, Papagelis K and Galiotis C 2010 Carbon nanotube–polymer composites: Chemistry, processing, mechanical and electrical properties *Progress in Polymer Science* 35 357-401

[4]     Slobodian P, Riha P and Saha P 2012 A highly-deformable composite composed of an entangled network of electrically-conductive carbon-nanotubes embedded in elastic polyurethane *Carbon* 50 3446-53

[5]     Kaushik P, Mehdi M, Chaneel P and Simon S P 2013 Effect of CNT alignment on the strain sensing capability of carbon nanotube composites *Smart Materials and Structures* 22 075006

[6]     Baughman R H, Zakhidov A A and de Heer W A 2002 Carbon nanotubes--the route toward applications *Science* 297 787-92

[7]     Ma P-C, Siddiqui N A, Marom G and Kim J-K 2010 Dispersion and functionalization of carbon nanotubes for polymer-based nanocomposites: A review *Composites Part A: Applied Science and Manufacturing* 41 1345-67

[8]     Mao Z, Wu W, Xie C, Zhang D and Jiang X 2011 Lipophilic carbon nanotubes and their phase-separation in SBS *Polymer Testing* 30 260-70

[9]     Theodosiou T C and Saravanos D A 2010 Numerical investigation of mechanisms affecting the piezoresistive properties of CNT-doped polymers using multi-scale models *Composites Science and Technology* 70 1312-20

[10]    Das A, Stöckelhuber K W, Jurk R, Saphiannikova M, Fritzsche J, Lorenz H, Klüppel M and Heinrich G 2008 Modified and unmodified multiwalled carbon nanotubes in high performance solution-styrene–butadiene and butadiene rubber blends *Polymer* 49 5276-83

[11]    Mazinani S, Ajji A and Dubois C 2009 Morphology, structure and properties of conductive PS/CNT nanocomposite electrospun mat *Polymer* 50 3329-42

[12]    Rahmat M and Hubert P 2011 Carbon nanotube–polymer interactions in nanocomposites: A review *Composites Science and Technology* 72 72-84

[13]    Li C, Thostenson E T and Chou T-W 2008 Sensors and actuators based on carbon nanotubes and their composites: A review *Composites Science and Technology* 68 1227-49

[14]    Obitayo W and Liu T 2012 A Review: Carbon Nanotube-Based Piezoresistive Strain Sensors *Journal of Sensors* 2012 1-15

[15]    Wang L, Xu C and Li Y 2013 Piezoresistive response to changes in contributive tunneling film network of carbon nanotube/silicone rubber composite under multi-load/unload *Sensors and Actuators A: Physical* 189 45-54

[16]    Loyola B, Saponara V and Loh K 2010 In situ strain monitoring of fiber-reinforced polymers using embedded piezoresistive nanocomposites *J Mater Sci* 45 6786-98

[17]    Huang C-T, Shen C-L, Tang C-F and Chang S-H 2008 A wearable yarn-based piezo-resistive sensor *Sensors and Actuators A: Physical* 141 396-403

[18]    Tsuchiya K, Sakai A, Nagaoka T, Uchida K, Furukawa T and Yajima H 2011 High electrical performance of carbon nanotubes/rubber composites with low

percolation threshold prepared with a rotation–revolution mixing technique *Composites Science and Technology* 71 1098-104

[19]    De Falco A, Goyanes S, Rubiolo G H, Mondragon I and Marzocca A 2007 Carbon nanotubes as reinforcement of styrene–butadiene rubber *Applied Surface Science* 254 262-5

[20]    Yi W, Wang Y, Wang G and Tao X 2012 Investigation of carbon black/silicone elastomer/dimethylsilicone oil composites for flexible strain sensors *Polymer Testing* 31 677-84

[21]    Bautista-Quijano J R, Avilés F and Cauich-Rodriguez J V 2013 Sensing of large strain using multiwall carbon nanotube/segmented polyurethane composites *Journal of Applied Polymer Science* 130 375-82

[22]    Hu N, Karube Y, Yan C, Masuda Z and Fukunaga H 2008 Tunneling effect in a polymer/carbon nanotube nanocomposite strain sensor *Acta Materialia* 56 2929-36

[23]    Rubinger C P L, Leyva M E, Soares B G, Ribeiro G M and Rubinger R M 2011 Hopping conduction on carbon black/styrene–butadiene–styrene composites *J Mater Sci* 47 860-5

[24]    Bautista-Quijano J R, Avilés F, Aguilar J O and Tapia A 2010 Strain sensing capabilities of a piezoresistive MWCNT-polysulfone film *Sensors and Actuators A: Physical* 159 135-40

[25]    Baughman R H, Cui C, Zakhidov A A, Iqbal Z, Barisci J N, Spinks G M, Wallace G G, Mazzoldi A, De Rossi D, Rinzler A G, Jaschinski O, Roth S and Kertesz M 1999 Carbon nanotube actuators *Science* 284 1340-4

[26]    Sun L, Huang W M, Ding Z, Zhao Y, Wang C C, Purnawali H and Tang C 2012 Stimulus-responsive shape memory materials: A review *Materials & Design* 33 577-640

[27]    Mirfakhrai T, Madden J and Baughman R 2007 Polymer artificial muscles *Materials Today* 10 30-8

[28]    Hu J, Zhu Y, Huang H and Lu J 2012 Recent advances in shape–memory polymers: Structure, mechanism, functionality, modeling and applications *Progress in Polymer Science* 37 1720-63

[29]    Wichmann M H G, Buschhorn S T, Gehrmann J and Schulte K 2009 Piezoresistive response of epoxy composites with carbon nanoparticles under tensile load *Physical Review B* 80 245437

[30]    Angelidis N, Wei C Y and Irving P E 2004 The electrical resistance response of continuous carbon fibre composite laminates to mechanical strain *Composites Part A: Applied Science and Manufacturing* 35 1135-47

[31]    Ferrreira A, Rocha J G, Ansón-Casaos A, Martínez M T, Vaz F and Lanceros-Mendez S 2012 Electromechanical performance of poly(vinylidene fluoride)/carbon nanotube composites for strain sensor applications *Sensors and Actuators A: Physical* 178 10-6

[32]    Pham G T, Park Y-B, Liang Z, Zhang C and Wang B 2008 Processing and modeling of conductive thermoplastic/carbon nanotube films for strain sensing *Composites Part B: Engineering* 39 209-16

[33]    Inpil K, Mark J S, Jay H K, Vesselin S and Donglu S 2006 A carbon nanotube strain sensor for structural health monitoring *Smart Materials and Structures* 15 737

[34]    W. Zhang, J. Suhr and N. Koratkar 2006 Multi-functional Polymer Nano-Composite for Self Strain Sensing *Journal of Nanoscience and Nanotechnology* 6 4

[35]    Oliva-Avilés A I, Avilés F and Sosa V 2011 Electrical and piezoresistive properties of multi-walled carbon nanotube/polymer composite films aligned by an electric field *Carbon* 49 2989-97

[36]    Kim T A, Kim H S, Lee S S and Park M 2012 Single-walled carbon nanotube/silicone rubber composites for compliant electrodes *Carbon* 50 444-9

[37]    Zhang R, Deng H, Valenca R, Jin J, Fu Q, Bilotti E and Peijs T 2013 Strain sensing behaviour of elastomeric composite films containing carbon nanotubes under cyclic loading *Composites Science and Technology* 74 1-5

[38]    Luo S and Liu T 2013 Structure–property–processing relationships of single-wall carbon nanotube thin film piezoresistive sensors *Carbon* 59 315-24

# Chapter 2.  Materials and Experimental Procedure

The polymer matrices and reinforcement fillers used for the preparation of the composites are presented in this chapter. The main properties of these materials are described and the main reasons for the selection of the materials indicated. After the description of the processing methods and conditions for development of the composites, the principal characterization techniques and experimental conditions are presented.

## 2.1  Materials

With the purpose of developing composites for large deformation sensors, elastomeric matrices are the most suitable option due to their elastic properties. As the electrical conductivity of the polymer matrix has to be increased, carbon nanoallotropes have been selected as fillers.

Thermoplastic elastomers (TPEs) appeared in the 1960s as a family of materials with characteristics between thermoplastics, characterized by easy processing but low elasticity, and elastomers, with outstanding elastic properties but more complex processing. TPEs are copolymers or compounds of thermoplastics and rubber [1]. Rigid and flexible phases can be obtained by two main ways [1]:

- Copolymerization of rigid and flexible sequences in the same molecule, for example:

    - styrene-butadiene-styrene for SBS

    - polyester (or polyether) – isocyanate for TPU

    - polyether-amide for PEBA

- Blending of a soft rubber, possibly partially vulcanized, dispersed in a rigid thermoplastic matrix. This family can be divided into thermoplastic polyolefin blends (TPOs) and dynamically vulcanized blends (TPVs) [2].

These two methods can be combined and some TPEs are alloys or blends of a copolymer with soft and rigid sequences and a thermoplastics and cross-linked rubbers [1].

One advantage SBS-based TPEs (figure 2.1) is that they can be processed by conventional thermoplastic processing methods such as extrusion and injection molding [3], with similar characteristics to conventional thermoplastic and the advantage of low-temperature flexibility, damping properties chemical stability and electrical insulator [3]. The properties of TPEs are similar to vulcanized rubber, e. g., softness, flexibility, extensibility and resilience [3].

The consumption of TPEs is increasing with relatively high growth rates, though these differ largely from one TPE family to another and from one country to another [1].

A variety of styrene-butadiene (SB) block copolymers constitute an important class of TPE. Different molecular architectures and block lengths are manufactured commercially in large volumes with a high degree of control over molecular characteristics to produce block copolymers with particular domain microstructures

suitable for specific applications [4]. These copolymers are synthesized through anionic polymerization via either sequential or coupling methods [4]. To produce styrene-butadiene-styrene tri-block copolymers, the synthesis comprises initiation of styrene polymerization using mono-anionic organolithium compound to form living polystyryl anion, followed by addition of butadiene monomer to form living SB di-block. In the sequential method a second quantity of styrene is added to the living SB di-block in order to complete the formation of SBS tri-block copolymer [4]. The efficiency of each process depends on temperature, polarity of the solvent and presence of impurities (water, alcohol, etc.) [4].
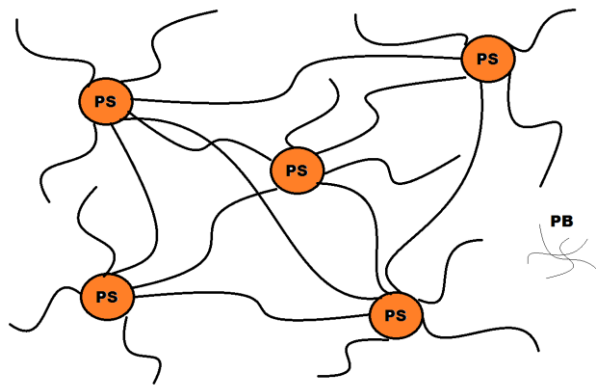


Figure 2.1- Schematic of styrene-butadiene-styrene tri-block copolymer, with polystyrene and polybutadiene blocks.

Other important advantage of TPEs for many applications is their biocompatibility. Styrene–ethylene/butylene–styrene (SEBS) polymers derive from SBS are obtained by hydrogenation of SBS polymers; this process allows removing insaturations typical of the butadiene components (carbon–carbon double bonds are saturated with hydrogen), which has a positive effect on environmental, thermal and UV radiation resistance, while maintaining the thermoplastic behavior. In this way, SEBS is useful in applications in which the use of SBS is restricted due to its sensitivity to degradation [5].

Butadiene, is usually 1,3-butadiene, with formula $C_4H_6$ (figure 2.2A). It is an important industrial chemical used in the production of synthetic rubber and the softer compound in SBS. The butadiene unit can have three different components, 1,2-, cis-1,4-, and trans-1,4 units [6] and the thermoplastic can show various microstructures depending on the ratios of the different units.

The polymer formed just from the polymerization process of the monomer 1,3-butadiene is the synthetic rubber, polybutadiene (PB), represented in figure 2.2B.

A                                                    B
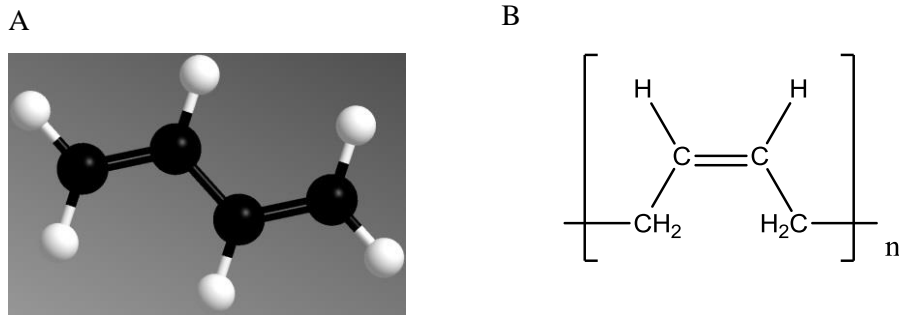


Figure 2.2 – A) 3D scheme for butadiene monomer and B) polybutadiene polymeric chain.

Styrene, also known as vinyl benzene and phenyl ethene, is an *organic compound* with the *chemical formula* $CH_2 = CH(C_6H_5)$[1], represented in figure 2.3A.

Polystyrene (PS) is a synthetic polymer (figure 2.3B) based on the monomer styrene and can be rigid or foamed. It is usually transparent, hard and brittle. The chemical formula is $-[CH_2(C_6H_5)]_n -$[1].

A                                                    B
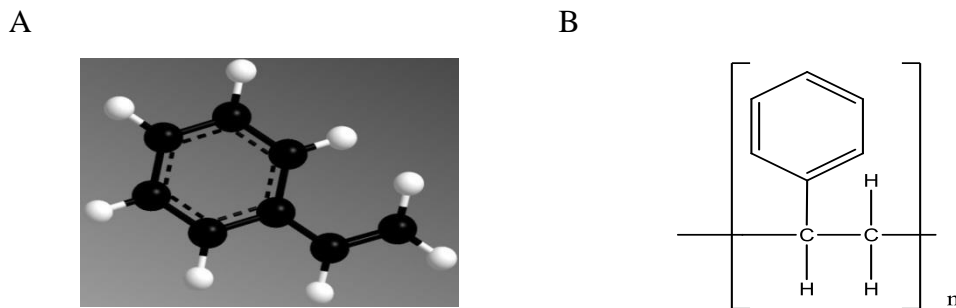


Figure 2.3 – A) 3D scheme for styrene monomer and B) polystyrene polymeric chain.

Polystyrene is valued for its good properties as transparency, mechanical properties and rigidity at room temperature, low price, easy processing and versatility of processing methods, inertness to certain chemicals, weak absorption of water, good electrical insulator even in wet environments, possibility of food contact for specific grades and thermal insulation properties, particularly in the form of foams [1]. Polystyrene ability for foaming has allowed the mass-production of foams for insulation and damping applications [1].

14

Some disadvantages of polystyrene are the sensitivity to heat, low temperature, UV, light and weathering, weak impact resistance, poor scratch resistance, low flexibility, creep when the temperatures rises, easy combustion with dripping and release of abundant black fumes, electrostatic build-up and some machining difficulties [1].

High-impact grades have lower rigidity, weak chemical resistance and are more difficult to join and weld. Blends made of polystyrene and polybutadiene are opaque [1].

Some relevant characteristics of 1,3 butadiene and styrene are summarized in table 2.1.

Table 2.1 – Properties of 1,3 butadiene and styrene.

| | Molecular formula | Mass Molar (g/mol) | Density (g/cm3) | Melting Point (°C) | Boiling Point (°C) |
|---|---|---|---|---|---|
| 1,3 Butadiene | C4H6 | 54.09 | 0.61 at 25 °C, solid 0.64 at – 6 °C, liquid | -108.9 | -4.4 |
| Styrene | C8H8 | 104.15 | 0.91 at 20 °C | -30.0 | 130.0 |

The composites prepared in this work used as matrix the thermoplastic elastomers tri-block copolymer styrene-butadiene-styrene, supplied by Dynasol Elastomers (Madrid), with different copolymer structures and ratios of butadiene/styrene. Table 2.2 shows the main characteristics of the SBS matrix.

Table 2.2 – Characteristics and denomination of the SBS used in this work.

| SBS reference | C401 | C411 | C500 | C540 |
|---|---|---|---|---|
| Block copolymer structure | radial | radial | linear | linear |
| Styrene/Butadiene ratio | 20/80 | 30/70 | 30/70 | 40/60 |

Thermoplastic elastomer is an insulator matrix and in order to tailor electrical conductivity it is necessary to add conductive fillers during composite processing. This electrical conductive behavior is based on the formation of percolation pathways of the conductive nanofillers impregnated in the matrix, which leads to a sudden increase in the conductivity at a certain critical filler concentration, commonly referred as the percolation threshold [7].

CNT has been proved to be the filler providing larger electrical conductivity at lower percolation thresholds [8].

The main properties of CNTs are high flexibility, low mass density, large aspect ratio (typically > 1000), high tensile modulus and strengths. Electrical conductivity is higher

than $10^4$ S/cm, tensile strength near 10 GPa and initial modulus (E) larger than 1TPa. The thermal conductivity can be near 2000 W/mK.

Individual single-walled carbon nanotubes can be metallic or semiconducting [9], being the electrical conductivity in some cases larger than copper [10, 11]. It is this combination of mechanical and electrical properties of individual nanotubes that makes them the ideal reinforcing agents in a number of technological applications. The first ever polymer nanocomposites using CNTs as fillers was reported in 1994 by Ajayan et al. [12]. Since then, there have been many works dedicated to polymer nanocomposites to improve mechanical and/or electrical properties of composites.

In this work three different types of CNT were used (table 2.3): MWCNT from Baytubes with reference C150P; purity > 95%, outer mean diameter of 13–16 nm and length of 1–10 $\mu$m) supplied from Bayer materials science; MWCNT from Nanocyl with reference NC7000; purity 90%, outer mean diameter of 9.5 nm and length of 1.5 $\mu$m) and SWCNT with purity 60-70% and 30% of metal content, mean diameter of 1.4 nm from Carbon Solutions with reference AP-SWNT. Table 2.3 shows the main properties of the used CNT.

Table 2.3 – Properties of the carbon nanotubes used for the preparation of the composites.

| CNT Reference | C150P (Baytubes) | NC7000 (NanoCyl) | AP-SWNT (Carbon Solutions) |
|---|---|---|---|
| Carbon Purity (wt%) | > 95 | 90 | 60-70 |
| Number of Walls | 3 - 15 | | |
| Outer mean diameter (nm) | 5 - 20 | 9.5 | 1.4 |
| Inner mean diameter (nm) | 2 - 6 | | |
| Length ($\mu$m) | 1 - >10 | 1.5 | |
| Density (kg/m$^3$) | 150 - 350 | | |
| Metal content (wt%) | | 10 | 30 |

Pristine CNT typically mixture various chiralitys, aspect ratios, some impurities and defects [9]. The effort is to establish the most suitable preparation method for the transfer of mechanical reinforcement or electrical conductivity to a polymer composite. Dispersion of CNT and chemical affinity (covalent or non-covalent) functionalization with the surrounding polymer matrix is a key issue to improve the composite properties [9].

The surface modification of CNTs to improve composite preparation can be divided into two categories, involving covalent or non-covalent bonding between CNT and polymer [9]. Non-covalent modification concerns the physical adsorption and/or wrapping of polymers to the surface of the CNTs [9] and the advantage is that this functionalization does not destroy the conjugated system of the CNT sidewalls and therefore it does not affect the final structural properties of the material [9].

Covalent modification is the chemical bonding (grafting) of polymer chains to CNTs, where strong chemical bonds are established between the polymer and the CNTs [9]. There are two main methods for the grafting of CNTs depending on the building of polymer chains. The "grafting to" approach involves the synthesis of a polymer with a specific molecular weight terminated with reactive groups or radical precursor. In a subsequent reaction, the polymer chain is attached to the surface of the carbon nanotubes by addition reactions. A disadvantage of this method is that the grafted polymer content is limited because of the relatively low reactivity and high steric hindrance of the macromolecules. In comparison, the "grafting from" approach involves growing polymers from CNT surfaces via in situ polymerization of monomers initiated by chemical species immobilized on the CNT sidewalls and CNT edges [9].

In this work, covalent and non-covalent functionalization were performed by styrene group, for covalent functionalization and styrene and butadiene for non-covalent functionalization, to modify surface interaction between carbon nanotubes and the TPE matrix and to explore the impact in the physical properties of the composites materials. Both functionalization procedures, present in table 2.4, are detailed in section 2.2.4.

Table 2.4- Covalent and non-covalent Carbon nanotube functionalizations.

| Functionalization | Reaction |
|---|---|
| Covalent | diazonium salt - styrene |
| Non-Covalent | $C_6H_5CH=CH_2$ – styrene<br>$CH_2=CHCH=CH_2$ - butadiene |

## 2.2  Processing of composites

Processing methods affect composite properties. Three methods were used for the preparation of the composites: solvent casting, extrusion and electrospinning. Further, CNT were functionalized by covalent and non-covalent functionalization.

### 2.2.1  Solvent Casting

For the preparation of the composites by solvent casting, the different CNT were placed in an Erlenmeyer with toluene and kepted in an ultrasound bath (*Bandelin*, Model Sonorex Super RK106) for 6 h or in and tip sonicated (Hielscher DRH-P400S; 400 W maximum power; 24 kHz maximum frequency) for 30 min (60% amplitude and 0.5 cycle time) to promote CNTs dispersion. After this stage, respective weight percentage of SBS was added to the solution and stirred at room temperature until complete dissolution was achieved. The relation of SBS to toluene was 1 g for 5.5 ml. Thin and highly flexible composites films were obtained by spreading the solution on a clean glass substrate. The evaporation of toluene was performed at room temperature. Thickness of the composites films varies between 150-300 μm. The CNT content in the composites ranged from 0 wt% up to 8 wt%. Functionalized (covalent and non-covalent) CNT/SBS composites have also been used following the same procedure.

### 2.2.2 Extrusion

The CNT/SBS composites were processed on a co-rotating Microlab Twinscrew extruder from Rondol Technology Ltd, designed to process small amounts of material while retaining the characteristics of larger equipment. The screw has a diameter of 10 mm and a length of 200 mm, and the die has a circular channel with a diameter of 2 mm. Prior to extrusion, the raw polymer was milled to reduce its original size until 1 mm in average in order to guarantee a continuous feeding of the twin-screw extruder. Both polymer and nanoallotropes were previously dried in a dry air dehumidifier according to the supplier instructions, pre-mixed in powder form and fed into the extruder by gravimetric feeding. Along the barrel and at the die, the temperature profile was set, after an optimization procedure for CNT/SBS composites, from 150 $^{o}$C (at the feed zone) to 190 $^{o}$C (at the die) (table 2.5) and the rotational velocity was set at 35 rpm.

Table 2.5 – Temperature profile along the extruder.

|  | Die | Zone 3 | Zone 2 | Zone 1 | Feed Zone |
|---|---|---|---|---|---|
| Temperature (ºC) | 190 | 180 | 170 | 160 | 150 |

After extrusion, the obtained composite wire was cooled at room temperature. Composites from SBS with 0, 4, 6, 8 and 10 wt% CNT (NC7000) were prepared for both C401 and C540 SBS matrices.

### 2.2.3 Electrospinning

SBS was dissolved in a mixture by volume of 75% tetrahydrofuran (THF, Panreac) and 25% of dimethylformamide (DMF, Merck) to form a solution that contained 14% (w/v) polymer. THF is a good solvent for the styrene and butadiene blocks, and the addition of 25% DMF improved the electrospinning jet stability. Dissolution was performed with the help of a magnetic stirrer (JPselecta) at room temperature.

Carbon nanotubes (NC7000) were dispersed by sonication (Bandelin, Model Sonorex Super RK 106) during 6 hours in the solvent mixture and then the SBS polymer was added to the solution, followed by magnetic stirring at room temperature until complete dissolution.

The polymer solution was placed in a commercial plastic syringe (10 ml) fitted with a steel needle with inner diameter of 0.5 mm. Electrospinning was conducted with an applied electric field of 1 kV.cm$^{-1}$ with a high voltage power supply from Glassman (model PS/FC30P04). A syringe pump (from Syringepump) was used to feed the polymer solutions into the needle tip at rate of 5 ml/h. The electrospun fibers were collected in a grounded collecting plate (random fibers) or in a rotating drum at 1000 rpm (drum diameter of 8 cm, oriented fibers).

Composites from SBS with 0, 0.05, 0.1, 0.5 wt% CNT (NC7000) were prepared for C540 SBS matrix.

### 2.2.4 CNT Functionalization

To modify surface interaction between carbon nanotubes and the TPE matrix and to explore the impact in the physical properties of the composites, the nanotubes were functionalized with covalent and non-covalent functionalization.

Covalent functionalization (CF) with styrene groups was accomplished by reaction with the corresponding in situ generated diazonium compound (figure 2.4).
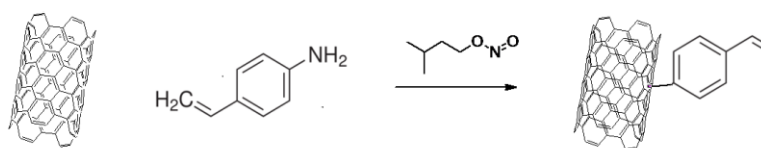


Figure 2.4 – Functionalization of CNTs with styrene by diazonium salt reaction

CNT were placed in tip sonication during 30 min (60% amplitude and 0.5 cycle time) with DMF in a ratio of 100 g of CNT to 50 ml of DMF. Then, 1.2 g of 4-vinylaniline (97%) (Sigma Aldrich) with 50 ml of acetonitrile (Sigma Aldrich) were added to the CNT/DMF solution at 60 ºC under constant magnetic stirring. The process was completed by adding 1 ml of isoamyl nitrite and keeping the solution under magnetic stirring for 8 h. After this process, the CNT were completely dried at 60 ºC during 6 hours. After obtaining covalent functionalized CNT, composites were prepared following the same procedure explained before for the pristine CNT.

Non-covalent functionalization (NCF) was achieved with two different reagents, one for styrene and one for butadiene, both from Sigma Aldrich. For styrene, $C_6H_5CH=CH_2$ was used whereas butadiene functionalization was achieved with $CH_2=CHCH=CH_2$. These reagents were added to the CNT and tip sonicated during 30 min 20 mg of CNT were mixed with 6 ml of the respective reagent for styrene or butadiene. Then, non-covalent functionalized CNT were added to the SBS matrix with toluene (2 g of SBS for 6 ml of toluene) and the solution was placed under magnetic stirring for 3 h until complete dissolution of the composite. Thin (150-300 µm) and highly flexible composite films were obtained by spreading the solution on a clean glass substrate and evaporating the toluene at room temperature.

## 2.3 Characterization techniques and conditions

After sample preparation, the influence of polymer matrix type, CNT type, concentration and functionalization, on the composite morphology, filler dispersion, mechanical, electrical, thermal and electromechanical properties of the composites was evaluated.

### 2.3.1 Composites morphology and CNT dispersion

Scanning electron microscopy (SEM) experiment was performed in order to evaluate the composites microstructure and the dispersion of the fillers within the polymer matrix. Three different SEM equipments were used: a Hitachi S3400N set-up working in the secondary electrons mode at a voltage of 15 kV and a distance of 5 mm, a Leica Cambridge apparatus at room temperature and a SEM Phillips X230 FEG apparatus. Cross section images were obtained after cutting the composites previously immersed in liquid nitrogen and coating the surface gold using a sputter coating.

Interaction between CNT and polymer matrix was analyzed using Fourier Transformed Infrared Spectroscopy (FTIR) performed at room temperature in a Perkin-Elmer Spectrum 100 apparatus in ATR mode from 4000 to 650 $cm^{-1}$. FTIR spectra were collected with 32 scans at a resolution of 4 $cm^{-1}$.

### 2.3.2 Thermal Analysis

Thermal behavior of the composites was analyzed to understand thermal stability and glass transition variations using Thermogravimetric analyses (TGA) and Differential scanning calorimetry (DSC), respectively. TGA analyses were carried out using a Pyris 1 TGA – Perkin-Elmer set-up under nitrogen atmosphere supplied at a constant 50 ml $min^{-1}$ flow rate. The composite holders were ceramic crucibles with a capacity of 60 µl. The composites were subjected to different heating rates from $5 \pm 0.1$ up to $30 \pm 0.4$ ºC.$min^{-1}$ in a temperature range between 30 and 900 ºC.

Differential scanning calorimetry was performed from -20 to 200 °C at a rate of 10 °C $min^{-1}$ using a DSC-2010 from TA instruments under dry nitrogen atmosphere.

### 2.3.3 Electrical conductivity measurements

Electrical resistance of the composites was calculated from the slope of I–V curves measured with an automated Keithley 487 picoammeter/voltage source. I–V data points were collected between gold contacts deposited on both sides of the composites with a Polaron SC502 sputter coater. Volume resistivity was measured with circular contacts of D = 5 mm diameter with an applied voltage ranging between $\pm$ 10 V and measuring the current. The resistivity of the composites (ρ) was calculated by [13]:

$$\rho = \frac{RA}{d} \qquad (2.1)$$

where R is the resistance of the composite, d its thickness of the sample and A the area of the electrodes. Electrical conductivity ($\sigma$) is the inverse value of electrical resistivity.

### 2.3.4 Mechanical measurements

Mechanical measurements were performed using a universal testing machine Shimadzu model AG-IS with a load cell of 1 kN for solvent casting and extruder samples, and with load cell of 50 N for electrospinning samples. Measurements were performed in tensile mode at room temperature in composites with dimensions presented in table 2.6 at a test velocity of 1-2 mm/min.

Table 2.6 – Typical dimensions of the samples, obtained by the different processing methods, for mechanical measurements.

| | Solvent Casting | Electrospinning | | Extruder |
|---|---|---|---|---|
| length (mm) / width (mm) / thickness ($\mu m$) | 60 / 20 / 150-300 | 60 / 20 / 50 | length (mm) / diameter (mm) | 60 / 1.5 |

### 2.3.5 Electromechanical measurements

Electromechanical tests were performed by measuring the electrical resistance of the composites, through gold electrodes deposited by sputtering with a Polaron Coater SC502, with an Agilent 34401 A multimeter during the mechanical deformation of the composite, applied with an universal testing machine from Shimadzu (model AG-IS, with a load cell of 1 kN) on samples with similar dimensions than the ones used for the mechanical tests (table 2.6).

Uniaxial stretching mechanical solicitation was applied to the composites. The mechanical experiments clamping apparatus is show in figure 2.5. Electrodes in the composites are in contact with the clamps of the universal testing machine and do not suffer any deformation during the stress-strain tests.
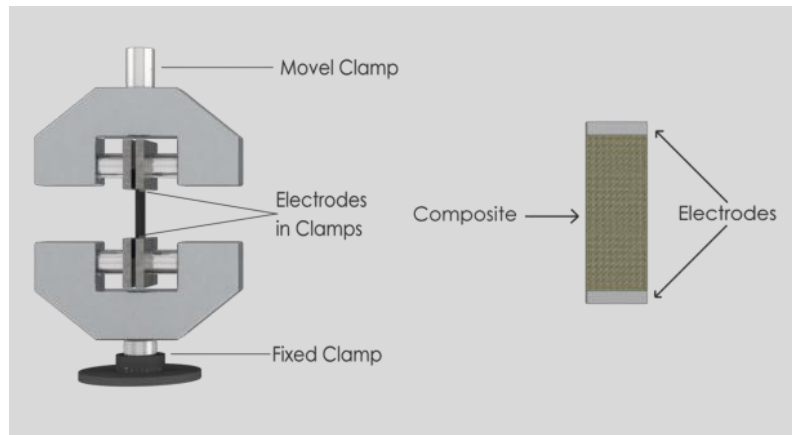
Figure 2.5 – Schematic representation of the experimental configuration of the clamps for the stress-strain experiments with simultaneous electrical measurements for electromechanical response evaluation of the composites.

For the 4-point-bending measurements (figure 2.6), the sample was glued to the bottom of a poly (propylene) board. Gold electrodes with an area of 6x1 mm were placed at the bottom of the composite. For all experiments, 4 loading-unloading cycles were performed and the average electromechanical response evaluated at room temperature.
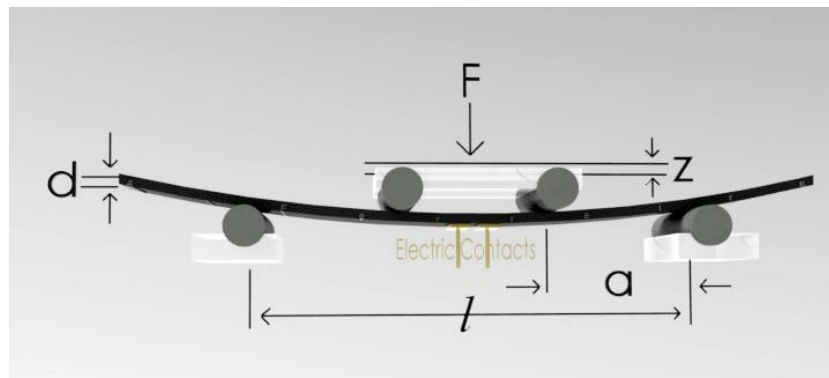


Figure 2.6 – Representation of the 4-point-bending tests (method 2) apparatus where z is the vertical displacement, d is the samples thickness (150–300 μm) and a is the distance between the first and the second bending points (15 mm). The electrodes are in the center of the samples.

The experimental conditions for the electromechanical measurements are summarized in the table 2.7.

Table 2.7 – Experimental conditions for the electromechanical tests for the two mechanical solicitations (methods).

|  | Description | Stress-strain cycles | Strain | Velocity (mm/min) |
|---|---|---|---|---|
| Method 1 | Uniaxial stress | 10 | 1% to 50% | 1 to 50 |
| Method 2 | 4-point bending | 4 | 0.1 to 1 mm | 1 to 50 |

In uniaxial stretching mode experiments (method 1) equation 2.2 was used for the calculation of the Gauge Factor (GF), using the evolution of the resistance during the stress-strain measurements. In 4-point-bending mode experiments (method 2), the strain was calculated from the theory of a pure bending of plate, valid between the inner loading points, and given by [14]:

$$\varepsilon = \frac{3dz}{5a^2} \tag{2.2}$$

Here, d, z and a are represented in Figure 2.6. Experiments were performed in samples of the different polymer matrices for CNT filler contents between 0 and 8 wt%. The GF value was calculated for each cycle from the z-displacement and the electrical resistance data by taking the fit curve by a linear regression. Finally, an average GF value was calculated for each sample.

The electromechanical response sensitivity of the composite is quantified by the gauge factor (equation 2.3), which is defined as the slope between relative change in electrical resistance $\left(\frac{dR}{R_0}\right)$ with the applied relative mechanical deformation $\left(\frac{dl}{l_0}\right)$ [14, 15].

$$GF = \frac{dR/R_0}{dl/l_0} \tag{2.3}$$

where $R_0$ is the steady-state electrical resistance of the material without deformation and $dR$ is the resistance variation caused by the deformation $dl$ [14, 15].

The gauge factor can be also written as:

$$GF = \frac{dR/R_0}{dl/l_0} = \frac{d\rho/\rho}{dl/l_0} + 1 + 2\nu \tag{2.4}$$

where $\nu$ is the Poisson ratio and $\rho$ the electrical resistivity. Equation 2.4 shows the two different contributions to the gauge factor: an intrinsic electromechanical term (first term in equation) and a geometrical term $\left(1 + 2\nu\right)$ [14, 15]. For thermoplastic elastomers, the Poisson ratio is around 0.5 [16], signifying that gauge factors smaller than 2 can be attributed mainly to geometrical contributions, whereas intrinsic electromechanical contributions will lead to gauge factors higher than 2.

**References**

[1]     Biron M 2007 *Thermoplastics and Thermoplastic Composites,* (Oxford: Elsevier) pp 217-714

[2]     Kong R S a I 2012 *Thermoplastic Elastomers*: In Tech)

[3]     Wu J-H, Li C-H, Wu Y-T, Leu M-T and Tsai Y 2010 Thermal resistance and dynamic damping properties of poly (styrene–butadiene–styrene)/thermoplastic polyurethane composites elastomer material *Composites Science and Technology* 70 1258-64

[4]     Canto L B, Mantovani G L, deAzevedo E R, Bonagamba T J, Hage E and Pessan L A 2006 Molecular Characterization of Styrene-Butadiene-Styrene Block Copolymers (SBS) by GPC, NMR, and FTIR *Polym. Bull.* 57 513-24

[5]     Juárez D, Ferrand S, Fenollar O, Fombuena V and Balart R 2011 Improvement of thermal inertia of styrene–ethylene/butylene–styrene (SEBS) polymers by addition of microencapsulated phase change materials (PCMs) *European Polymer Journal* 47 153-61

[6]     Choi S-S 2002 Characteristics of the pyrolysis patterns of styrene-butadiene rubbers with differing microstructures *Journal of Analytical and Applied Pyrolysis* 62 319-30

[7]     Tsuchiya K, Sakai A, Nagaoka T, Uchida K, Furukawa T and Yajima H 2011 High electrical performance of carbon nanotubes/rubber composites with low percolation threshold prepared with a rotation–revolution mixing technique *Composites Science and Technology* 71 1098-104

[8]     Wang L, Xu C and Li Y 2013 Piezoresistive response to changes in contributive tunneling film network of carbon nanotube/silicone rubber composite under multi-load/unload *Sensors and Actuators A: Physical* 189 45-54

[9]     Spitalsky Z, Tasis D, Papagelis K and Galiotis C 2010 Carbon nanotube–polymer composites: Chemistry, processing, mechanical and electrical properties *Progress in Polymer Science* 35 357-401

[10]    Dürkop T, Kim B M and Fuhrer M S 2004 Properties and applications of high-mobility semiconducting nanotubes *Journal of Physics: Condensed Matter* 16 R553

[11]    Wei B Q, Vajtai R and Ajayan P M 2001 Reliability and current carrying capacity of carbon nanotubes *Applied Physics Letters* 79 1172-4

[12]    Ajayan P M, Stephan O, Colliex C and Trauth D 1994 Aligned Carbon Nanotube Arrays Formed by Cutting a Polymer Resin—Nanotube Composite *Science* 265 1212-4

[13]    Costa P, Silva J, Sencadas V, Simoes R, Viana J C and Lanceros-Méndez S 2013 Mechanical, electrical and electro-mechanical properties of thermoplastic elastomer styrene-butadiene-styrene/multiwall carbon nanotubes composites *Journal of Materials Science* 48 1172-9

[14]    Cao C L, Hu C G, Xiong Y F, Han X Y, Xi Y and Miao J 2007 Temperature dependent piezoresistive effect of multi-walled carbon nanotube films *Diamond and Related Materials* 16 388-92

[15]    Wichmann M H G, Buschhorn S T, Gehrmann J and Schulte K 2009 Piezoresistive response of epoxy composites with carbon nanoparticles under tensile load *Physical Review B* 80 245437

[16]    Golaz B, Tetouani S, Diomidis N, Michaud V and Mischler S 2012 Processing and tribology of thermoplastic polyurethane particulate composite materials *Journal of Applied Polymer Science* 125 3745-54

# Chapter 3. Mechanical, Electrical and Electromechanical Properties of Thermoplastic Elastomer Styrene-Butadiene-Styrene/Multiwall Carbon Nanotubes Composites

## Abstract

Composites of styrene-butadiene-styrene (SBS) block copolymer with multiwall carbon nanotubes (MWCNT) were processed by solution casting in order to investigate the influence of filler content, the different ratio of styrene/butadiene in the copolymer and the architecture of the SBS matrix on the electrical, mechanical and electromechanical properties of the composites. It was found that filler content and elastomer matrix architecture influence the percolation threshold and consequently the overall composite electrical conductivity. The mechanical properties are mainly affected by the styrene and filler content. Hopping between nearest fillers is proposed as the main mechanism for the composite conduction. The variation of the electrical resistivity is linear with the deformation. This fact, together with the gauge factor values in the range of 2 to 18, results in appropriate composites to be used as (large) deformation sensors.

## 3.1 Introduction

Elastomers and thermoplastics are known for their capability to exhibit high deformation capability and high electrical and thermal resistances [1]. These properties can be significantly modified by the addition of conductive fillers such as carbon allotropes [1]. Within this family, carbon nanotubes (CNT) are known to produce composites with superior electrical and mechanical properties compared with other carbon allotropes such as carbon black (CB) or carbon nanofibers (CNF) [1]. The CNT unique electrical and mechanical properties [2] allows that even at low concentrations (less than 5 wt%) they can strongly affect the composites electrical and mechanical properties [3-4].

Thermoplastic elastomer tri-block copolymer styrene-butadiene-styrene (SBS) copolymers can be composed by different ratios of styrene and butadiene, influencing strongly their macroscopic properties.

The application range of SBS, once suitably reinforced with CNT, can be extended to a variety of products such as sensors and actuators [5], materials with electromagnetic shielding properties [6], vapour and infrared sensors [7] and capacitors [8], among others. Previous studies on SBS − carbon nanotube composites indicate that the final properties of the composite can change for different ratios of styrene and butadiene [9].

Despite the intensive use of SBS in industry, the potential of CNT/SBS nanocomposites for sensor applications has been scarcely explored and systematic studies on the interrelationship of styrene/butadiene ratio and CNT loading on the electrical, mechanical and electromechanical response, have yet to be done.

The composites using CNT show higher enhancement in the electrical properties that can be interpreted within the framework of percolation theory [10, 11]. The percolation theory predicts for fibres with a capped cylinder shape the following bounds for the percolation threshold [10, 12]:

$$1 - e^{\frac{-1.4V}{\langle V_e \rangle}} \leq \Phi_c \leq 1 - e^{\frac{-2.8V}{\langle V_e \rangle}} \tag{3.1}$$

Equation 3.1 links the average excluded volume $\langle V_e \rangle$ ,i.e., the volume around an object in which the centre of another similarly shaped object is not allowed to penetrate, averaged over the orientation distribution, with the critical concentration ($\Phi_c$). Here, 1.4 corresponds to the lower limit for infinitely thin cylinders and 2.8 correspond to spheres

(V is the particle volume). For high aspect ratio fillers the percolate network can be formed with lower concentrations producing a composite with higher electrical and mechanical properties. The percolation threshold found for this type of nanocomposites depends on the properties of the materials (matrix and nanoparticles) [13], nanofiller dispersion agent and method [14] and can be reduced down to 0.1 % volume using CNT [1]. The typical percolation threshold is between 10-25 % volume for CB [1] and 1-5 % volume to CNF [1].

An important property of CNT/polymer composites that can be used for sensor applications is the fact that by the application of uniaxial or hydrostatic stress, the composite electrical resistivity changes, due to the so called piezoresistance (electromechanical response) [15]. It is important to note that this change on the composite electrical resistivity due to the applied stress is not solely related to changes in the dimension of the solid or to the intrinsic electromechanical properties of the components. These properties in CNT/polymer composites can be mainly attributed to the variations of the conductive networks with strain, such as loss of contact between the fillers, tunnelling or hopping effect in neighbouring fillers and conductivity change due to the deformation of CNT [15]. It is also known that, even for the same kind of carbon allotrope, the electromechanical effect is highly dependent on the physical and chemical properties of the filler [16]. The electromechanical effect of CNT/polymer composites makes them particularly interesting materials to be used as highly sensitivity strain sensors for structural health monitoring [17], damage and fracture detection [18]. In particular, elastomeric based composites are exceptionally appropriate for high strain and high compliant deformation sensors, due to the difficulties of other materials in achieving high level reversible deformations.

The electromechanical effect results from the strain-induced variation of the electrical resistance of the material. At low strains, in thermoplastic elastomer/CNT composites, the resistance changes linearly with strain. This linearity is sometimes referred as Gauge Factor [19].

In the present work, MWCNT/SBS composites were processed by solution casting for different styrene/butadiene ratios and matrix architecture (radial and linear), as well for different filler loadings. The influence of these parameters on the mechanical and electrical response of the material was studied as well as their electromechanical performance through the calculation of the Gauge Factor. In this way, the fundamental

properties concerning the electrical and mechanical performance of the material were discussed, as well as its potential for use in large strain sensor applications.

## 3.2 Results and Discussion

### 3.2.1 MWCNT dispersion

SEM images of CNT/SBS composites for the C540 matrix with 1 wt% and 4 wt% of CNT are presented in figure 3.1 for two magnifications. Similar images are observed for the different polymer matrices. The samples are characterized by small CNT clusters well dispersed in the different SBS matrix. Therefore, composites with some degree of agglomeration of the nanotubes are obtained, but with a relatively good cluster distribution. This fact is independent of the polymer matrix.
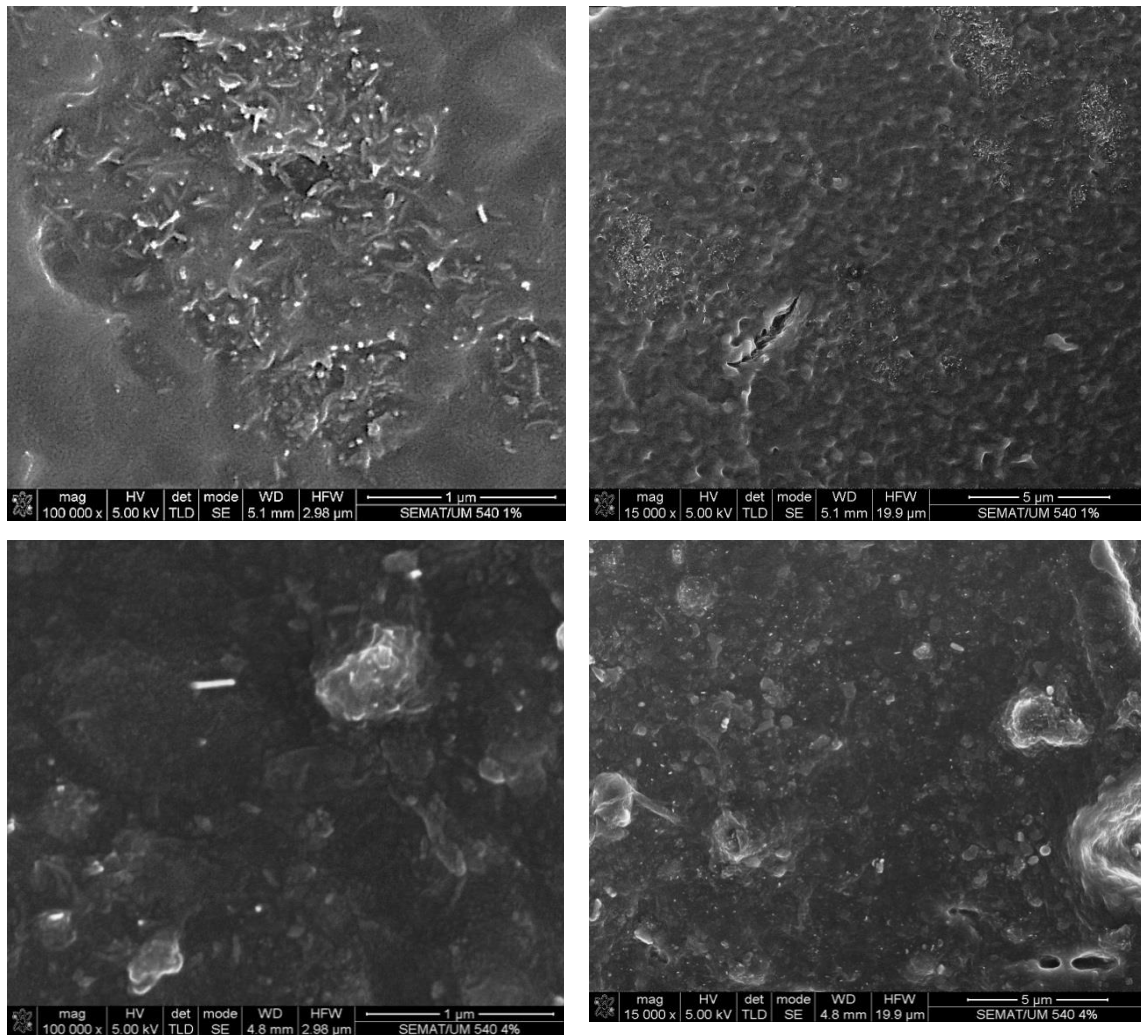


Figure 3.1 – SEM images for CNT/SBS composites (C540 with 1 wt% -above, and 4 wt% -below) with two different magnification where is possible to observe both clusters dispersed in the polymer matrix and individual CNT. The small CNT clusters are observed for all composites, well distributed within the different polymer matrices.

### 3.2.2 Mechanical Properties

Representative quasi-static stress/strain curves for the different SBS matrices are presented in figure 3.2. The materials undergo yielding and strain hardening as the strain increases. A first maximum stress is observed for all samples followed by a post-yielding plateau and a strain hardening stage before the rupture of the material. The stress-strain curves of figure 3.2 reveal that the SBS with radial morphology has lower tensile strength and presents a strain at rupture of approximately 1100%. On the other hand, the SBS with linear morphology shows higher tensile strength. The highest strain at rupture (~ 1400%) is found for the sample C540, which has a linear structure and the higher amount of the styrene in its composition (40%). The linear morphology SBS leads to higher strain-hardening modulus. It is also observed for both types of SBS architectures that the maximum sustained stress level of the SBS increases with increasing styrene content in the copolymer.
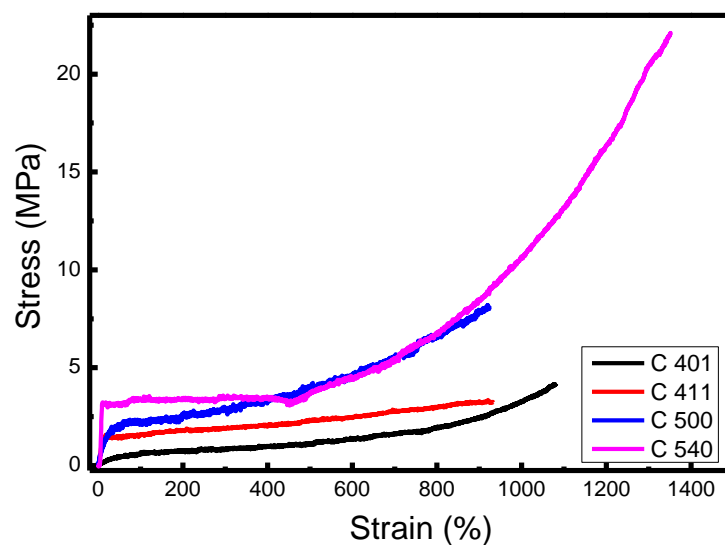


Figure 3.2 – Stress-Strain curves for different pure SBS.

It has been reported that the deformation induced in the SBS block copolymer depends strongly on the morphology and microdomain orientation [20]. In principle, the solution cast films do not have any preferable molecular orientation. During stretching, the orientation of the macromolecular chains and individual phases along the draw direction plays an important role in the material deformation. A linear architecture of the block copolymer allows also a higher material stretchability rather than a radial one.  In figure 3.2, the initial moduli of the neat SBS matrices are substantially higher for linear

architecture and for a high amount of styrene. The amount of styrene present in the copolymer increases the sustained stress level of the material, especially for the matrices with linear structure (C500 and C540). The measured stress at 300% of strain ($\sigma_{300}$) and at 900% of strain ($\sigma_{900}$) reveal that $\sigma_{300}$ and $\sigma_{900}$ increases with the increasing amount of PS present in the matrix and it is also higher for the material with linear morphology (figure 3.2).

Figure 3.3a) shows the stress-strain curves for C540 CNT/SBS (the matrix showing the highest initial modulus and deformation at break) composites with filler volume fractions up to $3.83 \times 10^{-2}$. For low filler volume fractions (up to $9.87 \times 10^{-3}$) increasing CNT content increases slightly the strain hardening response of the material without compromising its deformation capabilities (figure 3.3a). However, for higher CNT contents the strain hardening is substantially reduced, still without reducing the maximum strain at break. Table 3.1 presents the main mechanical properties of the C540 CNT/SBS composites. It is also observed that the initial modulus increases with increasing CNT content, suggesting a good adhesion between the SBS and the CNT. The $\sigma_{300}$ values are quite similar for all samples, suggesting that the CNTs are homogeneous and uniformly dispersed into the polymer matrix. This is further corroborated by the small variation of the strain at break with increasing CNT content. Finally, the ultimate tensile strength increases for small amounts of nanofiller added to the SBS until $1.95 \times 10^{-2}$ volume fraction, decreasing slightly for higher filler concentrations.

Table 3.1 – Mechanical properties of C540 CNT/SBS composites.

| Composite | E | $\sigma_{300}$ | $\sigma_{900}$ | $\sigma_{break}$ | $\varepsilon_{break}$ |
|---|---|---|---|---|---|
| | MPa | MPa | MPa | MPa | % |
| 0 | $43.9 \pm 2.21$ | $3.47 \pm 0.17$ | $8.55 \pm 0.35$ | $22.1 \pm 1.13$ | $1350 \pm 75$ |
| $1.24 \times 10^{-3}$ | $43.2 \pm 2.20$ | $3.31 \pm 0.16$ | $8.94 \pm 0.39$ | $23.6 \pm 1.16$ | $1344 \pm 77$ |
| $4.96 \times 10^{-3}$ | $54.4 \pm 2.51$ | $1.90 \pm 0.10$ | $10.19 \pm 0.52$ | $11.8 \pm 0.61$ | $970 \pm 48$ |
| $9.87 \times 10^{-3}$ | $50.2 \pm 2.42$ | $3.17 \pm 0.16$ | $10.39 \pm 0.54$ | $27.6 \pm 1.36$ | $1330 \pm 75$ |
| $1.95 \times 10^{-2}$ | $60.4 \pm 3.11$ | $3.47 \pm 0.17$ | $10.9 \pm 0.57$ | $16.96 \pm 0.75$ | $1157 \pm 71$ |
| $3.83 \times 10^{-2}$ | $114.0 \pm 5.51$ | $3.17 \pm 0.16$ | $6.63 \pm 0.32$ | $10.9 \pm 0.53$ | $1370 \pm 76$ |

The inclusion of CNT into the polymer matrix leads to an increase in the initial modulus, which is a common behaviour of this kind of polymeric systems [16]. It

should be noted that the strength is almost similar for all samples until $\varepsilon \sim 700\%$, but for the sample with $3.83 \times 10^{-2}$ filler volume fraction, the tensile stress is smaller than the ones found for the composite samples with lower filler contents. The formation of CNT aggregates in the polymer composite [14] represent a common defect that for higher strains explains the decrease of the tensile tress for the sample with highest filler content. The retaining of the tensile strength observed in the samples suggests the presence of just small extent of agglomerates (table 3.1).
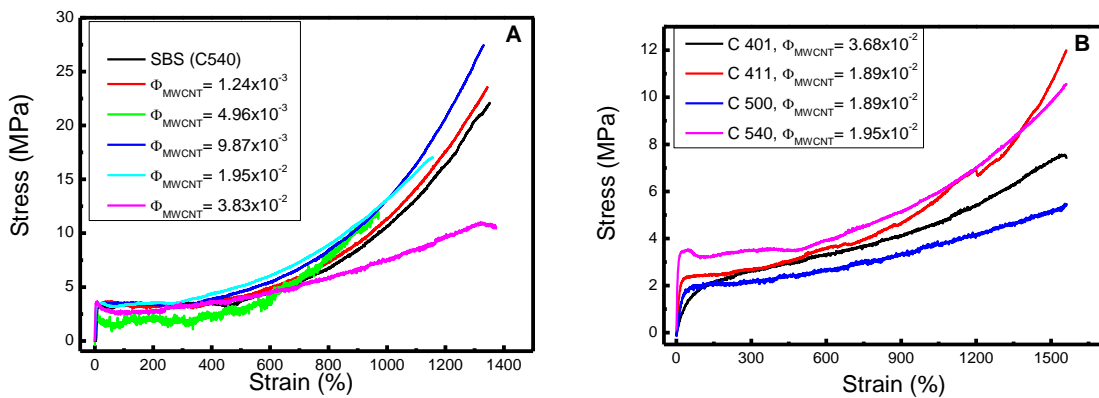


Figure 3.3- A) Stress-strain curves of SBS C540 filled with different contents of CNT and B) stress-strain curves for CNT/SBS composites with 1.95-3 to $3.68 \times 10^{-2}$ volume fraction of CNT.

In order to understand the effect of the CNTs into the different SBS morphologies, several samples were processed with $1.95 \text{-} 3.68 \times 10^{-2}$ filler volume fractions. Figure 3.3B shows the stress-strain curves indicating that all SBS nanocomposites show the same deformation trends. The C540 matrix (with linear SBS architecture and high styrene content) filled with $1.95 \times 10^{-2}$ volume fraction of CNT shows the best mechanical performance, namely the highest sustained stresses. The C500 matrix (with linear SBS architecture and low styrene content) presents the lowest stress levels. The C411 matrix (with radial SBS architecture and high styrene content) shows the highest strain hardening slope. The architecture type and the styrene content in the SBS matrix have distinct effects on the mechanical response of the CNT/SBS composites.

Comparing with the neat SBS stress-strain curves (figure 3.3A) the incorporation of CNT improves the mechanical response of the SBS matrices. In general, the initial modulus increases significantly, showing linear SBS nanocomposites lower initial modulus when compared to the radial ones. Increasing styrene content leads to higher initial modulus of the nanocomposites. For the radial SBS morphologies, the ultimate

stress increases significantly with the incorporation of the fillers, but for the linear SBS, adding the nanofillers reduces the maximum stress level. As already mentioned, the initial modulus of the SBS nanocomposites depend upon the copolymer morphology (radial vs. linear) and the styrene content on the SBS.

Figure 3.4 shows the variation of the initial modulus of the SBS systems with the CNT content. For a given SBS matrix, E increases with increasing filler content. The initial modulus is higher for the C540 samples due to the larger styrene (40%) content, leading to a stiffer material. Conversely the C401 sample shows the lowest E values. Finally, comparing similar styrene/butadiene ratios, C411 and C500, the initial modulus is larger for the SBS with a radial structure, C411, than that with a linear structure, C500, and this behaviour is correlated to the distribution and uniformity of the styrene phase among the copolymer.
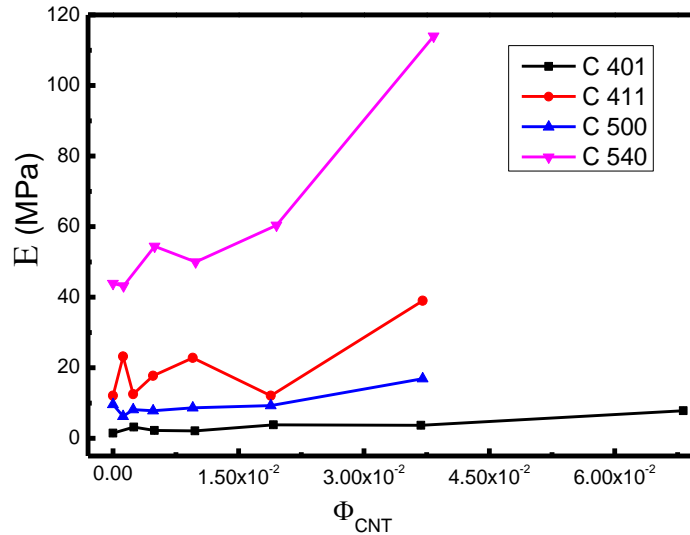


Figure 3.4- Initial modulus for the different matrix as a function of the CNT contents. See also table 3.1 for the C540/CNT composites.

### 3.2.3 Electrical Properties

The electrical response of the CNT/SBS composites was evaluated by measuring the bulk electrical resistivity (figure 3.5A).
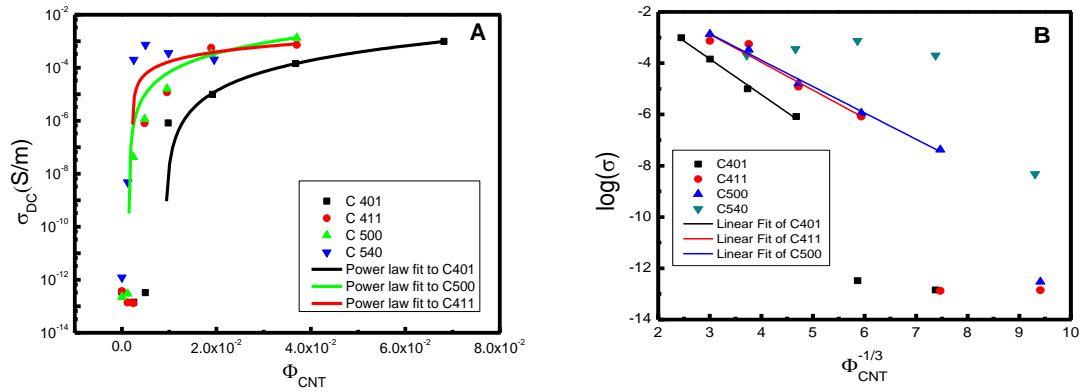
Figure 3.5- A) Log-Linear plot of the electrical conductivity versus volume fraction of CNT for the SBS matrices and B) volume electrical conductivity of CNT/SBS nanocomposites versus volume fraction. The linear relations indicate that the electrical conductivity is due to hopping between the fillers.

Figure 3.5A shows the electrical conductivity of the SBS nanocomposites as a function of the volume fraction of CNT. For C401, C411 and C500 nanocomposites there is a critical volume fraction were a change of several orders of magnitude in the electrical conductivity is observed. For the C540, the position of the critical volume fraction is not clear, but a sharp increase in the electrical conductivity is observed, leading to a quasi-plateau for the highest volume fractions. The electrical conductivity seems to be also dependent on the morphology and styrene content of the SBS block copolymers. Interestingly, the variations of the electrical conductivity for the SBS nanocomposites are similar to those of the initial modulus. The C540 shows the highest values of the initial modulus and electrical conductivity, followed by C411, C500; the C401 showing the lowest values. In this way, the electrical conductivity of the nanocomposites, such as the modulus, is also dependent upon the copolymer morphology (radial vs. linear) and the styrene content.

In fact, as the same type of CNT are used for all composites, the matrix characteristics should also be used to explain the observed differences in the electrical behaviour. Together with the fibre characteristics (e.g., size, aspect ratio), typically taken into account by different theoretical models, the range of the matrix-mediated interactions between the fillers has also to be considered [21]. The percolation threshold, $\Phi_c$, depends also upon the type of matrix [21]:

$$\Phi_c = \frac{D^2}{2L\delta_{max}} \tag{3.2}$$

where, D is the CNT outer diameter, L their length and $\delta_{max}$ is related to the maximum interaction range between two adjacent CNT (matrix dependent) [22]. Usually, the length of the CNT is not uniform, exhibiting a length distribution. Assuming that this distribution can be described by a Gaussian distribution with an average length $L_{av}$ and a variance $\sigma^2$, the effect of the CNT length distribution in the percolation threshold can be studied by substituting the length by an weighted average length $\langle L \rangle_w$ in Equation (3.2) [22], leading to:

$$\Phi_c = \frac{D^2}{2\langle L \rangle_w \delta_{max}} \tag{3.3}$$

with $\langle L \rangle_w \propto L_{av} + \dfrac{\sigma^2}{L_{av}}$, where $L_{av}$ is the average CNT length. Usually the electrical conductivity of the composites is understood within the percolation theory, which predicts a power law dependence for the electrical conductivity, $\sigma$, upon the volume fraction of conductive particles, valid for $\Phi \geq \Phi_c$, and expressed by:

$$\sigma \propto \left( \Phi - \Phi_c \right)^t \tag{3.4}$$

where, $t$ is a universal critical exponent depending only on the system dimension, $\Phi$ is the volume fraction and $\Phi_c$ is the critical concentration at which an infinite cluster appears in the composite [21]. Using equation (3.4), the percolation threshold and the critical exponent were calculated for all composites, with the exception of the C540, were the fits were inconclusive. Further, the maximum interaction range ($\delta_{max}$) was established using Equation 3.3 with the average values for the CNT diameter and length presented in the experimental section and assuming that $\sigma = \frac{L_{av}}{2}$ is equal for all composites. It was also assumed that the value for the standard deviation is the same for all composites due to the fact that all CNT came from the same batch and that the processing conditions for the preparation of the nanocomposites were the same. It is also important to note that CNT aggregate into clusters and, therefore, CNT clusters must be considered as conductivity units, comprised of several individual CNT with a given effective length. The latter reasoning leads to choose large values for the length standard deviation (table 3.2).

Table 3.2 – Percolation threshold and critical exponents calculated for the different SBS nanocomposites (R2 is the coefficient of linear correlation).

| C401 | | | | C411 | | | | C500 | | | |
|------|---|------|--------------|------|---|------|--------------|------|---|------|--------------|
| $\Phi_c$ | t | $R^2$ | $\delta_{max}$ (nm) | $\Phi_c$ | t | $R^2$ | $\delta_{max}$ (nm) | $\Phi_c$ | t | $R^2$ | $\delta_{max}$ (nm) |
| $9.18E^{-3}$ | ~3 | 0.999 | 1.67 | $2.22E^{-3}$ | ~1 | 0.843 | 6.89 | $1.47E^{-3}$ | ~2 | 0.998 | 10.4 |

It can be concluded from table 3.2 that the percolation threshold, $\Phi_c$, decreases with the addition of styrene (C401 and C411). Furthermore, for composites with the same ratio of styrene/butadiene (C411, C500) the percolation threshold is lower for SBS with a linear structure (C500) as compared to those with a radial one (C411). It is also observed that the lower percolation threshold implies that $\delta_{max}$ is higher, this meaning a higher interaction range between two CNT for a specific matrix. The high percolation threshold observed for the radial SBS structure can be attributed to electrostatic screening by the radial structures, lowering the maximum effective interaction distance between two CNT and therefore increasing the percolation threshold.

In table 3.2, the critical exponents, t, for the power law described by equation 3.4 are also shown. A wide range of values for the critical exponents were found: the C401 composites have a value typical of a Bethe lattice [21], the C411 has the electrical mean field approximation value [11] and the critical exponent for the C500 has the typical value of a 3D system [21].The fact that the expected power law value predicted by the percolation theory was found within a wide range of values leads to consider that, indeed, there exists a giant component that spans the system, but that the conduction mechanism can be attributed to a matrix mediated hopping leading to a weak disorder regime [19-20]. This weak disorder regime can be described by:

$$G_{eff} = G_{cut} \exp\left(\frac{-l_{opt}}{(N_{max}\Phi)^{1/3}}\right)$$

(3.5)

were, $l_{opt}$ is the length of the optimal path. When most of the links of the path contribute to the sum, the system is said to be in the "weak disorder" regime [23]. Conversely, the case where a single link dominates the sum along the path is called the "strong disorder" limit [23]. In equation 3.5, $N_{max}$ is the maximum number of fillers in the domain and $G_{cut}$ is the effective electrical conductance of the system before a bond with maximum

conductance is added to (or removed from) the system [23]. The $l_{opt}$ parameter is related to the disorder strength when the system is in the weak disorder regime. The disorder strength is just the inverse of the scale over which the wave function decays in the polymer ($x_0$), as expressed by the hopping conductivity expression at room temperature [24-25]:

$$\sigma_{ij} = \sigma_0 \exp\left(-\frac{x_{ij}}{x_0}\right) \qquad (3.6)$$

where $\sigma_0$ is the dimension coefficient and $x_{ij}$ is the distance between two fillers. As described in [26], applying equation 3.6 to the gap between the fillers (described as the minimum distance between two rods) and thus defining the electrical conductivity by hopping between adjacent fillers, leads to equation 3.6. This agrees well with recent results [26], which demonstrate that hopping between adjacent fillers gives rise to the expression $\log(\sigma) \propto \Phi^{-\frac{1}{3}}$, as given by equation 3.4, which corresponds to a weak disorder regime. This relation is also found in fluctuation-induction tunnelling [27] for the DC conductivity. In order to prove the latter assumptions, the $\log(\sigma) \propto \Phi^{-1/3}$ dependence was tested for all composites (figure 3.5B).

Figure 3.5B shows that there is a linear relation between the logarithm of the electrical conductivity and the volume fraction of CNT (with a $R^2 > 0.9$). It is important to note that for the SBS C401, C411 and C500 matrices there is a deviation from the linear relation for the lower CNT volume fractions, indicating that the conductive network is not yet formed, and implying that $G_{eff} = G_{cut}$ [26], i.e., the effective electrical conductance is controlled by the matrix conductance. On the other hand, for the C540 nanocomposite there are also deviations from the linear relationship for the higher volume fractions, which may be explained by the earlier formation of a spanning cluster [21]. For the C540 composite the spanning cluster is established at lower filler volume fractions (figure 3.5B), which implies that increasing CNT content does not further contribute to the overall composite electrical conductivity. Hopping between nearest fillers leads to the deviation from the percolation theory and the overall nanocomposite electrical conductivity is explained by the existence of a weak disorder regime.

### 3.2.4 Electromechanical Properties

The electromechanical effect was assessed for the CNT/SBS nanocomposites in the strain range between 5 to 20 % in order to test the suitability of these materials for strain sensor applications. The measurements were performed in composites with volume fractions just above the percolation threshold in order to maintain suitable resistance values to be measured as large stretching is applied (i.e., at volume fractions of $1.95 \times 10^{-2}$). The obtained GF ranges from 2 to 18, the highest values being obtained for the composite C540 at 20 % strain (figure 3.6B).

In figure 3.6A are presented the variations of the electrical resistance with a reversible strain loading (loading and unloading cycles). The relationship is linear and the electrical resistance increases with the deformation. This fact, together with the large values obtained for the GF, indicates the suitability of these nanocomposites for high strain deformation sensors.
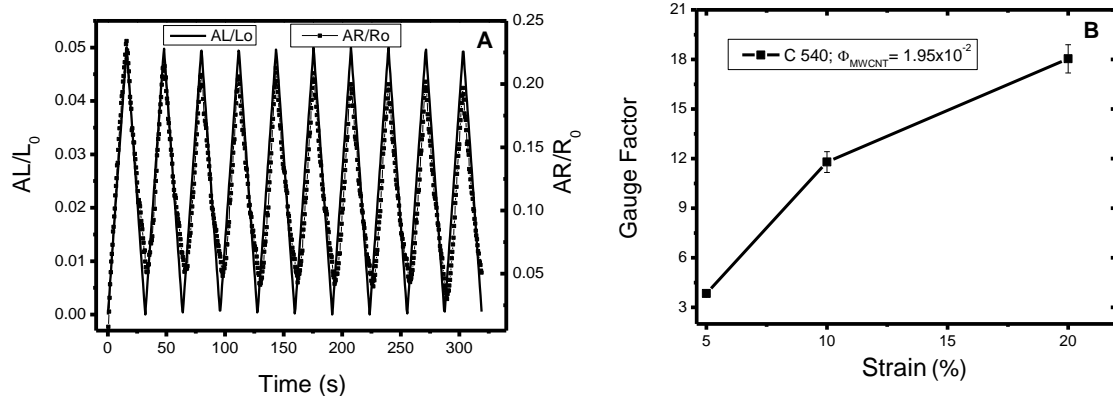


Figure 3.6- A) Variation of the electrical resistance ($\Delta R / R_0$) with strain ($\Delta L / L_0$) for the CNT/SBS composite (for 10 loading-unloading cycles. B) Gauge Factor as a function of strain for the C540 matrix with $1.95 \times 10^{-2}$ volume fraction CNT.

Figure 3.6B shows the variation of GF with strain for the C540 matrix. GF increases with increasing strain. There are still no consolidated theories explaining electromechanical properties in conducting particle-reinforced insulating matrix composites. Theories for the GF based on elastic heterogeneity, where the conducting phase is stiffer than the insulating one, indicate that the local strains within the latter are higher with respect to the averaged macroscopic strains, thus inducing higher GF values [28]. In this case, the increase of the GF with increasing strain is ascribed to larger

induced variations in the conductive network due to larger induced local strains on the matrix.

### 3.3  Conclusions

CNT/SBS composites were processed by solution casting with different CNT contents. It was found that both the architecture of the block copolymer elastomer (i.e., radial vs linear) and the styrene/butadiene ratio influence the electrical conductivity of the CNT/SBS composites. Conversely, regarding the mechanical properties, the influence of the SBS architecture was not observed, with the mechanical response being dominated by the styrene/butadiene ratio. Hopping between nearest fillers is the main mechanism for the composite electrical conduction; the overall composite conductivity is explained by the existence of a weak disorder regime. Finally, the obtained values for the Gauge Factor reveal the potential of these materials for large strain sensor applications.

**References**

[1]     Lorenz H, Fritzsche J, Das A, Stöckelhuber K W, Jurk R, Heinrich G and Klüppel M 2009 Advanced elastomer nano-composites based on CNT-hybrid filler systems *Composites Science and Technology* 69 2135-43

[2]     J-H. Du, J. Bai and Cheng H-M 2007 The present status and key problems of carbon nanotube based polymer composites *Express Polymer Letters* 1 253-73

[3]     Ma P-C, Siddiqui N A, Marom G and Kim J-K 2010 Dispersion and functionalization of carbon nanotubes for polymer-based nanocomposites: A review *Composites Part A: Applied Science and Manufacturing* 41 1345-67

[4]     Sahoo N G, Rana S, Cho J W, Li L and Chan S H 2010 Polymer nanocomposites based on functionalized carbon nanotubes *Progress in Polymer Science* 35 837-67

[5]     De Falco A, Goyanes S, Rubiolo G H, Mondragon I and Marzocca A 2007 Carbon nanotubes as reinforcement of styrene-butadiene rubber *Applied Surface Science* 254 262-5

[6]     Koerner H, Liu W, Alexander M, Mirau P, Dowty H and Vaia R A 2005 Deformation-morphology correlations in electrically conductive carbon nanotube--thermoplastic polyurethane nanocomposites *Polymer* 46 4405-20

[7]     Li C, Thostenson E T and Chou T-W 2008 Sensors and actuators based on carbon nanotubes and their composites: A review *Composites Science and Technology* 68 1227-49

[8]     Tsuchiya K, Sakai A, Nagaoka T, Uchida K, Furukawa T and Yajima H 2011 High electrical performance of carbon nanotubes/rubber composites with low percolation threshold prepared with a rotation-revolution mixing technique *Composites Science and Technology* 71 1098-104

[9]     Pedroni L G, Soto-Oviedo M A, Rosolen J M, Felisberti M I and Nogueira A F 2009 Conductivity and mechanical properties of composites based on MWCNTs and styrene-butadiene-styrene block™ copolymers *Journal of Applied Polymer Science* 112 3241-8

[10]    Celzard A, McRae E, Deleuze C, Dufort M, Furdin G and Marêché J F 1996 Critical concentration in percolating systems containing a high-aspect-ratio filler *Physical Review B* 53 6209-14

[11]    Kirkpatrick S 1973 Percolation and Conduction *Reviews of Modern Physics* 45 574-88

[12]    Balberg I, Anderson C H, Alexander S and Wagner N 1984 Excluded volume and its relation to the onset of percolation *Physical Review B* 30 3933-43

[13]    Silva J, Ribeiro S, Lanceros-Mendez S and Simões R 2011 The influence of matrix mediated hopping conductivity, filler concentration, aspect ratio and orientation on the electrical response of carbon nanotube/polymer nanocomposites *Composites Science and Technology* 71 643-6

[14]    Wang P, Geng S and Ding T 2010 Effects of carboxyl radical on electrical resistance of multi-walled carbon nanotube filled silicone rubber composite under pressure *Composites Science and Technology* 70 1571-3

[15]    Taya M, Kim W J and Ono K 1998 Piezoresistivity of a short fiber/elastomer matrix composite *Mechanics of Materials* 28 53-9

[16]    Paleo A J, Hattum F W J v, Pereira J, Rocha J G, Silva J, Sencadas V and Lanceros-Méndez S 2010 The piezoresistive effect in polypropylene—carbon

nanofibre composites obtained by shear extrusion *Smart Materials and Structures* 19 065013

[17] Kang I, Heung Y Y, Kim J H, Lee J W, Gollapudi R, Subramaniam S, Narasimhadevara S, Hurd D, Kirikera G R, Shanov V, Schulz M J, Shi D, Boerio J, Mall S and Ruggles-Wren M 2006 Introduction to carbon nanotube and nanofiber smart materials *Composites Part B: Engineering* 37 382-94

[18] Thostenson E T and Chou T W 2006 Carbon Nanotube Networks: Sensing of Distributed Strain and Damage for Life Prediction and Self Healing *Advanced Materials* 18 2837-41

[19] Oliva-Avilés A I, Avilés F and Sosa V 2011 Electrical and piezoresistive properties of multi-walled carbon nanotube/polymer composite films aligned by an electric field *Carbon* 49 2989-97

[20] Huy T A, Adhikari R and Michler G H 2003 Deformation behavior of styrene-block-butadiene-block-styrene triblock copolymers having different morphologies *Polymer* 44 1247-57

[21] Stauffer D and Aharony A 1992 *Introduction to percolation theory* (London

[22] Kyrylyuk A V and van der Schoot P 2008 Continuum percolation of carbon nanotubes in polymeric and colloidal media *Proceedings of the National Academy of Sciences* 105 8221-6

[23] Sreenivasan S, Kalisky T, Braunstein L A, Buldyrev S V, Havlin S and Stanley H E 2004 Effect of disorder strength on optimal paths in complex networks *Physical Review E* 70 046133

[24] Ambegaokar V, Halperin B I and Langer J S 1971 Hopping Conductivity in Disordered Systems *Physical Review B* 4 2612-20

[25] Miller A and Abrahams E 1960 Impurity Conduction at Low Concentrations *Physical Review* 120 745-55

[26] Silva J, Simoes R, Lanceros-Mendez S and Vaia R 2011 Applying complex network theory to the understanding of high-aspect-ratio carbon-filled composites *EPL (Europhysics Letters)* 93 37005

[27] Connor M T, Roy S, Ezquerra T A and Baltá Calleja F J 1998 Broadband ac conductivity of conductor-polymer composites *Physical Review B* 57 2286-94

[28] Grimaldi C, Ryser P and Strassler S 2000 Gauge factor of thick-film resistors: Outcomes of the variable-range-hopping model *Journal of Applied Physics* 88 4164-9

# Chapter 4. Electromechanical properties of triblock copolymer styrene-butadiene-styrene/carbon nanotube composites for large deformation sensor applications

### Abstract

Thermoplastic elastomer/carbon nanotube composites are studied for sensor applications due to their excellent mechanical and electrical properties. Electromechanical properties of tri-block copolymer styrene-butadiene-styrene (SBS)/carbon nanotubes (CNT) prepared by solution casting have been investigated. The initial modulus of the CNT/SBS composites increases with increasing the CNT filler content present in the samples, without losing the high deformation capability of the polymer matrix (~1500%). Furthermore, above the percolation threshold these materials are unique for the development of large deformation sensors due to the strong electromechanical response. Electromechanical properties evaluated by uniaxial stretching in tensile mode and 4-point bending showed Gauge Factors up to 120. The linearity obtained between strain and electrical resistance makes these composites interesting for large strain electromechanical sensors applications.

## 4.1 Introduction

Elastomeric polymers are promising materials for the development of composite samples for sensors and actuator applications, among other factors, due to their large deformation, flexibility and impact resistance [1].

In order to expand their range of applicability, in particular to the sensor field, the electrical properties of elastomers can be tailored through the incorporation of carbon nanotubes (CNT). Applying this approach, composites using carbon allotropes and thermoplastic elastomeric materials (TPE) have found applications in electrostatic charge dissipation, electromagnetic interference shielding, field emission devices, pressure or deformation sensors [2]. Due to the large strains and the high impact resistance, such materials are also promising for the substitution of silicon based force and deformation sensors, as well as strain gages [3]. Conductive TPE composites exhibit excellent mechanical and electrical properties and can be used as artificial muscles, electromechanical actuators, touch control, switches and shape-memory polymers [2]. Small amounts of CNT incorporated in the TPE matrix can enhance the mechanical properties, electrical and thermal conductivity. The filler can be randomly distributed or oriented within the TPE matrix, by applying a magnetic or electric field, in order to optimize the electromechanical properties in the desire direction [4].

The dispersion of CNT in a polymer matrix is one of the most studied issues in polymer composites, and physical and chemical strategies for CNT cluster segregation are commonly used. Several chemical agents are used for this purpose, including xylene [2], dehydrated ethyl alcohol [5], toluene and ethanol [6], among others, in order to achieve higher composite homogeneity [2, 7] and reduced the clusters size [2]. By applying such dispersion agents, the aims are to obtain a better dispersion of the fillers within the polymer matrix and, as a result, to decrease the percolation threshold and enhance electrical properties while maintaining proper elastomeric behavior [5, 8].

Thermoplastic elastomers based on a tri-block copolymer styrene-butadiene-styrene (SBS) have similar properties than rubber without the need of the vulcanization step. They show good chemical stability, low temperature flexibility and damping properties [9]. SBS is an interesting elastomer material for scientific and technological applications due to its large elongation at break and durability and when obtained without the vulcanization chemical treatment, no degradation of the mechanical and electrical properties occurs [10]. The different butadiene/styrene ratio and architecture

in the copolymer influences the material morphology, mechanical, electrical and thermal properties. Usually, butadiene is the larger component and the quantity of styrene can go up to 50%.

Studies on CNT/polymer composites can be found regarding the evaluation of dispersion, mechanical, electrical and thermal properties, as well as the development of applications [5, 8]. Within this field, thermoplastic elastomeric polymers with CNT are gaining increasing attention [2, 5, 8, 11]. The electrical properties of these composites are strongly dependent on CNT type and concentration present in the composite [2, 5, 8] and on chemical modification of the surface of the CNTs [5, 8, 12].

SBS shows a good thermal stability with the glass transition at -80 ºC, due to the butadiene phase, and at 100 ºC, assigned to the styrene compound present in the copolymer [2], and the incorporation of the CNT filler does not change them significantly [2] . Furthermore, the CNT/SBS composites have excellent mechanical properties like strain higher than 1000 %, similar stress-strain curves with amount of CNT and several ratios of styrene and butadiene in matrix of these composites. The initial modulus increases with decreasing butadiene in SBS and electrical percolation threshold is similar for the different SBS matrices [13].

One key issue of these composites for electromechanical sensor development is the linearity between electrical resistivity and the strain. The GF can be tailored by changing CNT concentration or pre-strain  to the material, in order to obtain  sensors with tailored sensibility [13]. The gauge factor of polymer/CNT composites with different CNT type and polymer matrix can lie within a quite wide range, 0.74-50 [14-20]. The piezoresistivity depends on parameters related to CNT conductivity, surface characteristics and dispersion and polymer matrix, the GF being typically larger for filler concentrations in the composite around the percolation threshold [14, 20]. Piezoresistivity composites with thermoplastics or thermosetting polymer matrixes have been most often studied than elastomeric composites [15]. Epoxy composites with carbonaceous fillers show typically gauge factors between 3.4 to 4.3 [20]. Poly(methyl methacrylate) and polycarbonate as matrix and CNT as fillers show higher gauge factors for ~ 0.6% of strain which are 3.5 times more sensitive than metallic strain gages [15].

Elastomeric silicon composite have been studied for pressure sensors [16] and electromechanical sensors based on polyurethane are being developed [15].

In the present work, CNT/SBS composites with different SBS morphologies, radial and linear, and with different filler contents were prepared by solvent casting in order to

study the influence of the carbon nanotubes in the electromechanical properties of the composite samples and to evaluate the performance of the composites for sensor applications. Four-point bending and uniaxial tensile mechanical tests were performed, while monitoring the variation of electrical resistance in composites samples.

## 4.2 Results and Discussion

Elastomeric materials are known for their outstanding deformation, that can reach ~1500 %, and it was observed that the incorporation of CNTs up to 8 wt% into the polymer matrix does not influence the maximum strain. On the other hand it is observed an increase of the initial modulus from ~1.5 MPa obtained for the SBS matrix up to 150 MPa for a CNT concentration of 8 wt% [13].

### 4.2.1 Morphological characterization

Dispersion and interaction between CNT and the SBS matrix are shown in the SEM images of different SBS matrix (C401, C411, C500 and C540) with 4 wt% of CNT in figure 4.1. Composite samples with higher loadings of CNT present similar dispersion patterns for all the SBS matrix.

C401 CNT/SBS with 4 wt% CNT



C411 CNT/SBS with 4 wt% CNT



C500 CNT/SBS with 4 wt% CNT



C540 CNT/SBS with 4 wt% CNT
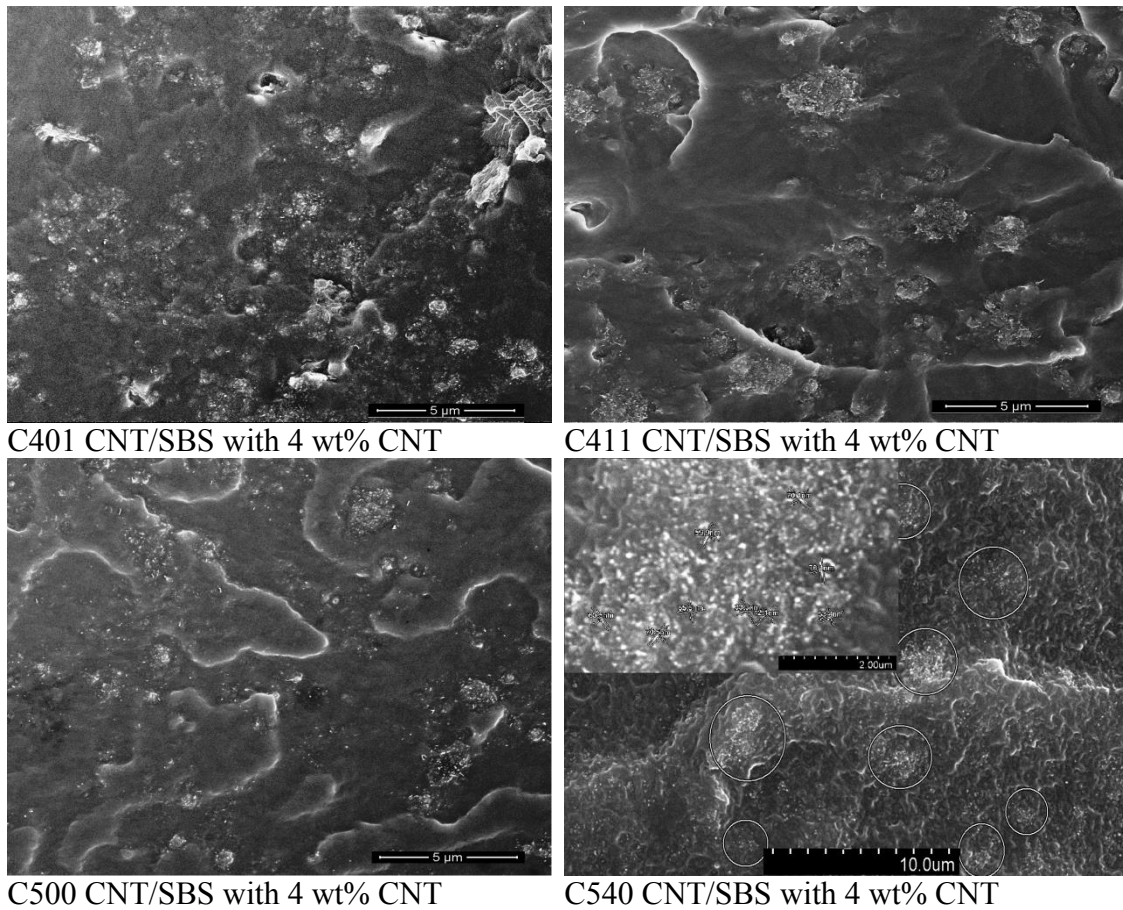
Figure 4.1 – SEM images for CNT/SBS composites with different SBS matrix (C401, C411, C500 and C540) filler loading of 4 wt% of pristine CNT.

CNT/SBS composites processed by solvent casting present a good cluster distribution of CNT for the different SBS matrix. CNT are agglomerated in clusters with ~1-2 μm in size for all composites. As it will be shown later, the SBS matrix does not has an important role in electrical conductivity network in composite samples, which correlated to the similar filler dispersion, results in overall similar electrical macroscopic response. It is also observed a good wetting between individual CNT and the SBS matrix (inset in figure 4.1 for the C540 CNT/SBS composite).

Electrical conductivity of composites depends on CNT distribution within the polymer matrix. It has been demonstrated that a distribution of well distributed small agglomerates or clusters is more important for achieving higher electrical conductivity [5, 17] than a good dispersion of individual fillers. The same is not the case for the mechanical properties [17]. Different parameters such as dispersion method and dispersion agent [18] and structural quality of carbon nanofillers [18] have influence in electrical properties of polymer/carbon composites. In the present case, nevertheless, it

is observed that the used polymer matrix does not influence the overall dispersion of the fillers.

Good wetting is observed SBS matrix and CNT in the composites as shown in figure 4.1, inset, and by the fact that during the electromechanical tests for large deformations up to 20% no degradation of the electromechanical cycles is observed (figure 4.2), indicating reversible electromechanical processes and therefore no detachment or irreversible reconfigurations of the filler network [13].

### 4.2.2 Mechanical hysteresis

The mechanical properties of SBS polymers, like initial modulus, maximum strain or hysteresis are key issues for their applications as electromechanical sensors, where mechanical properties play an important role in sensor response and reliability. The mechanical hysteresis is important to analyze reproducibility of stress-strain tests in sensor applications. Good linearity of electrical resistance depends on the mechanical properties of composites.

The mechanical hysteresis of these nanocomposites was characterized in stress-strain tests for ten cycles for several deformations levels of 5%, 10% and 20% (figure 4.2). It was observed that loading and unloading curves do not coincide during two successive cycles, given evidence of a mechanical hysteresis in these composites. The mechanical hysteresis decreases with increasing number of cycles in the composite, in particular for the first few cycles (figure 4.2A), and increases for increasing strain (figure 4.2B). For elastomeric matrices filled with carbon nanofillers, the mechanical hysteresis increases with the increment of nanofiller content in the composite, both in uniaxial tension and compression [19]. Initial stiffness (and initial modulus) and subsequent stretch-induced stiffening at larges strains were both found to increase with increasing filler content [13, 19].
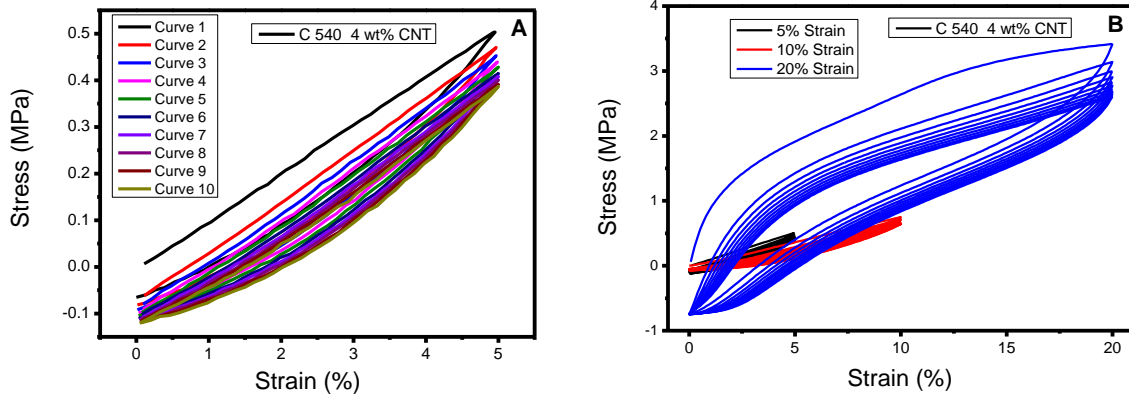
Figure 4.2 – Example of hysteresis for experimental stress-strain curves for composites SBS-C540 with 4 wt% CNT. A) with individual color for 10 curves for 5% of deformation and B) 10 cycles for 5%, 10% and 20% of deformation.

The hysteresis energy loss values are calculated by the area under the cycles in $J/m^3$ (figure 4.3) for the SBS copolymers. As mentioned, this value increases for increasing strain and decrease with increasing number of cycles for each composite.
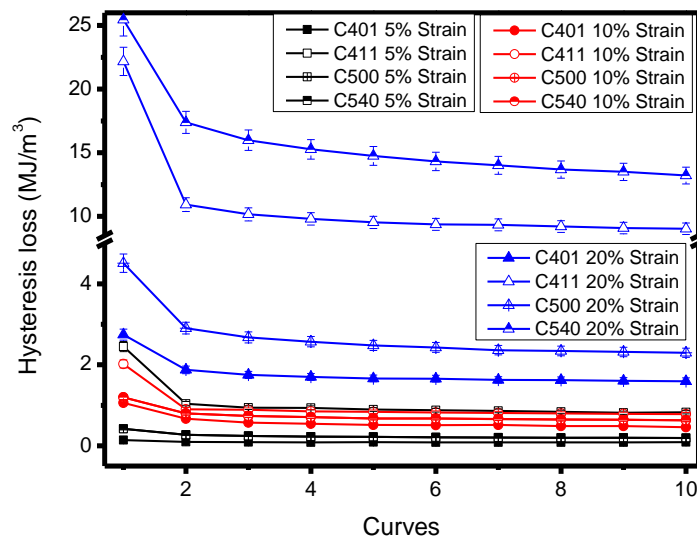


Figure 4.3 – Hysteresis for the different SBS copolymers as a function of strain during 10 cycles for 4 different matrixes and 5%, 10% and 20% of deformation.

Comparing the different ratios of butadiene/styrene in the polymer matrices, the larger hysteresis value is found for the harder copolymer (C540 with 40% of styrene), followed by C411 matrix for 20% of strain, as presented in figure 4.3. The copolymer with lower mechanical hysteresis is C401, the one with lower styrene content (20%). For copolymers with same styrene content (C411 and C500, with 30% of styrene), the larger hysteresis is for C411, as the radial structure shows slower recovery dynamics than the linear one [13]. This behavior is related to the one observed for the initial

modulus, with higher values for matrices with more styrene, and for same values of styrene, the radial structure showing superior Young modulus values [13].

## 4.3  Electrical and Electromechanical response

Electrical measurements on CNT/SBS composite samples prepared with different SBS ratios and morphologies (table 2.2) and with several amounts of conductive filler show that the composite electrical conductivity is not strongly dependent on the matrix morphology or styrene/butadiene relative content (figure 4.4), the conductivity being nevertheless higher for the sample with less butadiene present in the sample and with linear morphology (C540). The percolation threshold is found to occur at around 1wt% CNT concentration present in the material. The sample with less styrene and with radial structure (C401) showed a smaller value of electrical conductivity until percolation threshold, when compared to the other samples.
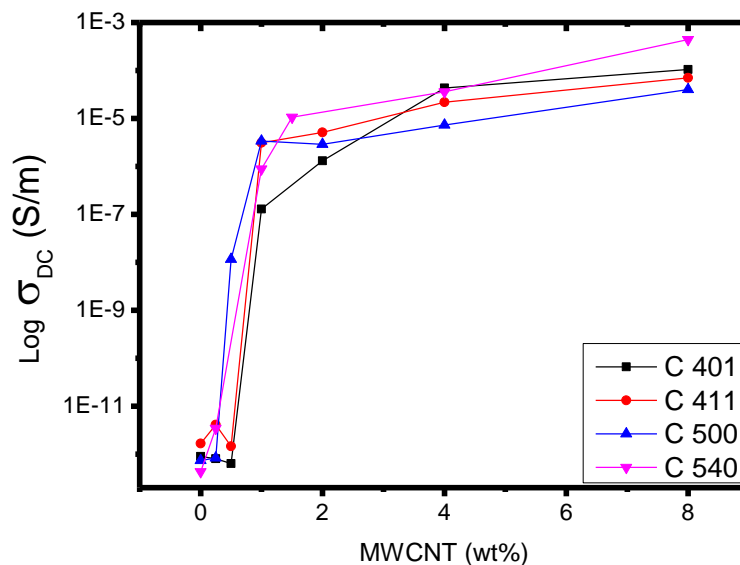


Figure 4.4 – Log of electrical conductivity as a function of CNT content for the four different matrices, C401, C411, C500 and C540.

Composites near electrical percolation threshold generally show the largest variation of the electrical resistance with the applied mechanical deformation [20, 21]. In the present case of these elastomeric materials, the GF is also large around the percolation threshold, but due to the small filler content at the threshold, just small deformations (below 5%) can be applied before a strong decrease of the electrical conductivity

occurred due to the strong decrease of the local concentration of the filler, which destroys the conductive path between fillers [22, 23]. Therefore, for large deformation sensors, composites with larger concentration of CNT, above the percolation threshold, have to be considered in order to undergo strains up to $\varepsilon \sim 50\%$ with linear variation of the electrical resistance and with resistance values compatible with the development of strain sensors [13]. Thus, we use in further electromechanical measurements, composites samples with 4 wt% CNT to analyze GF for larges deformation.

### 4.3.1 Electromechanical response under uniaxial stress

Electromechanical response was measured under uniaxial stress and in 4-point-bending tests. In uniaxial tensile tests, the mechanical measurements were performed with the composite with filler content of 4 wt% CNT (figure 4.5A) and the GF was determined by the variation of resistance during the loading and unloading cycles (figure 4.5A), according to equations 2.3 and 2.4. In figure 4.5B are shown different data points to demonstrate how the GF (relation between the variations of the electrical resistance with the mechanical deformation) was obtained for the different composite samples through the respective linear fits. The higher is the slope in linear fit, the larger is the GF value for composites, i.e., increasing their sensibility.

It was observed that the electrical response of the CNT/SBS composites follows linearly the mechanical deformation, both during the loading and the unloading cycles (figure 4.5A). Moreover, it is possible to observe that $\Delta R/R_0$ has a linear trend and fits well with $\Delta L/L_0$ in the data points for all cycles (figure 4.5a). In figure 4.5B, there are shown three different responses of the electrical resistance variation with mechanical strain of the SBS filled with 4 wt% of CNT and respective linear fits for different GF values. This demonstrates the different sensibility of the composites samples, related to the different test velocity or pre-strain applied during the measurements, as it will be discussed later. It is important to notice that the thermoplastic SBS elastomer composites fully recover the original properties after loading-unloading cycles at different pre-strains and experiments performed at different strain rates.
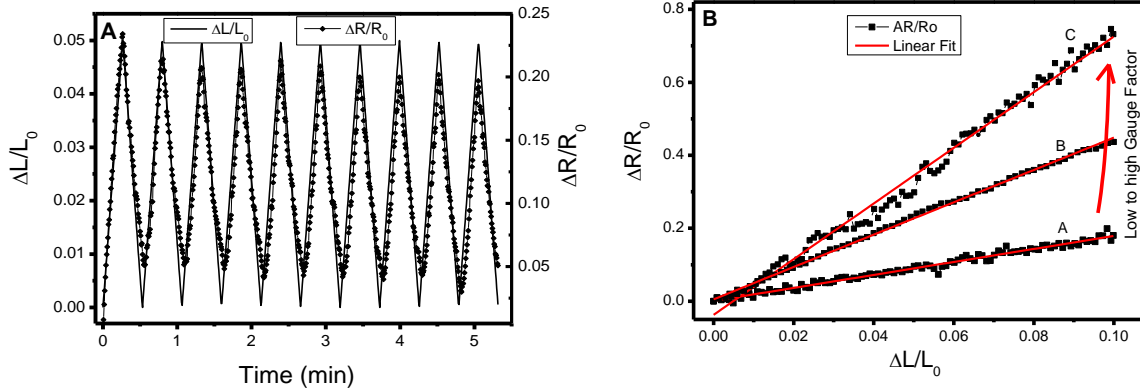
Figure 4.5 – A) Electromechanical measurements during uniaxial deformation (method 1) for the C411 elastomeric SBS matrix with 4 wt% CNT, obtained for a maximum strain of 5% and nominal strain-rate of 1 mm/min. B) $\Delta R/R_0$ vs $\Delta L/L_0$ and corresponding linear fit for the determination of Gauge Factor of composite samples with 4 wt% CNT within a C401 SBS matrix for A- 5%, B- 10% and C- 20% of strain.

The electromechanical response for uniaxial stress method was analyzed for C401, C411, C500 and C540 SBS matrices with 4 wt% CNT as a function of the deformation, between 5% to 20%. C540 SBS matrix was also pre-stressed (until 30%) and deformed until a maximum deformation of 20%, and for several velocities at four different deformations (5%, 10%, 20% and 50%). The GF was determined applying equation 2.3. The four different elastomeric matrices have distinct behavior for GF at different deformations (at a velocity of v =2 mm/min) as shown in figure 4.6A. SBS matrix with a linear structure (C540) showed a higher GF than the SBS samples with a radial morphology. This is influenced by the mechanical hysteresis, with radial structure showing slower recovery dynamics than the linear ones [13]. For the same butadiene/styrene ratios, the GF is higher for the SBS linear matrix structures, as observed by comparison of the C500 and C411 composite samples. C500 CNT/SBS composites with 4 wt% filler content show a GF≈ 9, whereas the GF for composites with C411 SBS matrix have a GF less than GF< 4 for all strains (figure 4.6A). Moreover, the amount of butadiene present in the composites influences the GF, which is lower for the samples with more butadiene in their composition (table 2.2), for strains up to 10% with C401 (low styrene content matrix) CNT/SBS shows a higher GF than for the SBS samples with 30% of butadiene at 20% of strain. C401, C411 and C500 SBS matrix have a lower GF value (GF < 10) and distinct behavior with deformation. Composite with higher amount of styrene with linear structure (C540 with 40% styrene) has the highest value of GF and an increase of the GF was observed with increasing deformation (up until a maximum of 20%). This GF behavior is related to the

mechanical response of the these composites, as the initial modulus is around 5 times higher for the C540 than for other elastomeric matrixes filled with 4 wt% CNT [13]. The results show that polymer morphology and styrene/butadiene ratio influence the mechanical behavior of the matrix.

Due to the nanoscale dimensions of the carbon nanotubes, the interfacial regions that surround the filler are also in nanometer dimensions and the applied load can be easily transferred from the matrix to CNTs network. There are three synergizing aspects of interactions in carbon nanotube based nanocomposites, i.e., polymer-nanotube interaction, nanotube-nanotube and intra polymer interactions. Despite an increase interest in carbon nanotube filled polymer composites, the mechanism and magnitude of load transfer between the polymer matrices and the filler are still unclear [24]. In the present work, it seems that the CNTs present in the SBS matrix with radial structure are poorly wrapped by elastomeric amorphous chains, and when a mechanical load is applied to such a nanocomposite, and due to the nature of such anisotropic structure, polymer chains will not aligned easily in the direction of the mechanical loading and consequently, the conductive filler will suffer minor spatial rearrangements due to the poor wrapping between the filler and the matrix, and the change in the electrical resistance will be smaller, giving origin to reduced GF values. On the other hand, it seems that for the linear structure, the SBS amorphous chains wrapped with more contact points the CNTs, and when the mechanical load was applied, the chains are more easily aligned in the stretch direction, giving origin to a local decrease of the concentration of CNT by increasing the distance between the each neighbor filler. Consequently there is an increment on the electrical response of the material, contributing for the highest GF values found in the samples with linear structure when compared to the radial ones.

Small values of uniaxial stretching do not change the CNT and consequently, the effect on the electrical response is not influenced in a strong manner by this type of loading [23]. The average number of electrical paths seems similar for stretching until 3% [23] and CNT displacements would not be sufficiently large to break the percolations network [23]. On the other hand, larger strains induce reorientation of the filler in the direction of the applied mechanical load, and therefore, stronger variations in the electrical properties of the composites [25].
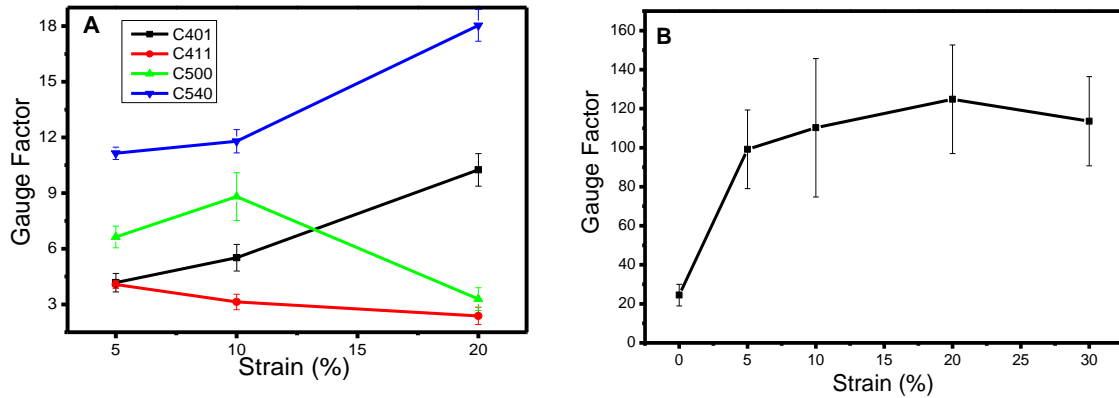
Figure 4.6 – Values of GF of method 1 for different matrices of composites CNT/SBS with 4 wt% CNT at v= 2 mm/min without pre-stress and b) values of the GF for C540 composite at deformation of ε= 20% and test velocity of v = 2 mm/min for different pre-stresses strains.

In order to maximize the GF response of the elastomeric nanocomposites, a pre-stress from until 30% of strain, was performed to the C540 matrix. In these measurements, the composites were pre-stressed at 30% of initial distance between jaws and then the electromechanical tests were performed at 20% of deformation at 2 mm/min. The obtained results shows an increase of the GF value with a small increase of the pre-stress of 5% of strain from GF of ~20 up to GF of ~100, and remaining almost constant for higher pre-stress values (Figure 4.6B). Pre-stretching will cause both an increase of the apparent initial modulus and a reorientation of the fillers to an unstable configuration. In this situation, a further increase of the stretching will lead both to larger internal stresses [26] and to larger variations on the CNT conductive network, leading to larger values of the GF. Theoretical predictions showed that aligned CNT make composites more sensitive (increase GF value) that non-aligned CNT [23] and this can be important to increase GF for higher deformations, if the CNTs align with the applied deformation during the electromechanical tests.

Proceeding on the searchof maximizing the electromechanical properties of SBS matrix composites, an effort was devoted to the understanding of the influence of the test velocity during mechanical solicitation on the GF values. This study was performed for several deformations of 5%, 10%, 20% and 50% at different velocities of 1 to 50 mm/min for the C540 SBS matrix filled with 4 wt% of CNT. The results are presented in figure 4.7. The gauge factor increase with velocity until 20 mm/min, decreasing for higher velocities (50 mm/min) for low strains analyzed. For the minimum and maximum velocities (5 and 50 mm/min) the behavior of GF is constant and the values are similar, being around 15 to 30 as function of the strain until 50%. For intermediate

velocities, GF shows higher values at low strains (up until 10%) decreasing thereafter down to the values of others velocities. The obtained results suggest that an applied pre-strain improves the electromechanical response of the nanocomposites. It seems that an increase of the GF values occurs, but this increase is especially stronger for the smaller pre-strain values and for intermediated deformation velocities. For smaller pre-stress, the alignment of the CNTs will be poor and their orientation will be similar to the obtained after processing and when a load is applied, especially at smaller velocities, the mechanical load transferred from the polymer matrix to the filler is not enough to promote alignment of the conductive filler in the loading direction due to the poor wrapping of the polymer amorphous chains on the CNT. Consequently the electrical response of the nanocomposites will be smaller. On the other hand, for higher deformation rates, the mechanical load is too fast and, due to the week bonding between the polymer chains and the conductive filler that only occurs at nanoscale points in the CNT, such higher mechanical solicitation will quickly destroy the bonds between the filler and the matrix. Consequently the polymer chains will align in the direction of the applied stress, but the CNTs only not suffer the same mechanical load and the electrical response will be smaller, being the effect similar to the one observed for the strain rate of 5 mm/min (figure 4.7). Further, when the strain was applied at 10 and 20 mm/min, the rate was not enough to destroy the bonds between the matrix and the conductive filler. Consequently the CNTs can follow the direction of the mechanical solicitation, contributing for higher alignment and local decrease of filler concentration, which promotes an increase of the GF values obtained (figure 4.7). The results for this SBS composite  show that the variations on the electrical resistance follows the stress-strain tests at a velocity of around 10mm/min, and denoting a major difficulty on this match for higher velocities.
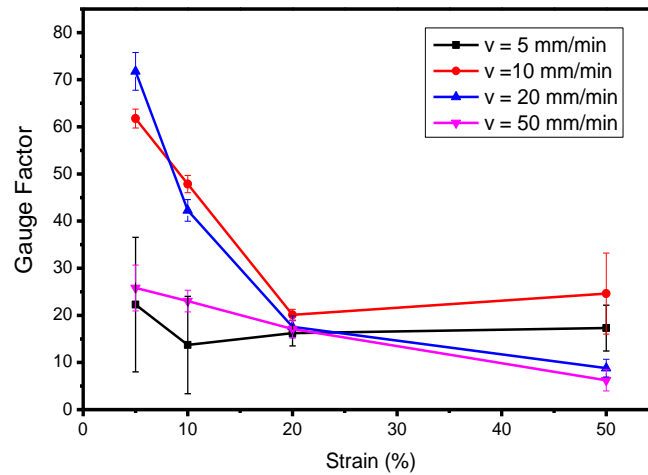
Figure 4.7 – GF values for C540 SBS with 4 wt% CNT at different strains (5%, 10%, 20% and 50%) for velocities of 5, 10, 20 and 50 mm/min.

### 4.3.2 Electromechanical response under 4-point-bending

Typical results from the 4-point-bending experiments are show in figure 4.8, where four loading-unloading cycles are shown for the C411 composite with 4 wt% of CNT content. The variation of electrical resistance follows linearly the mechanical deformation over time. The deformation in this method 2 is quite different from those applied in method 1: the applied force is parallel to the cross-section of the composite sample unlike the method 1 that is normal to the cross section. This implies a different stress and strain distribution through the cross section of the loaded samples. In method 1, the stress is uniform through the cross section, whilst in method 2 there is a non-uniform stress distribution along the cross section, which is maximum at the outer surfaces of the specimen (being the surface where load is applied in a compressive state, and in a tensile in the opposed surface).
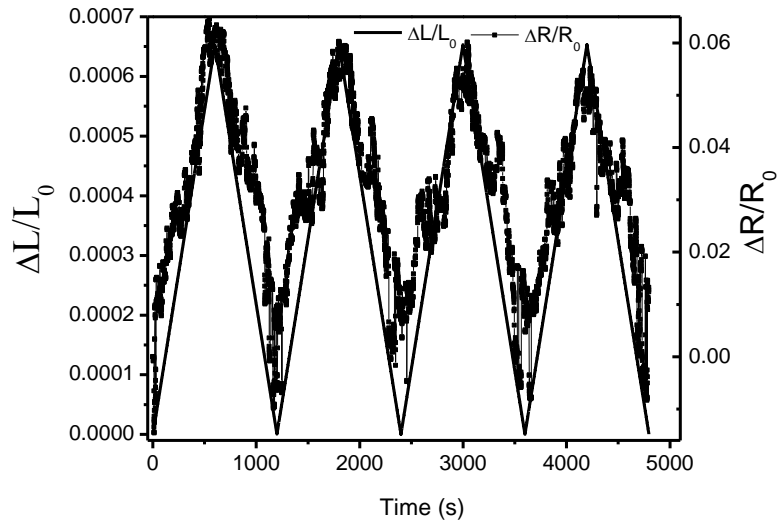
Figure 4.8 – Electromechanical measurements with 4-point-bending mechanical solicitation (method 2) for the C411 elastomeric SBS matrix with 4 wt% CNT. Maximum deformation: 1mm; deformation velocity: 0.1 mm/min.

The GF obtained for the different SBS sample composites with 4 wt% CNT for different maximum deformations and deformation velocities are shown in figures 4.9A and 4.9B, respectively. It was observed that the composite samples with SBS radial structure show higher GF values (C401 and C411), and the ones with large content of butadiene (C401 with 80%) present the highest GF values (figure 4.9A). The GF for SBS C540 varies between 40 and 100 for several strain levels. The remaining composites have GF values lower than 30. In general, the samples with linear structure (C500 and C540) present similar electromechanical response, and the composite samples with large butadiene amount present in their composition have the highest GF values. An increase of the deformation velocity reveals that the amount of butadiene phase in the elastomeric composition is responsible for the highest GF values found (figure 4.9B). The values of GF as function of velocity are practically constant up to until 50 mm/min for the SBS matrices C411, C500 and C540 and are similar to the values of the GF obtained for varying strains. For the C401 SBS matrix, the GF values are around 100 and they increase for lower velocity up to a maximum value, similar to the results obtained for method 1, and decrease thereafter with the increase of the velocity until 50 mm/min. This electromechanical behavior is related to the viscoelastic nature of the polymer matrix and therefore to the mechanical time response [20].

The two different electromechanical methods (tensile and bending) show how important is the SBS matrix in the electromechanical of the nanocomposites. In uniaxial uniform stress (tensile loading), the SBS matrix with the lowest butadiene content shows a

higher GF value, as well as the highest mechanical properties (namely, the initial modulus) . In 4-point-bending the SBS matrix with higher GF values is that with the largest butadiene content.
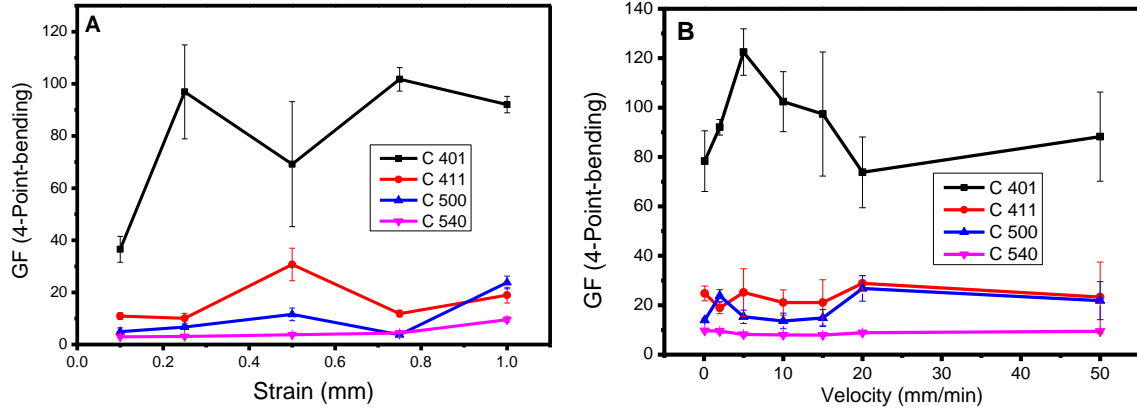


Figure 4.9- A) GF for 4-point-bending as a function of strain up to 1 mm and B) GF as a function of velocity up to 50 mm/min for C401, C411, C500 and C540 SBS matrix composites with 4 wt% CNT.

There are two different effects contributing to the GF values: the intrinsic electromechanical effect and the geometric variation effect (equation 2.4). For this type of materials, the Poisson ratio goes from 0.35 to 0.5 [27-29], which means that the geometric variation effect contribution to GF varies among 1.7 to 2. Metallic strain gauges show similar GF of ~2 for strains smaller than 4%, which are ascribed to geometrical variations [30, 31]. In elastomeric composites, the piezoresistivity values up to ~2 are also mostly due to geometrical contributions, being the larger contributions to the GF due to electrical resistance variation of network fillers in composites and therefore to intrinsic contributions. Figure 4.9 shows that for concentrations of the 4 wt% CNT, the geometric variation factor can be dominant for small deformations and C500 or C540 SBS matrix, but for larger deformations the intrinsic effect due to strain-induced modification of the conductive network is dominant. For C401 CNT/SBS composite samples, the intrinsic electromechanical effect is dominant for several deformations and velocity stress-strain tests.

## 4.4 Conclusions

The SBS tri-block copolymers have excellent properties for piezoresistivity sensors at large deformations when mixed with carbon nanotubes at percolation threshold or above, offering electrical properties to the isolator matrixes. The electrical percolation threshold is less than 1wt% for all different matrices of SBS composites and it has a similar behavior for electrical conductivity.

Electrical and mechanical properties generally depend on CNT distribution on the polymer matrix. In the present case, SEM images show a similar small cluster distribution of CNT in all SBS matrixes, which results in similar high electrical conductivity for all studied polymer/carbon nanotubes matrixes.

The nanocomposites with 4 wt% CNT can be used as sensors for larges deformations, up to 50% of deformation, with high GF values.

For uniaxial stress method, the SBS matrix that has the highest GF is C540 (linear copolymer architecture and lowest content of butadiene), which increase with deformation. For enhanced sensibility and GF values, to these composites is applied an initial pre-strain until 30%. Applying a pre-strain of 5% or higher, the GF increase for values around 100 for the C540 CNT/SBS composite with 4 wt% CNT. The gain in sensibility of the composite is huge with the application of pre-stress and can be as high as GF = 120. The GF as function of test velocity increases up to 10mm/min, and have a distinct behavior for the superior velocities for the different matrices. Thus, the maximum GF is obtained using a pre-strain (5% or 10%), velocity of around 10 mm/min. These CNT/SBS nanocomposites can be used in sensor for larger deformation, up to 50% of strain, with a high GF.

For method 2 (bending) the behavior of the GF for several velocities and deformations for all SBS matrices was measured. As function of deformation, the matrix that shows the highest values of GF is C401 (copolymer with a radial architecture, and high content of butadiene) and the values ranging between 40 < GF < 100. For the other matrices GF values are lower than 30. As function of the test velocity, the behavior is similar to the behavior of strain and it is varying from 80 < GF < 120 for C401 SBS, and for others matrices the GF shows similar values as function of the applied strain.

These composites present also a mechanical hysteresis that increase with strain and its higher for the initial loading cycles, decreasing in the course of the cyclic loading. Mechanical hysteresis is higher for the matrices with high content of styrene.

Overall, this investigation demonstrates the suitability of these materials for the development of large deformation electromechanical sensors.

## References

[1]     Zhi Feng W, Pei W, Xiong Ying Y and Bo J 2009 Processing and modeling of multi-walled carbon nanotube/styrene-butadiene-styrene (SBS) composites for force sensing. In: *Nanotechnology, 2009. IEEE-NANO 2009. 9th IEEE Conference on,* pp 756-7

[2]     Pedroni L G, Soto-Oviedo M A, Rosolen J M, Felisberti M I and Nogueira A F 2009 Conductivity and mechanical properties of composites based on MWCNTs and styrene-butadiene-styrene block™ copolymers *Journal of Applied Polymer Science* 112 3241-8

[3]     Wang P, Geng S and Ding T 2010 Effects of carboxyl radical on electrical resistance of multi-walled carbon nanotube filled silicone rubber composite under pressure *Composites Science and Technology* 70 1571-3

[4]     Oliva-Avilés A I, Avilés F and Sosa V 2011 Electrical and piezoresistive properties of multi-walled carbon nanotube/polymer composite films aligned by an electric field *Carbon* 49 2989-97

[5]     Lorenz H, Fritzsche J, Das A, Stöckelhuber K W, Jurk R, Heinrich G and Klüppel M 2009 Advanced elastomer nano-composites based on CNT-hybrid filler systems *Composites Science and Technology* 69 2135-43

[6]     De Falco A, Goyanes S, Rubiolo G H, Mondragon I and Marzocca A 2007 Carbon nanotubes as reinforcement of styrene–butadiene rubber *Applied Surface Science* 254 262-5

[7]     Liu Y-T, Xie X-M and Ye X-Y 2011 High-concentration organic solutions of poly(styrene-co-butadiene-co-styrene)-modified graphene sheets exfoliated from graphite *Carbon* 49 3529-37

[8]     Das A, Stöckelhuber K W, Jurk R, Saphiannikova M, Fritzsche J, Lorenz H, Klüppel M and Heinrich G 2008 Modified and unmodified multiwalled carbon nanotubes in high performance solution-styrene–butadiene and butadiene rubber blends *Polymer* 49 5276-83

[9]     Wu J-H, Li C-H, Wu Y-T, Leu M-T and Tsai Y 2010 Thermal resistance and dynamic damping properties of poly (styrene–butadiene–styrene)/thermoplastic polyurethane composites elastomer material *Composites Science and Technology* 70 1258-64

[10]    Munteanu S B, Brebu M and Vasile C 2005 Thermal and thermo-oxidative behaviour of butadiene–styrene copolymers with different architectures *Polymer Degradation and Stability* 89 501-12

[11]    Ocando C, Tercjak A and Mondragon I 2010 Nanostructured systems based on SBS epoxidized triblock copolymers and well-dispersed alumina/epoxy matrix composites *Composites Science and Technology* 70 1106-12

[12]    Li C, Thostenson E T and Chou T-W 2008 Sensors and actuators based on carbon nanotubes and their composites: A review *Composites Science and Technology* 68 1227-49

[13]    Costa P, Silva J, Sencadas V, Simoes R, Viana J C and Lanceros-Méndez S 2012 Mechanical, electrical and electro-mechanical properties of thermoplastic elastomer styrene-butadiene-styrene/multiwall carbon nanotubes composites *Journal of Materials Science* 1172-9

[14]    Wang Z and Ye X 2013 A numerical investigation on piezoresistive behaviour of carbon nanotube/polymer composites: Mechanism and optimizing principle *Nanotechnology* 24

[15]    Bautista-Quijano J R, Avilés F and Cauich-Rodriguez J V 2013 Sensing of large strain using multiwall carbon nanotube/segmented polyurethane composites *Journal of Applied Polymer Science* 130 375–382

[16]    Wang L, Wang X and Li Y 2012 Relation between repeated uniaxial compressive pressure and electrical resistance of carbon nanotube filled silicone rubber composite *Composites Part A: Applied Science and Manufacturing* 43 268-74

[17]    Cardoso P, Silva J, Klosterman D, Covas J A, van Hattum F W J, Simoes R and Lanceros-Mendez S 2012 The role of disorder on the AC and DC electrical conductivity of vapour grown carbon nanofibre/epoxy composites *Composites Science and Technology* 72 243-7

[18]    Tsuchiya K, Sakai A, Nagaoka T, Uchida K, Furukawa T and Yajima H 2011 High electrical performance of carbon nanotubes/rubber composites with low percolation threshold prepared with a rotation–revolution mixing technique *Composites Science and Technology* 71 1098-104

[19]    Cantournet S, Boyce M C and Tsou A H 2007 Micromechanics and macromechanics of carbon nanotube-enhanced elastomers *Journal of the Mechanics and Physics of Solids* 55 1321-39

[20]    Ferreira A, Cardoso P, Klosterman D, Covas J A, van Hattum F W J, Vaz F and Lanceros-Mendez S 2012 Effect of filler dispersion on the electromechanical response of epoxy/vapor-grown carbon nanofiber composites *Smart Materials and Structures* 21 075008

[21]    Dawson J C and Adkins C J 1996 Conduction mechanisms in carbon-loaded composites *Journal of Physics: Condensed Matter* 8 8321

[22]    Silva J, Ribeiro S, Lanceros-Mendez S and Simões R 2011 The influence of matrix mediated hopping conductivity, filler concentration, aspect ratio and orientation on the electrical response of carbon nanotube/polymer nanocomposites *Composites Science and Technology* 71 643-6

[23]    Theodosiou T C and Saravanos D A 2010 Numerical investigation of mechanisms affecting the piezoresistive properties of CNT-doped polymers using multi-scale models *Composites Science and Technology* 70 1312-20

[24]    Bikiaris D 2010 Microstructure and Properties of Polypropylene/Carbon Nanotube Nanocomposites *Materials* 3 2884-946

[25]    Jiang Y and Fan H 2013 A micromechanics model for predicting the stress–strain relations of filled elastomers *Computational Materials Science* 67 104-8

[26]    Grimaldi C, Ryser P and Strassler S 2000 Gauge factor of thick-film resistors: Outcomes of the variable-range-hopping model *Journal of Applied Physics* 88 4164-9

[27]    Buckley C P, Prisacariu C and Martin C 2010 Elasticity and inelasticity of thermoplastic polyurethane elastomers: Sensitivity to chemical and physical structure *Polymer* 51 3213-24

[28]    Motamedi M, Eskandari M and Yeganeh M 2012 Effect of straight and wavy carbon nanotube on the reinforcement modulus in nonlinear elastic matrix nanocomposites *Materials & Design* 34 603-8

[29]    Aoyama T, Carlos A J, Saito H, Inoue T and Niitsu Y 1999 Strain recovery mechanism of PBT/rubber thermoplastic elastomer *Polymer* 40 3657-63

[30]    Wichmann M H G, Buschhorn S T, Gehrmann J and Schulte K 2009 Piezoresistive response of epoxy composites with carbon nanoparticles under tensile load *Physical Review B* 80 245437

[31]    Cao C L, Hu C G, Xiong Y F, Han X Y, Xi Y and Miao J 2007 Temperature dependent piezoresistive effect of multi-walled carbon nanotube films *Diamond and Related Materials* 16 388-92

# Chapter 5. Effect of carbon nanotube type and functionalization on the electrical, thermal, mechanical and electromechanical properties of carbon nanotube/styrene-butadiene-styrene composites

### Abstract

Thermoplastic elastomer tri-block copolymer, namely styrene-butadiene-styrene (SBS) composites filled with carbon nanotubes (CNT) are characterized with the main goal of obtaining electromechanical composites suitable for large deformation sensor applications. CNT/SBS composites with different filler contents and filler functionalization are studied by morphological, thermal, mechanical and electrical analyses. It is shown that the different dispersion levels of CNT in the SBS matrix are achieved for pristine or functionalized CNT with strong influence in the electrical properties of the composites. In particular covalently functionalized CNTs show percolation thresholds higher than 8 wt% whereas pristine CNT show percolation threshold smaller than 1 wt%. On the other hand, CNT functionalization does not alter the conduction mechanism which is related to hopping between the CNT for concentrations higher than the percolation threshold.

Pristine single and multiwall CNT within the SBS matrix allow the preparation of composites with electromechanical properties appropriate for strain sensors for deformations up to 5% of strain, the gauge factor varying between 2 and 8. Composites close to the percolation threshold show larger values of the gauge factor.

This chapter is based on a paper, with same title, submitted to Carbon.

Effect of carbon nanotube type and functionalization on the electrical, thermal, mechanical and electromechanical properties of carbon nanotube/styrene-butadiene-styrene composites

## 5.1 Introduction

Composite materials research in order to tailoring material properties for novel applications has resulted in important advancements in materials science and engineering. In particular, the use of carbon nanoallotropes as fillers in polymer matrices resulted in applications in the areas of sensors, relying on the electrical properties of the carbon nanoallotropes [1, 2], low weight aerospace structural materials [1], optoelectronics [3], antistatic protection [4, 5], capacitors [4] and electromagnetic interference shielding materials [4, 5], among others.

Thermoplastic elastomers (TPE) are an important class of polymers that combine the mechanical properties of rubbers (e.g., high deformation materials) with the processability and recyclability of thermoplastics [6]. Tri-block copolymer poly(styrene-b-butadiene-b-styrene) (SBS) is a TPE known for its microphase separation into soft and hard domains, including spherical, cylindrical, gyroid and lamellar morphologies [7]. Tailoring the molecular architecture and the morphology of SBS block copolymers offers the possibility to tune the mechanical properties of the materials from thermoplastic elastomers to tough thermoplastics [7]. This requires a detailed understanding of the interrelations between the molecular architecture, the microphase separated morphology, the thermal and mechanical history and the resulting mechanical behavior [7]. SBS was first industrialized as a thermoplastic elastomer of styrene via anionic polymerization [7]. It did not find wide use in biomedical applications due to the biostability problem of the double bonds in the elastomeric block. However, after the entire saturation of the butadiene segments in SBS, the obtained poly (styrene-b-(ethylene-co-butylene)-b-styrene) (SEBS) shows a better oxidative stability [7], allowing biomedical applications such as medical gloves, transfusion bags, catheters, ureteral stents, microfluidic devices and DNA chips [7].

SBS can be manufactured by solvent casting using solvents such as toluene [8], ethanol and acetone [9], or by melt flow processes such as extrusion [10, 11]. It can be also used without vulcanization [12] which is an advantage as there is no degradation of the mechanical and electrical properties of the composites obtained from this copolymer [12]. The excellent mechanical properties of SBS such as its high deformation (can be larger than 1000% [8]) and the value of initial modulus depend on the styrene/butadiene ratio and copolymer architecture. SBS has two glass transition temperatures ($T_g$) due to the distinct $T_g$ of poly-butadiene (PB), around -80ºC, and poly-styrene (PS), around

+80 ºC [13-15]. This copolymer has a good thermal stability and its degradation temperature is around 230 ºC for PB and 430 ºC for PS [16], the incorporation of carbon nanoallotropes not inducing major variations on the thermal properties of the SBS matrix [16].

SBS is an interesting material for the development of force sensors for robotic and industrial automation [17] in order to replace silicones-based sensors that are not capable of sustaining large deformations and sudden impacts [17]. For these and related applications, the TPE insulator matrix needs conductive nanofillers for modifying its electrical properties. Carbon nanoallotropes have been studied as suitable fillers for the development of polymeric matrix composites. Carbon black, carbon nanofibers and carbon nanotubes have been investigated for the development of composites with TPE matrices in order to tune mechanical, electrical or thermal properties for specific applications as antistatic devices [4, 18, 19], electrostatic discharge [14, 18, 20], pressure [14, 18] or large deformation sensors [21-23] and also for better understanding of the matrix/filler interactions in order to achieve tuned composite properties [9, 24, 25]. From the different carbon nanoallotropes, CNT allow the lowest electrical percolation [22] thresholds in composites due to the high aspect ratio and lower defects [4, 9, 26]. Differences in the CNT characteristics strongly affect the overall performance of the composites [4] and, in particular,  the functionalization of the CNT surface is commonly used to tailor composite response and polymer/CNT compatibility and dispersion [9, 25]. Chemical functionalization is based on the covalent linkage of functional entities onto CNT surfaces [27]. It can be performed at the termini or the sidewalls of CNT. Direct covalent sidewall functionalization is associated to a change of hybridization from $sp^2$ to $sp^3$ and simultaneous loss of the $\pi$-conjugation system on the graphene layer [27]. Non-covalent functionalization is other method for tuning the interfacial properties of CNT where a suspension of CNT in the presence of polymers leads to the wrapping of the polymer around the CNT to form supermolecular complexes of CNT [27]. The polymer wrapping process is achieved through van der Waals interactions and $\pi$- $\pi$ stacking between CNTs and polymer chains [27]. Together with polymers, surfactants have also been employed to functionalize CNT [27].

The preparation method is also important to determine the properties of composites, in particular due to its effect on filler dispersion and orientation (in the case of high aspect ratio nanofillers) within the polymer matrix [9, 28]. Composite materials prepared by

solvent casting generally show lower electrical percolation thresholds and homogeneous dispersion of CNT than extruded composites [14, 29].

All together it is recognized that the addition of CNT into an insulator matrix allows to tune the electrical and mechanical properties of the composites to suit specific applications as pressure or deformation sensors [30, 31]. Using a TPE matrices, this sensors can be large deformation sensors, with deformations up to 20% [8]. This is an important fact due to the large interest of those sensors and the few material possibilities to develop them. The piezoresistivity, the variation of the electrical resistivity when a deformation is applied to a material, can be taken as advantage for the development of such sensors [30, 31] and, in the case of carbon nanofiller/polymer composites, this effect is mainly attributed to variations of the conductive network with strain due to loss of contact between the fillers, tunnelling or hopping effects in neighbouring fillers and/or conductivity variations due to the deformation of CNT [32-34]. These electromechanically active composites are characterized by a high electromechanical sensitivity [32] and can be used in applications such as strain sensors for structural health monitoring [24, 35], damage and fracture detection [36] and in biomechanical applications [37].

The electromechanical properties are determined by the mechanical and, mainly, by the electrical conductivity value and the electrical conductivity mechanism [30] within the composite. Further, the addition of CNT to the SBS matrix can also influence the overall conduction mechanism, i.e., with addtion of CNT to the composite the main contribution to the conduction mechanism can be ascribed to hopping or tunneling between CNT [34, 38].

This work aims at understanding how the different PB/PS ratio in the polymer matrix as well as the CNT characteristics, single - and multi-walled and functionalized, influences the mechanical, electrical and electromechanical properties of CNT/SBS composites.

## 5.2 Results and Discussion

### 5.2.1 Composites morphology and filler distribution

Characteristic SEM images for different SBS matrices, filler content and filler functionalization are shown in figure 5.1. SBS C401 (figure 5.1A) and C540 (figure 5.1B) polymer matrices filled with pristine nanotubes show a similar level of dispersion

with a well-defined cluster distribution with average cluster sizes of few micrometers in composites with 4 wt% CNT. Figures 5.1C and 5.1D show a better dispersion of the individual carbon nanotubes both for CF and NCF, respectively, for 1 wt% and 4 wt% functionalized composites. The improved dispersion of the nanotubes in the SBS matrix, is attributed to the stronger interactions between SBS and the carbon nanotubes [39] and to the chemical affinity of the styrene functional groups of the CNTs and the matrix.
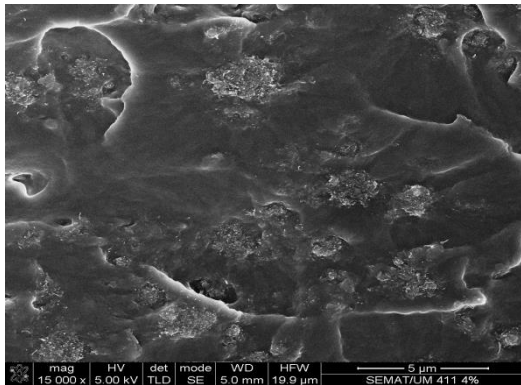


A) C401 matrix with 4 wt% of CNT.
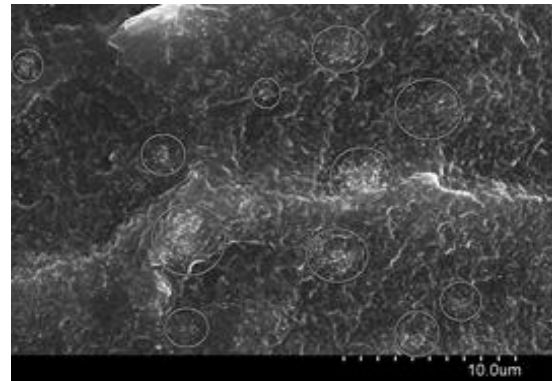


B) C540 matrix with 4 wt% of CNT.
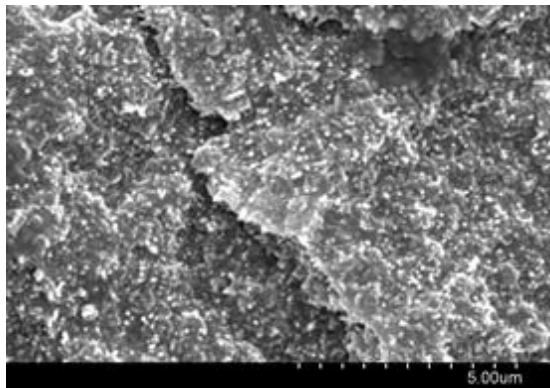


C) C540 matrix with 4 wt% CNT with covalent functionalization.
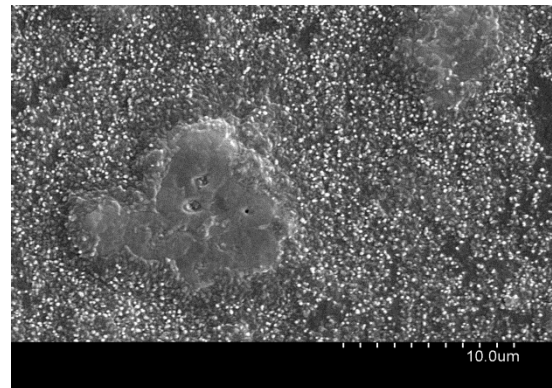


D) C540 matrix with 1 wt% CNT with non-covalent functionalization.

Figure 5.1 – SEM images for different SBS matrices composites, (SBS C401 (A) and C540 (B, C and D), CNT concentrations (1 and 4 wt%) with covalent or non-covalent functionalization of CNT.

It is concluded that the SBS matrix type is not relevant for the distribution of CNT within the composite, the composites C401 (figure 5.1A) and C540 (figure 5.1B) showing similar clusters size and distribution of CNT for a given CNT loading. Small agglomerates with a few micrometers of diameter can be found in both matrices, revealing that the ratio butadiene/styrene and the structure of the matrix does not have significant role in CNT distribution.

Functionalized covalent and non-covalent CNT (figure 5.1C and 5.1D) show better distribution for all studied concentrations, the distribution being similar for both functionalization strategies. No large clusters are found in these cases, but homogeneous distributions of the fillers all over the composites.

As it will be shown later, the different dispersion levels of the CNT within the SBS matrix has strong influence in the electrical and electromechanical properties of the composites.

The FTIR results are shown in figure 5.2. For the four different SBS matrices the characteristic bands of styrene and butadiene are identified (figure 5.2A). The peaks at the wave-number of 966 cm$^{-1}$, relative to the C-H *oop* bending of trans alkenes, and 699 cm$^{-1}$, relative to C-H *oop* bending in monoalkylated aromatics, were selected as the most suitable ones for analysis of polybutadiene (PB) and polystyrene (PS), respectively [40]. The styrene/butadiene ratio and structure (linear or radial) does not affect the characteristic peaks in SBS composites. In the same way, the filler type and content did not induce any change in the SBS matrix identifiable in the FTIR spectra (figure 4B) due to the filler inclusion. No new bonds attributable to CNT-matrix interactions are identified.
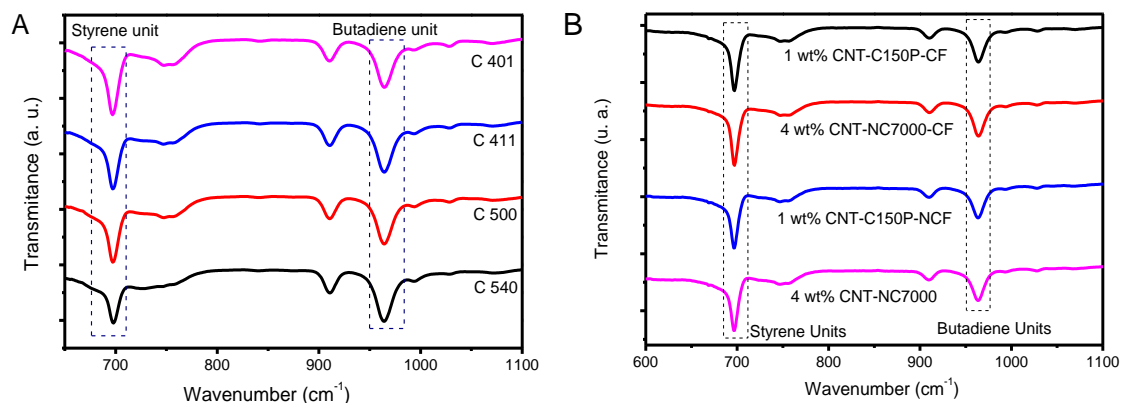


Figure 5.2 – FTIR spectra for pure SBS matrix and composites. A) Pure SBS matrixes (C401, C411, C500 and C540). B) C540 CNT/SBS for different CNT (1 or 4 wt%) and covalent or non-covalent CNT functionalization.

### 5.2.2 Thermal Properties

The thermal properties of the composites are measured using TGA and DSC in order to investigate variations of the thermal degradation and transition temperatures.

### 5.2.2.1 Thermal degradation

The thermogravimetric (TG) curves of the composites for the four different matrices, different CNT contents and functionalization is shown in Figure 5.3.

The thermal degradation behavior of the different matrices is similar (figure 5.3A). The temperature of maximum rate in the differential thermal gravimetry (DTG) increases with increasing nanotube content in the composites (figure 5.3B and 5.3D). Functionalized CNT/SBS composites also present similar behavior than pure SBS matrix and non-functionalized CNT composites.

A

B

C

D
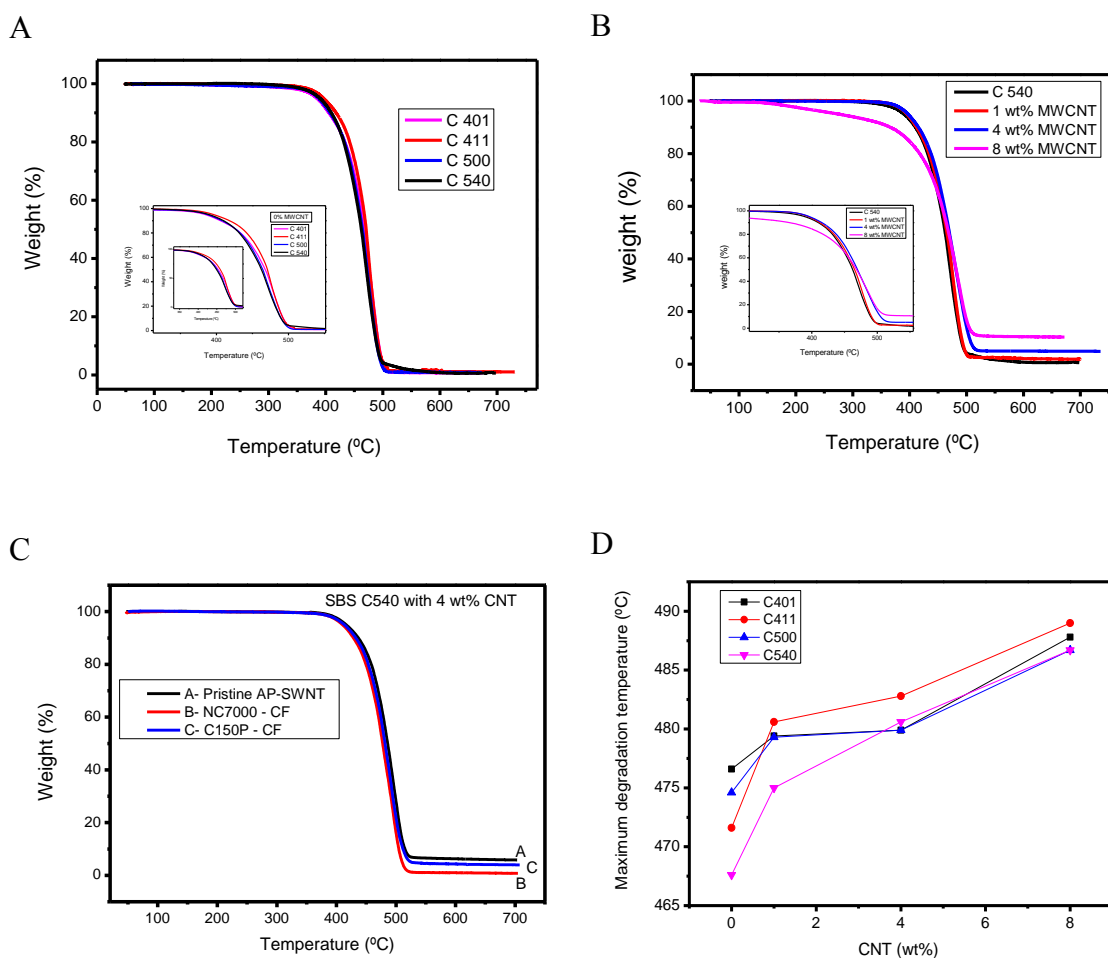


Figure 5.3 – Thermal degradation of CNT/SBS composites with multi-walled CNT C150P from Baytubes. A) Pure SBS matrixes (C401, C411, C500 and C540). B) Composite C 540 CNT/SBS for different CNT content. C) C540 CNT/SBS with 4% of CNT for several CNT types and functionalization. D) DTG for all composites as a function of CNT content.

CNT do not suffer degradation until 700 ºC, temperature at which the SBS matrix is completely degraded [39, 41]. The DTG occurs between 465-490 ºC for the different SBS matrices and multi-walled CNT C150P concentrations in the composites (figure 5.3A). The degradation temperature increases with increasing CNT content for all

polymer matrices (figure 5.3D), being the larger variation for the SBS C540 matrix with a $\Delta T = 19$ ºC with respect to the pure copolymer. The minimum variation of the degradation temperature was for the C401 SBS matrix, with a $\Delta T = 11$ ºC between the non-loaded and the 8 wt% CNT loaded composite (figure 5.3D). This increase in temperature is due to the interactions between CNT and SBS conferring larger thermal stability [39].

Functionalized carbon nanotubes in the composite do not change the thermal degradation behavior of the composites (figure 5.3C). The AP-SWNT pristine carbon nanotubes composites have a DTG at 496 ºC. Functionalized CNT have a similar DTG, around T = 488 ºC for both NC7000 and C150P nanotube type. For pristine C150P CNT the DTG is 481 ºC. The higher degradation  temperature for the AP-SWNT can be ascribed to the presence of metal impurities( between 30-40%) or to their higher graphitization due to they have been produced by arch-discharge; for covalent functionalized CNT, the increase in degradation temperature can be attributed to the individual CNT dispersion in the SBS matrix, instead of clusters dispersion in pristine composites, and a higher interaction energy in  the functionalization than in the pristine CNT bonds [39].

### 5.2.2.2   *Transition temperature*

The glass transition temperature (Tg) of composites was measured by DSC for the different SBS matrices and composites with 4 wt% CNT (C150P) (figure 5.4 A). SBS shows two different Tg ascribed to polybutadiene and polystyrene domains [42]. The glass transition of polybutadiene appears around 10 ºC for C540 SBS with 60% butadiene and between 15 ºC and 17 ºC for C401 with 80% butadiene, although SBS showing different structures. The polystyrene glass transition is less pronounced and appears around 70 ºC for all composites. It shows a less pronounced feature at Tg due to the lower styrene content in the SBS matrices.

A                                                    B
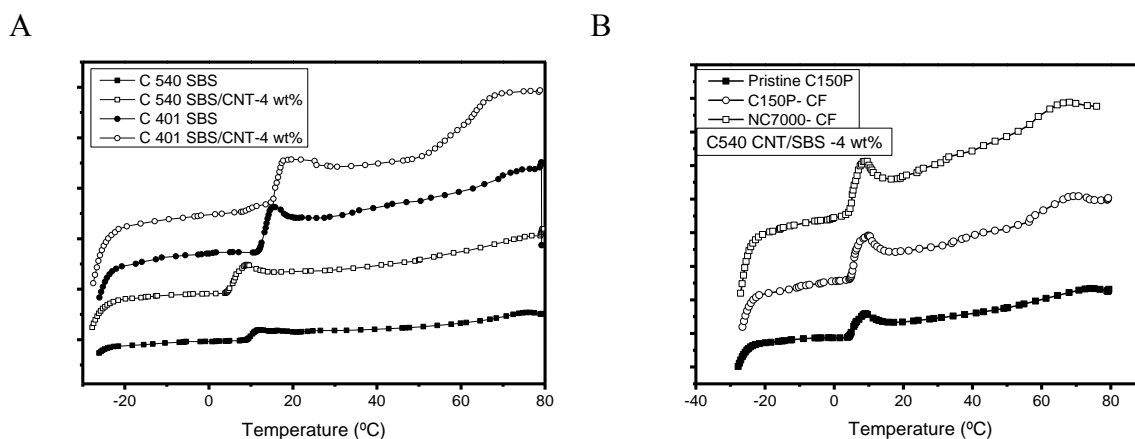


Figure 5.4 – DSC thermograms of the composites: A) Two different SBS matrixes (C401 and C540) and respective composites with 4 wt% CNT. B) Composites with 4 wt% CNT for different CNT and functionalization.

The incorporation of CNT into the SBS matrices seems to alter the Tg of PB in different ways. For SBS C401 with a radial structure, adding CNT leads to a slight increase of Tg of the polybutadiene component and therefore a more restrained macromolecular mobility of the soft segments. Conversely, adding CNT to SBS C540 with a linear structure the Tg of the PB regions decrease thus evidencing a higher mobility of the soft phase on the copolymer.

For the same SBS matrix (C540) and percentage of the loading of CNT (4 wt%), the glass transition temperature shows a similar behavior for all composites (figure 5.4B) independently of the nanotubes type and functionalization. Thus, the glass transition temperature depends on the SBS matrices and by the CNT. Do not depend of CNT with different properties, as single or multi-walled.

### 5.2.3 Mechanical Properties

The mechanical properties of the SBS composites are particularly interesting due the large deformations in comparison to common thermoplastics and thermo sets and low mechanical hysteresis [8].

Figure 5.5 shows the stress-strain curves with deformations up to 400% for composites with different CNT both without and with chemical functionalization. In general, the mechanical behavior is similar to that for the pure SBS matrix and it is similar for the different matrices [8]. For both pure SBS and composites large deformations around

1500% [8] can be achieved with yielding at of strains around ~3% (here yielding is refers to the point where there is a large increment of strain at almost constant load).
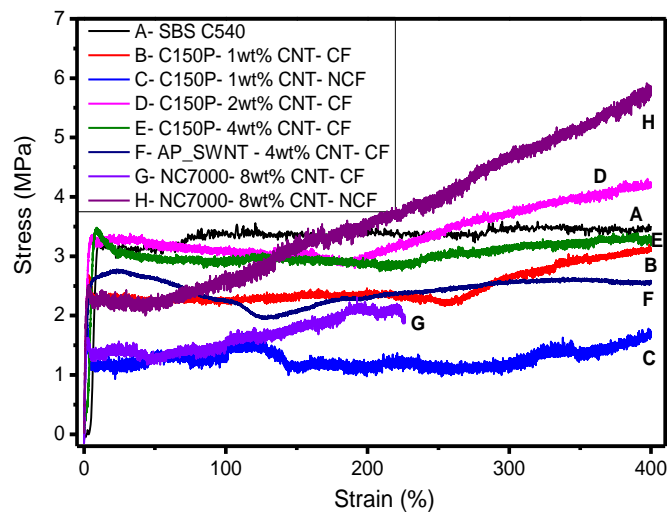


Figure 5.5- Mechanical properties of SBS C540 composites for several CNT contents and functionalizations.

The composites with pristine carbon nanotubes (C150P) show an increase of the initial modulus with increasing nanotube content in the composites (table 5.1). For neat SBS the value of the initial modulus is around 43MPa and increases until 114 MPa for composites with 8 wt% filler content [8].

Initial modulus of composites using chemical covalent functionalized CNT increase almost double at low amount of CNT in the composites (1 to 4 wt%) for different nanotubes, single or multi-walled CNT. With larger CNT content (8 wt%), composite CNT/SBS with covalent functionalized NC7000 have similar initial modulus than composite using pristine C150P CNT. Different dispersion, CNT or cluster dispersion, influence therefore mechanical properties with low CNT content, but this effect vanishes with increasing amount of CNT inside SBS matrix.

Non-covalent functionalization increase initial modulus in composites compared to pristine or covalent functionalization with same amount and nanotubes, for C150P and NC7000.

Table 5.1 – Mechanical properties of composites CNT/SBS for different nanotubes and functionalization.

| $E\ (MPa)$ $CNT(wt\%)$ | no Functionalization (C150P) | CF/NCF C150P | CF AP-SWNT | CF/NCF NC7000 |
|---|---|---|---|---|
| 0 | $43.9 \pm 2.2$ | | | |
| 0.25 | $43.2 \pm 2.2$ | | | |
| 1 | $54.4 \pm 2.5$ | $118 \pm 6.2/123 \pm 6.6$ | | |
| 2 | $50.2 \pm 2.4$ | $121 \pm 5.9$ | | |
| 4 | $60.4 \pm 3.1$ | $120 \pm 5.8$ | $99.9 \pm 4.9$ | |
| 8 | $114.0 \pm 5.5$ | | | $110 \pm 5.2/145 \pm 6.8$ |

Covalent or non-covalent functionalization increase initial modulus in composites due to the different dispersion of CNT within composites. CNT dispersion increase therefore the initial modulus of the composites when compared to cluster dispersion due to the surface area interaction between fillers and polymer matrix.

### 5.2.4 Electrical Properties

The electrical conductivity of the composites with different CNT and functionalizations are shown in figure 5.6. Functionalized CNT are used in composites for improving mechanical, electrical and electromechanical properties with eventual different interactions between CNT and the polymer matrix. Covalent and non-covalent functionalization are used to introducing functional groups in the fillers surface to guide structural assembly and improve the interface adhesion of nanofillers and matrix [43]. These treatments of carbon nanofillers are mostly carried out in aqueous oxidations and can reduce their length and remove amorphous carbon [43]. The agent of dispersion also has an important role in the electrical properties of the composites [9, 25].

The linear relation between current and voltage (figure 5.6A) in pure polymers and composites allows calculating the electrical conductivity of the materials (figure 5.6B).
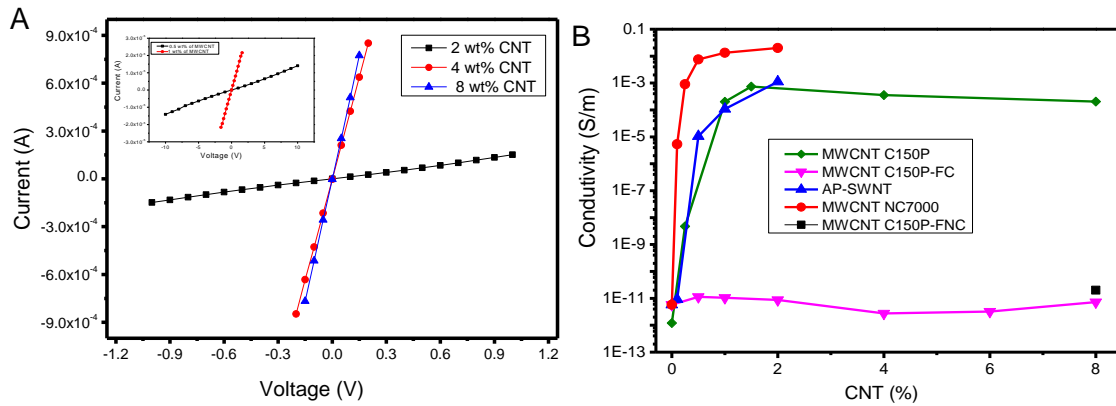
Figure 5.6- Electrical properties of composites CNT/SBS. A) Current vs voltage (I-V) measurements. B) Electrical conductivity of composites with C540 matrix and different carbon nanotubes, C150P, NC700, AP-SWNT and C150P with covalent and non-covalent functionalization.

Using the C540 SBS matrix, with the largest quantity of styrene (larger initial modulus), the electrical response strongly depends on the filler type and functionalization. The electrical conductivity for composites with pristine CNT is similar for incorporation of AP-SWNT and C150P CNT. They are CNT with distinct properties like single or multi-walled, purity and diameter and present similar conductivity for SBS matrix until 2 wt% of CNT, which is above the percolation threshold. The NC7000 shows higher electrical conductivity values for low CNT concentrations and lower percolation threshold (around 0.5 wt%). The percolation threshold is about half than the one obtained for the composites with AP-SWNT and C150P and the maximum value of the conductivity is one order of magnitude larger. For getting conductive in CNT/SBS composites, the NC7000 are the most effective carbon nanotube filler. The high aspect ratio and larger surface area by volume faction of these fillers is the main responsible for this percolation threshold at low loading of CNT [25, 27].

Both covalently and non-colvalently functionalization CNT prevent the increase of the electrical conductivity in CNT/SBS composites with CNT contents up to 8 wt%. This is related to both the better dispersion of the CNT, as verified in the SEM images (figure 5.1) and the disturbance of the conductance of the CNT [44, 45].

In order to get some hints on the electric conduction mechanism, figure 5.7 shows the linear relation between the logarithm of the conductivity and the filler content for the larger volume fractions of pristine CNT.
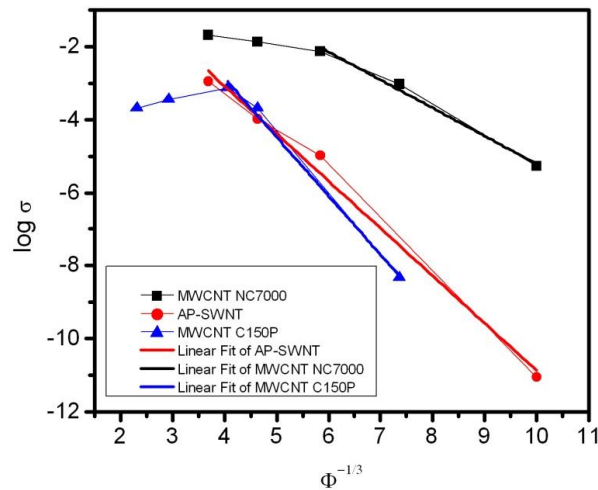
Figure 5.7- Logarithmic plot of the conductivity (σ) as function of the volume fraction ($\phi^{-\frac{1}{3}}$) for the different composites. Thick lines are linear fits to the presented data, with a coefficient of correlation of $R^2$ =0.99.

The latter linear relationship can be explained by the network theory [46], by the formation of a CNT network were the nodes of the network are the CNT and the edges are formed by inter tube conductance. Specifically, the linear relation $\log(\sigma) \propto \Phi^{-1/3}$ is a consequence of a hopping mechanism between nearest CNT neighbors [46]. One important aspect in figure 5.7 is that when the network is not formed, the conductivity deviates from the linear relation. This type of behavior was also observed for another type of CNT composites [47, 48]. The latter leads to an effective conductivity that is mediated by the matrix as described in [47].

### 5.2.5 Electromechanical Properties

The electromechanical response of the SBS composites with pristine CNT is dependent on both mechanical and electrical properties. Stress-strain cycles are non-linear in the elastic region up to 5% of strain (figure 5.8A) and show mechanical hysteresis [8]. On the other hand the composites show a linear variation of electrical resistance for strains up to 5% (figure 5.8B). It is worthy to notice that the literature mostly refers to deviation from linearity of the electrical resistance variation with strain when composites are in the plastic zone, and linear variations for deformations within the elastic regime [49], as observed in the present case (although with a non-linear character).
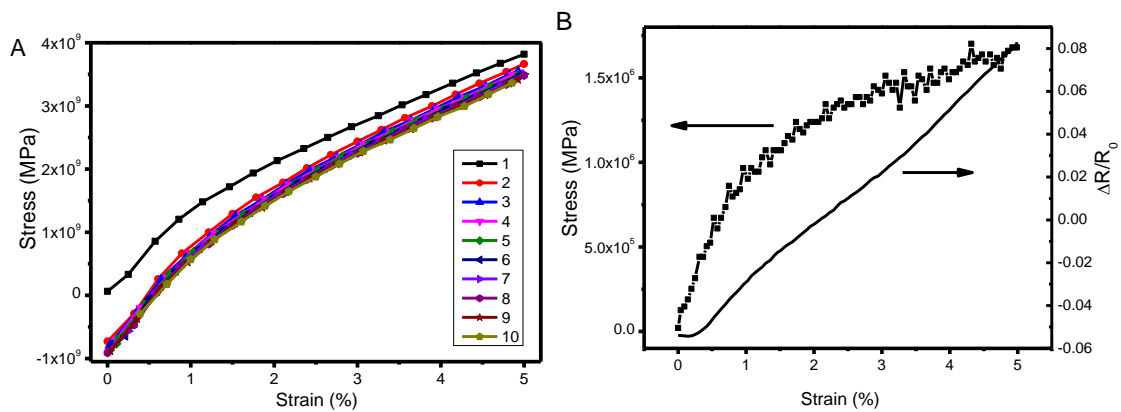
Figure 5.8- A) Stress-Strain curves for 10 cycles for the C540 CNT/SBS with 1.5 wt% CNT for 5% of strain and B) stress-strain curve for 5% of strain and relative electrical resistance change.

The linearity between electrical resistance variations with strain in the electromechanical tests for the composites is shown in figure 5.9.

The SBS composites with pristine CNT within and above percolation threshold show electromechanical properties that make then suitable for sensor applications [8]. Good linearity between relative strain and electrical resistance change as function of time for these composites is presented in figure 5.9A, with ten loading-unloading strain cycles. Gauge factor for deformations up to 5% of strain for different pristine CNT in C540 SBS matrix are shown in figure 5.9B.
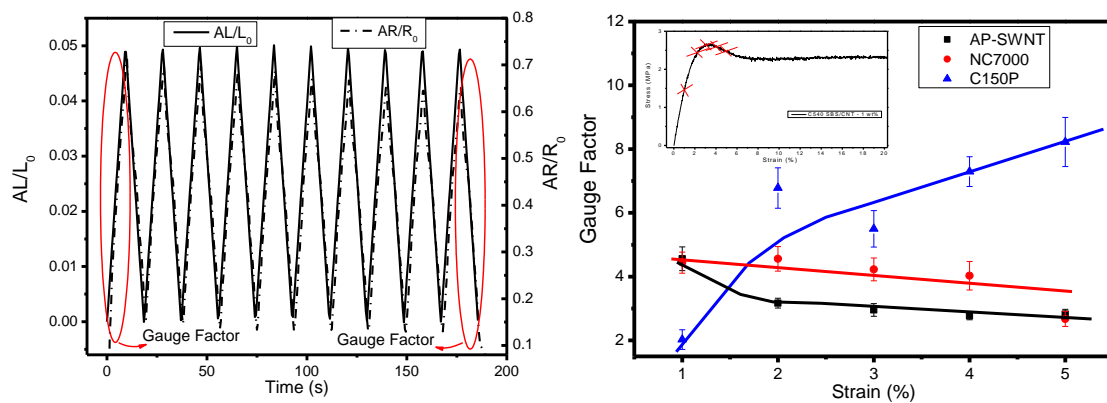


Figure 5.9 – A) Typically loading-unloading cycles for piezoresistivity tests. B) Gauge factor for composites C540 CNT/SBS with 1 wt% filler content of different CNT (C150P, NC7000 and AP-SWNT) as a function of strain up to 5% strain, for 1 mm/min of deformation velocity. The lines are for guiding the eyes.

Different CNT types show different behavior with NC7000 and AP-SWNT leading to decreasing GF with increasing deformation, whereas it increases significantly for C150P CNT.

Figure 5.9B shows that the value of the GF, between 2 and 8 for C150P CNT, indicates strong intrinsic contributions to the GF, due to variations of the CNT network on the CNT/SBS composite.

The electromechanical properties of CNT/SBS composites are independent upon the strain level in the stress-strain tests of composites. Yield strain of the composites is near 2-3%, and the electromechanical properties do not change significantly at this point due to the hiper-elastic nature of TPE.

The Gauge Factor is larger for composites close to the percolation threshold (in this work ~1% CNT) in agreement with the literature [49, 50]; for low CNT loadings, tunneling or hopping effects play a dominant role in the conduction mechanism and they increase exponentially with increasing CNT distance [50, 51]. In several CNT filled composites, it can be observed for large strains a nonlinear behavior in the electrical resistance change which means that the tunneling effect plays a dominant role, in these cases [50]. Others works in the literature refer that main electrical conduction mechanism in these related composites is hopping intra-tube or from one CNT to another [52, 53]. For composites CNT/SBS with 1-1.5% CNT the nonlinear effect in electrical resistance variation is noticed for strains up to around 10% (higher than the yield strain of these composites, typically 3%). For composites with larger CNT content the electrical resistance is linear with strain up to 50% of strain [54].

In order to assess the effect of CNT loading on the electromechanical response of CNT/SBS composites, in figure 5.10A shows the gauge factor values until 5% of strain for the composites with 4 wt% CNT and figure 5.10B compares composites with 3 different CNT loadings (1, 1.5 and 4wt% CNT).
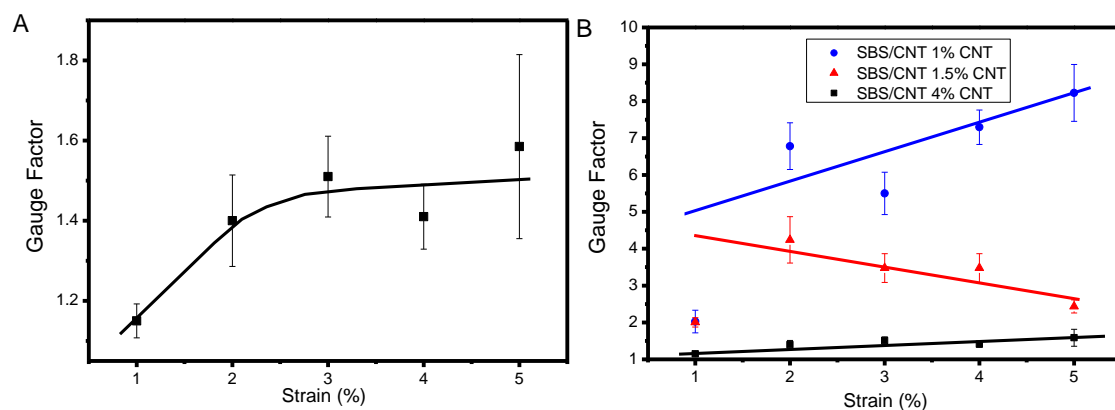


Figure 5.10 – Gauge factor as a function of strain for composites C540 CNT/SBS for A) 4 wt% CNT until 5% of strain and B) comparison of CNT/SBS with 1, 1.5 and also 4 wt% CNT for same electromechanical tests. The lines are for guiding the eyes.

CNT/SBS composites well above the percolation threshold (Figure 5.10A for CNT/SBS with 4 wt% CNT) show electromechanical properties with gauge factors lower than 2, i.e. with higher geometrical electromechanical contribution, unlike composites near percolation threshold, which show strong intrinsic electromechanical effect and GF increasing up to 8 for increasing strain up to 5%.

Figure 5.10B compares the electromechanical response of the SBS composites for different CNT loadings. The CNT/SBS composites near percolation threshold show higher gauge factor values for strains up to 5%. These results are well above the ones found in the literature in which CNT/polysulphone electromechanical properties up to 1% of strain showed higher gauge factor for composite with 0.5 wt% of CNT with GF = 0.74 ± 0.08 [55], i.e. due to the geometrical contribution.

Furthermore, traditional strain gauges show gauge factors around 2 [50], the present CNT/SBS composites showing higher gauge factors for low CNT loadings and also allowing larger maximum strains.

Finally, figure 5.11 shows the gauge factor variations for small strains at several tests velocities (figure 5.11A) and with a pre-stress (figure 5.11B).

Gauge factor is larger than 2 (the geometric term for thermoplastic elastomers with Poisson coefficient close to 0.5 [49]), and arises up to near 4 for 2% of strain. Gauge factor is practically independent of the test velocity up to 1mm/min (figure 5.11A), indicating the same time response of the CNT networks reorientation for the considered deformations.

The sensibility of composites changes when a pre-stress is applied is presented in figure 5.11B. For 1% of strain, the SBS composite shows a higher value of GF with 10% of pre-stress applied before electromechanical measurements. The pre-stress strongly increases the sensitivity of the CNT network, again the deformation velocity having no effect. Pre-stress in electromechanical tests increases the CNT distance and conductivity mechanism [50, 52] causing higher variation in electrical resistance with increasing deformation in the composites.
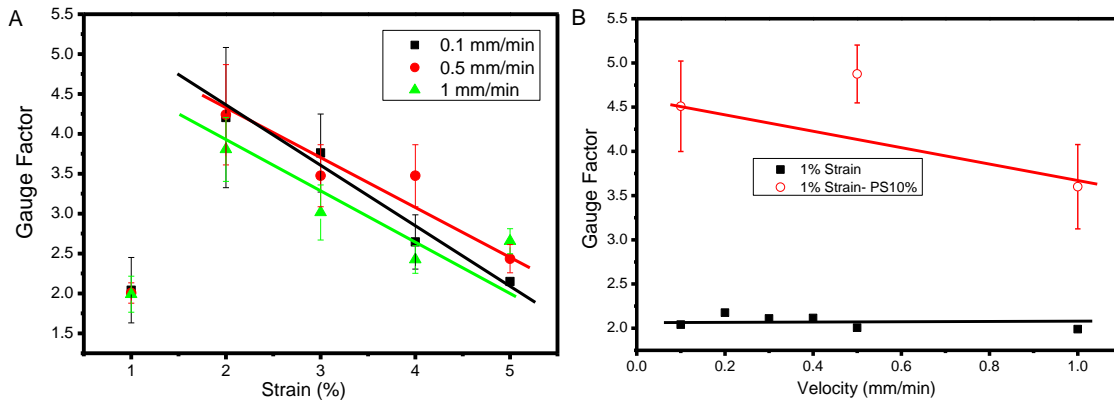
Figure 5.11 – Electromechanical properties of C540 CNT/SBS with 1.5 wt% CNT. A) For small strains (1% to 5%) at v = 0.1, 0.5 and 1mm/min and B) without and with 10% of pre-stress for 1% of strain at several velocities (v = 0.1 to 1 mm/min). The lines are for guiding the eyes.

## 5.3  Conclusions

Tri-block copolymer SBS can be proceeded by solvent casting with carbon nanotubes with interesting electromechanical properties for sensor applications.

The electrical properties of these composites are similar for pristine CNT with percolation threshold near 1 wt% for three different types of CNT, multi-walled (CNT NC7000 and C150P) and single-walled CNT (AP-SWNT), where composites with nanotubes NC7000 have the smallest percolation threshold. Near percolation threshold it is observed higher electromechanical sensibility with gauge factors up to 8.

Covalent and non-covalent functionalization improve CNT dispersion but prevent conductivity increase for increasing filler contents up to 8 wt% CNT, therefore hindering the use of the materials for electromechanical sensors.

The mechanical properties show the typical stress-strain curves of thermoplastic elastomers with maximum deformation of CNT/SBS composites larger than 400% and yield strain around 3%. Electromechanical properties of CNT/SBS composites have similar behavior before and after yielding.

**References**

[1]     Logakis E, Pandis C, Peoglos V, Pissis P, Stergiou C, Pionteck J, Pötschke P, Mičušík M and Omastová M 2009 Structure-property relationships in polyamide 6/multi-walled carbon nanotubes nanocomposites *Journal of Polymer Science Part B: Polymer Physics* 47 764-74

[2]     Oliva-Avilés A I, Avilés F and Sosa V 2011 Electrical and piezoresistive properties of multi-walled carbon nanotube/polymer composite films aligned by an electric field *Carbon* 49 2989-97

[3]     Pradhan B, Kohlmeyer R R, Setyowati K, Owen H A and Chen J 2009 Advanced carbon nanotube/polymer composite infrared sensors *Carbon* 47 1686-92

[4]     Tsuchiya K, Sakai A, Nagaoka T, Uchida K, Furukawa T and Yajima H 2011 High electrical performance of carbon nanotubes/rubber composites with low percolation threshold prepared with a rotation–revolution mixing technique *Composites Science and Technology* 71 1098-104

[5]     Dang Z-M, Shehzad K, Zha J-W, Mujahid A, Hussain T, Nie J and Shi C-Y 2011 Complementary percolation characteristics of carbon fillers based electrically percolative thermoplastic elastomer composites *Composites Science and Technology* 72 28-35

[6]     Drozdov A D and Christiansen J 2009 Thermo-viscoplasticity of carbon black-reinforced thermoplastic elastomers *International Journal of Solids and Structures* 46 2298-308

[7]     Hölzer S, Ganß M, Schneider K, Knoll K and Weidisch R 2013 Deformation mechanisms in lamellar S–S/B–S triblock copolymers *European Polymer Journal* 49 261-9

[8]     Costa P, Silva J, Sencadas V, Simoes R, Viana J C and Lanceros-Méndez S 2013 Mechanical, electrical and electro-mechanical properties of thermoplastic elastomer styrene–butadiene–styrene/multiwall carbon nanotubes composites *Journal of Materials Science* 48 1172-9

[9]     Lorenz H, Fritzsche J, Das A, Stöckelhuber K W, Jurk R, Heinrich G and Klüppel M 2009 Advanced elastomer nano-composites based on CNT-hybrid filler systems *Composites Science and Technology* 69 2135-43

[10]    Siengchin S and Karger-Kocsis J 2013 Binary and ternary composites of polystyrene, styrene–butadiene rubber and boehmite produced by water-mediated melt compounding: Morphology and mechanical properties *Composites Part B: Engineering* 45 1458-63

[11]    Wu J-H, Li C-H, Wu Y-T, Leu M-T and Tsai Y 2010 Thermal resistance and dynamic damping properties of poly (styrene–butadiene–styrene)/thermoplastic polyurethane composites elastomer material *Composites Science and Technology* 70 1258-64

[12]    Munteanu S B, Brebu M and Vasile C 2005 Thermal and thermo-oxidative behaviour of butadiene–styrene copolymers with different architectures *Polymer Degradation and Stability* 89 501-12

[13]    Shih R-S, Kuo S-W and Chang F-C 2011 Thermal and mechanical properties of microcellular thermoplastic SBS/PS/SBR blend: effect of crosslinking *Polymer* 52 752-9

[14]    Pedroni L G, Soto-Oviedo M A, Rosolen J M, Felisberti M I and Nogueira A F 2009 Conductivity and mechanical properties of composites based on MWCNTs

and styrene-butadiene-styrene block™ copolymers *Journal of Applied Polymer Science* 112 3241-8

[15] Ocando C, Tercjak A and Mondragon I 2010 Nanostructured systems based on SBS epoxidized triblock copolymers and well-dispersed alumina/epoxy matrix composites *Composites Science and Technology* 70 1106-12

[16] Liu Y-T, Xie X-M and Ye X-Y 2011 High-concentration organic solutions of poly(styrene-co-butadiene-co-styrene)-modified graphene sheets exfoliated from graphite *Carbon* 49 3529-37

[17] Zhi Feng W, Pei W, Xiong Ying Y and Bo J 2009 Processing and modeling of multi-walled carbon nanotube/styrene-butadiene-styrene (SBS) composites for force sensing. In: *Nanotechnology, 2009. IEEE-NANO 2009. 9th IEEE Conference on,* pp 756-7

[18] Rubinger C P L, Leyva M E, Soares B G, Ribeiro G M and Rubinger R M 2011 Hopping conduction on carbon black/styrene–butadiene–styrene composites *Journal of Materials Science* 47 860-5

[19] Tang W, Liu B, Liu Z, Tang J and Yuan H 2012 Processing-dependent high impact polystyrene/styrene-butadiene-styrene tri-block copolymer/carbon black antistatic composites *Journal of Applied Polymer Science* 123 1032-9

[20] Shehzad K, Dang Z-M, Ahmad M N, Sagar R U R, Butt S, Farooq M U and Wang T-B 2013 Effects of carbon nanotubes aspect ratio on the qualitative and quantitative aspects of frequency response of electrical conductivity and dielectric permittivity in the carbon nanotube/polymer composites *Carbon* 54 105-12

[21] Tjahyono A P, Aw K C and Travas-Sejdic J 2012 A novel polypyrrole and natural rubber based flexible large strain sensor *Sensors and Actuators B: Chemical* 166-167 426-37

[22] Yi W, Wang Y, Wang G and Tao X 2012 Investigation of carbon black/silicone elastomer/dimethylsilicone oil composites for flexible strain sensors *Polymer Testing* 31 677-84

[23] Johnson O K, Kaschner G C, Mason T A, Fullwood D T and Hansen G 2011 Optimization of nickel nanocomposite for large strain sensing applications *Sensors and Actuators A: Physical* 166 40-7

[24] Theodosiou T C and Saravanos D A 2010 Numerical investigation of mechanisms affecting the piezoresistive properties of CNT-doped polymers using multi-scale models *Composites Science and Technology* 70 1312-20

[25] Das A, Stöckelhuber K W, Jurk R, Saphiannikova M, Fritzsche J, Lorenz H, Klüppel M and Heinrich G 2008 Modified and unmodified multiwalled carbon nanotubes in high performance solution-styrene–butadiene and butadiene rubber blends *Polymer* 49 5276-83

[26] PÖTSCHKE, P, HÄUSSLER, L, PEGEL, S, STEINBERGER, R, SCHOLZ and G 2007 Thermoplastic polyurethane filled with carbon nanotubes for electrical dissipative and conductive applications *KGK. Kautschuk, Gummi, Kunststoffe* 60 432-7

[27] Ma P-C, Siddiqui N A, Marom G and Kim J-K 2010 Dispersion and functionalization of carbon nanotubes for polymer-based nanocomposites: A review *Composites Part A: Applied Science and Manufacturing* 41 1345-67

[28] Cardoso P, Silva J, Klosterman D, Covas J A, van Hattum F W J, Simoes R and Lanceros-Mendez S 2012 The role of disorder on the AC and DC electrical conductivity of vapour grown carbon nanofibre/epoxy composites *Composites Science and Technology* 72 243-7

[29] Pedroni L G, Araujo J R, Felisberti M I and Nogueira A F 2012 Nanocomposites based on MWCNT and styrene–butadiene–styrene block copolymers: Effect of the preparation method on dispersion and polymer–filler interactions *Composites Science and Technology* 72 1487-92

[30] Xiao H, Li H and Ou J 2010 Modeling of piezoresistivity of carbon black filled cement-based composites under multi-axial strain *Sensors and Actuators A: Physical* 160 87-93

[31] Wang P, Geng S and Ding T 2010 Effects of carboxyl radical on electrical resistance of multi-walled carbon nanotube filled silicone rubber composite under pressure *Composites Science and Technology* 70 1571-3

[32] Hu N, Karube Y, Arai M, Watanabe T, Yan C, Li Y, Liu Y and Fukunaga H 2010 Investigation on sensitivity of a polymer/carbon nanotube composite strain sensor *Carbon* 48 680-7

[33] Taya M, Kim W J and Ono K 1998 Piezoresistivity of a short fiber/elastomer matrix composite *Mechanics of Materials* 28 53-9

[34] Nigro B, Grimaldi C, Miller M A, Ryser P and Schilling T 2012 Tunneling conductivity in composites of attractive colloids *The Journal of chemical physics* 136 164903

[35] Inpil K, Mark J S, Jay H K, Vesselin S and Donglu S 2006 A carbon nanotube strain sensor for structural health monitoring *Smart Materials and Structures* 15 737

[36] Thostenson E T and Chou T W 2006 Carbon Nanotube Networks: Sensing of Distributed Strain and Damage for Life Prediction and Self Healing *Advanced Materials* 18 2837-41

[37] Li X, Luan S, Shi H, Yang H, Song L, Jin J, Yin J and Stagnaro P 2013 Improved biocompatibility of poly (styrene-b-(ethylene-co-butylene)-b-styrene) elastomer by a surface graft polymerization of hyaluronic acid *Colloids and surfaces. B, Biointerfaces* 102 210-7

[38] Gupta K, Chakraborty G, Jana P C and Meikap A K 2011 Temperature dependent dc and ac electrical transport properties of the composite of a polyaniline nanorod with copper chloride *Solid State Communications* 151 573-8

[39] Wu G, Zhou L, Ou E, Xie Y, Xiong Y and Xu W 2010 Preparation and properties of hydroxylated styrene–butadiene–styrene tri-block copolymer/multi-walled carbon nanotubes nanocomposites via covalent bond *Materials Science and Engineering: A* 527 5280-6

[40] Canto L B, Mantovani G L, deAzevedo E R, Bonagamba T J, Hage E and Pessan L A 2006 Molecular Characterization of Styrene-Butadiene-Styrene Block Copolymers (SBS) by GPC, NMR, and FTIR *Polym. Bull.* 57 513-24

[41] Lu L, Yu H, Wang S and Zhang Y 2009 Thermal degradation behavior of styrene-butadiene-styrene tri-block copolymer/multiwalled carbon nanotubes composites *Journal of Applied Polymer Science* 112 524-31

[42] Lu L, Zhou Z, Zhang Y, Wang S and Zhang Y 2007 Reinforcement of styrene–butadiene–styrene tri-block copolymer by multi-walled carbon nanotubes via melt mixing *Carbon* 45 2621-7

[43] Carmona F, Canet R and Delhaes P 1987 Piezoresistivity of heterogeneous solids *Journal of Applied Physics* 61 2550

[44] Wladyka-Przybylak M, Wesolek D, Gieparda W, Boczkowska A and Ciecierska E 2011 Functionalization effect on physico-mechanical properties of multi-

walled carbon nanotubes/epoxy composites *Polymers for Advanced Technologies* 22 48-59

[45] Yadav S K, Mahapatra S S and Cho J W 2013 Tailored dielectric and mechanical properties of noncovalently functionalized carbon nanotube/poly(styrene-b-(ethylene-co-butylene)-b-styrene) nanocomposites *Journal of Applied Polymer Science* 129 2305-12

[46] Silva J, Simoes R, Lanceros-Mendez S and Vaia R 2011 Applying complex network theory to the understanding of high-aspect-ratio carbon-filled composites *EPL (Europhysics Letters)* 93 37005

[47] Carabineiro S A C, Pereira M F R, Nunes-Pereira J, Silva J, Caparros C, Sencadas V and Lanceros-Méndez S 2012 The effect of nanotube surface oxidation on the electrical properties of multiwall carbon nanotube/poly(vinylidene fluoride) composites *J Mater Sci* 47 8103-11

[48] Silva J, Ribeiro S, Lanceros-Mendez S and Simões R 2011 The influence of matrix mediated hopping conductivity, filler concentration, aspect ratio and orientation on the electrical response of carbon nanotube/polymer nanocomposites *Composites Science and Technology* 71 643-6

[49] Wichmann M H G, Buschhorn S T, Gehrmann J and Schulte K 2009 Piezoresistive response of epoxy composites with carbon nanoparticles under tensile load *Physical Review B* 80 245437

[50] Hu N, Karube Y, Yan C, Masuda Z and Fukunaga H 2008 Tunneling effect in a polymer/carbon nanotube nanocomposite strain sensor *Acta Materialia* 56 2929-36

[51] Li C, Thostenson E T and Chou T-W 2008 Sensors and actuators based on carbon nanotubes and their composites: A review *Composites Science and Technology* 68 1227-49

[52] Feng C and Jiang L 2013 Micromechanics modeling of the electrical conductivity of carbon nanotube (CNT)–polymer nanocomposites *Composites Part A: Applied Science and Manufacturing* 47 143-9

[53] Psarras G C 2006 Hopping conductivity in polymer matrix–metal particles composites *Composites Part A: Applied Science and Manufacturing* 37 1545-53

[54] Costa P F A, Sencadas V, Viana J C and Lanceros-Méndez S 2013 Electro-mechanical properties of triblock copolymer styrene-butadiene-styrene / carbon nanotube composites for large deformation sensor applications *Sensors and Actuators A: Physical* Submitted

[55] Bautista-Quijano J R, Avilés F, Aguilar J O and Tapia A 2010 Strain sensing capabilities of a piezoresistive MWCNT-polysulfone film *Sensors and Actuators A: Physical* 159 135-40

Effect of carbon nanotube type and functionalization on the electrical, thermal, mechanical and electromechanical properties of carbon nanotube/styrene-butadiene-styrene composites

# Chapter 6. Upscale processing for thermoplastic elastomers styrene-butadiene-styrene/carbon nanotubes composites for strain sensor applications

## Abstract

Tri-block copolymer styrene-butadiene-styrene (SBS) composites with different butadiene/styrene ratios and multi-walled carbon nanotubes (MWCNT) can be used for the development of electromechanical sensors for large strains applications. Extruded CNT/SBS composites show percolation thresholds around 5 wt%, electromechanical properties with high sensibility at larger strain and the gauge factor reach values up to 30 at strains of 20%. The butadiene/styrene ratio has influence in the mechanical and electromechanical properties. In one hand, the increase of the styrene content in copolymer increasing initial mechanical modulus, on the other hand, the increase of the butadiene content leads to larger maximum deformations and higher electromechanical sensibility for strains up to 20%. Further, applied initial pre-stress increases the electromechanical sensibility of the composites.

## 6.1 Introduction

Conducting polymer composites based on an insulator polymeric matrix with an electrical conducting nanofiller dispersed within the matrix have been extensively studied for their applications as antistatic materials, electromagnetic interference, capacitors [1-4], temperature, pressure, gas and electromechanical sensors [1, 2]. Conductive electrospun composites can be used in the fabrication of tiny electronic devices or machines such as scottky junctions, sensors and actuators [5]. Due to the properties of electrospinning composites, conductive nanofibrous membranes are also quite suitable for using as porous electrodes in the development of high performance batteries [5, 6] and electrostatic dissipation, corrosion protection, electromagnetic interference shielding, photovoltaic device, etc [5, 7].

The most widespread uses of industrial polymer composites with carbon nanoallotropes are as packing and structural materials. The majority of polymers are thermally and electrically insulators but for packing purposes it is required that polymers do not accumulate static charge during manufacturing, assembling, storage and service [3]. The amount of carbon nanoallotropes necessary for obtaining a given level of electrical conductivity depends on the type of nanofiller. In the case of carbon black (CB), widely used due to its low cost, a loading between 15-20 weight percentage (wt%) is necessary for reaching the percolation threshold [3, 4]. These large filler contents, on the other hand, brings negative effects on the processability of the composites  and their mechanical properties [3]. The use of carbon nanotubes (CNT) lead to composites with superior electrical and mechanical properties when compared to other carbon allotropes such as carbon black or vapor grown carbon nanofibers (CNF) and these properties are achieved with lower nanoallotropes loadings [8, 9]. CNF have higher density and diameter than CNT [10]. Electrical percolation threshold in composites with CNF as filler materials is around 4-6 wt% [10]. The unique mechanical, electrical and thermal properties of CNT have largely accelerated their applications in the development of structural and electrical components [11]. CNT/polymer composite materials have further enhanced multifunctionality in terms of stress and strain sensing capabilities, even at the nanofiller-matrix interface level [12].

As polymer matrix, the thermoplastic elastomer tri-block copolymer styrene-butadiene-styrene (SBS) is widely studied and used in industry due to its high elongation at break, abrasion resistance and durability [13-16]. SBS can be used without vulcanization,

which is an advantage as it does not degrade the mechanical and electrical properties obtained in composites [8]. SBS copolymers can be composed by different ratios of styrene and butadiene, which strongly influences its mechanical, electrical and thermal properties. Usually, butadiene is the component in larger quantity with the styrene content being up to 50%.

The SBS has high thermal stability with the butadiene glass transition (Tg) around -80ºC [13] and the styrene around 100 ºC [13] . The incorporation of carbon nanotubes within the copolymer matrix does not change them significantly, being observed just a slight shift of the glass transitions to higher temperatures [17, 18]. The most outstanding property of CNT/SBS composites is therefore their mechanical properties, showing strains higher than 1000% for CNT contents up to 8 wt% independently of the styrene/butadiene ratio within the SBS (20/80, 30/70 or 40/60) [2]. Further, the initial modulus increases with decreasing butadiene (softer phase) in SBS and the electrical percolation threshold is independent of the SBS matrix [2].

Properties of polymer composites strongly depend on the processing, characteristics and functionalization of the nanoallotropes, as well as on the dispersion and distribution level of the nanofillers in the polymer matrix [10, 19].

Processing methods typically used in this type of composites are solvent casting, in situ polymerization, electrospun process, melt blending and chemical modifications [5, 19, 20]. The ability to disperse individual CNT homogeneously within matrix has a strong influence in composite characteristics and therefore in their application potential [20].

Percolation threshold below 0.01 wt% [21] have been reported under specific processing conditions such as solvent casting [22], but values around 1 to 3 wt% are most typically found for composites based on thermoplastic polymers with CNT processed with industrially-viable methods such as melt compounding and extrusion [22]. Thus, up scaled industrial processes for composites preparation typically lead to an increase of carbon nanofiller loading for achieving similar electrical properties when compared with solvent casting methods processed in laboratory environment.

The percolation threshold can be further tailored  in polymer extrusion by adding a second filler working in synergy with the CNT [22], but this second filler can have both positive implications such as decreasing the percolation threshold and adding novel functionalities to the polymer matrix, but also negative, such as increasing fragility, price and difficult recyclability of composites [22]. Nanoclays are of the best example of second fillers added in polymer/carbon nanofiller composite [23, 24].

It has been shown that CNT/SBS composites prepared by solvent casting show excellent electromechanical properties appropriate for the development of large deformation sensors with good and linear sensibility [25], when compared to traditional strain gages [26]. Composites with percolation thresholds near 0.5 wt% and good electromechanical properties characterized by gauge factors (GF) up to 100 for 4 wt% CNT of composites have been achieved [25].

This work investigates the electrical, mechanical and electromechanical performance of CNT/SBS composites prepared by extrusion in the form of wire and electrospun fibers (oriented and randomly oriented) in order to evaluate the possibly of up-scaled production and performance of these materials for sensor and actuator applications. The matrices studied are C401 and C540 for extruded composites and C540 for electrospun materials. The CNT (NC7000) content is 0.05, 0.1 and 0.5 wt% for electrospun composites, and 4, 6, 8 and 10 wt% for extruded composites.

## 6.1  Results and Discussion

### 6.1.1 Nanofiller distribution and sample morphology

SEM images (figure 6.1) show the CNT distribution in the SBS matrices. The dispersion process energy was not capable of breaking all CNT clusters, but overall, the SEM images reveal a homogeneous distribution of CNT clusters with diameters around 1 to 2 micrometers. Cluster size and homogeneous distribution is similar for both composites with different ratio of butadiene/styrene matrices (80/20 for C401 and 60/40 for C540), being nevertheless an apparently better distribution of smaller clusters for the C540 sample, that can be attributed to a better distribution of the fillers in the styrene compound during the extrusion process. It has been proven CNT interact similarly with the polybutadiene and the polystyrene phases and show similar distribution in both phases when prepared from solution [2, 15]. Small distribution variations in each polymer phase can be related to the preparation method and the different thermal behavior of styrene and butadiene.
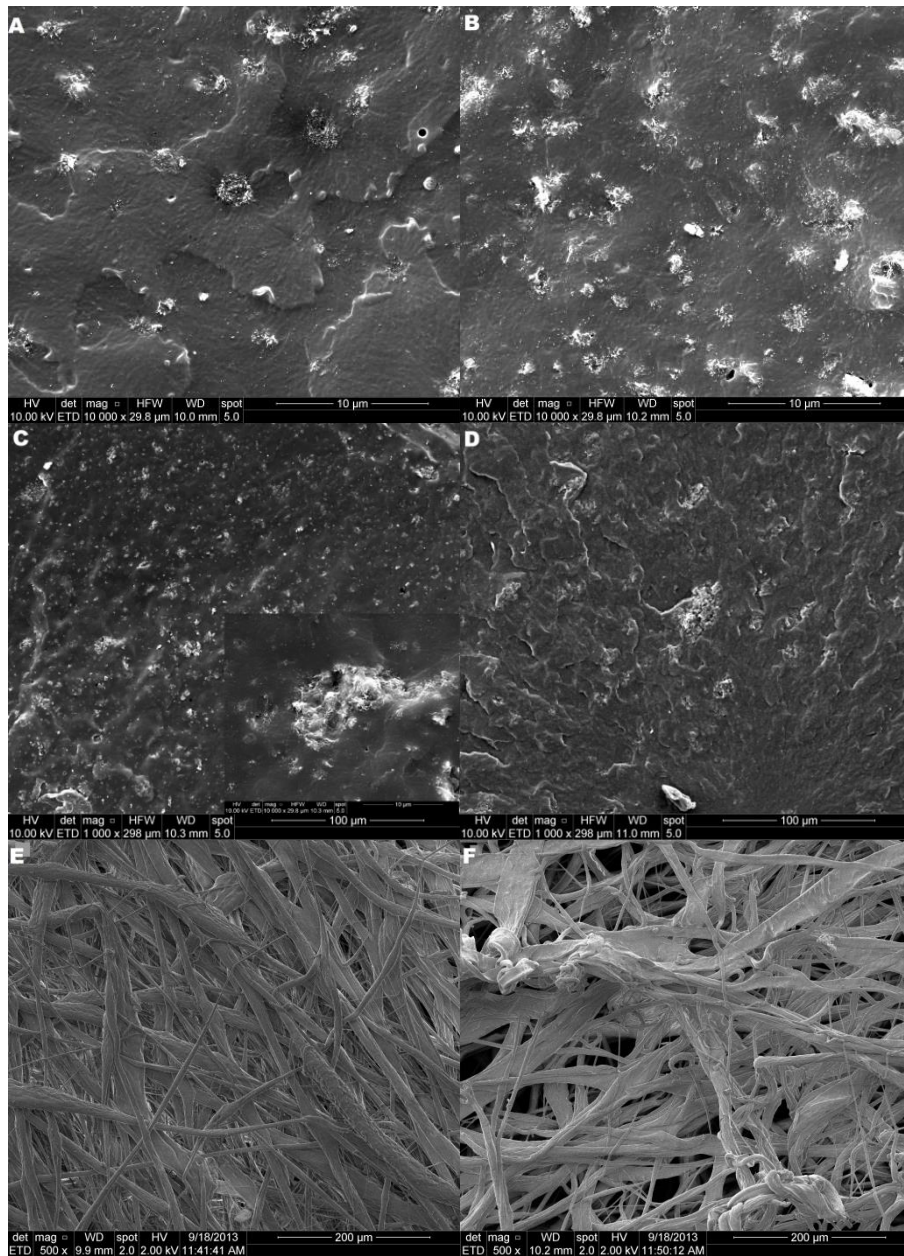
Figure 6.1- SEM images of composites with extruded SBS C401 and C540 matrices (A, B, C and D) and electrospun C540 matrix (E and F), for different CNT loadings. A and B- C401 CNT/SBS with 4 and 6 wt% CNT, respectively. C- C401 CNT/SBS with 8 wt% CNT; the inset corresponds to a cluster. D- C540 CNT/SBS with 8 wt% CNT. E- Oriented fibers of C540 CNT/SBS with 0.1 wt% CNT. F- Randomly oriented fibers of C540 CNT/SBS with 0.5 wt% CNT.

Together with a good distribution of clusters, figure 6.1C (inset) indicates that clusters are wrapped by the SBS matrices. Closer examination of the CNT reveals a thicker layer of SBS that seems to cover the CNT surface, which indicates some degree of wetting and phase adhesion in all clusters. Figure 6.1 E and F shows electrospinning composites with 0.1 and 0.5 wt% CNT, respectively, with fibers diameters around 10

μm. The fibers can be oriented in electrospinning process with differences on mechanical properties.

### 6.1.2 Molecular and thermal characterization

FTIR measurements for pure SBS and for the composites (figure 6.2A) for extruder method show the typical bands of the copolymer with no new bands or band energy deviation in the composites, indicative of no chemical interaction between the fillers and the polymer matrix. Butadiene is the softer matter in the copolymer and is characterized by the FTIR band at 966 cm$^{-1}$ whereas styrene is the harder matter and its characteristic peak appear at 699 cm$^{-1}$ [15], as represented in figure 6.2A. The results are similar independently of the copolymer matrix, the difference being just the relative intensity of the butadiene and styrene bands, depending on their relative content in the sample.
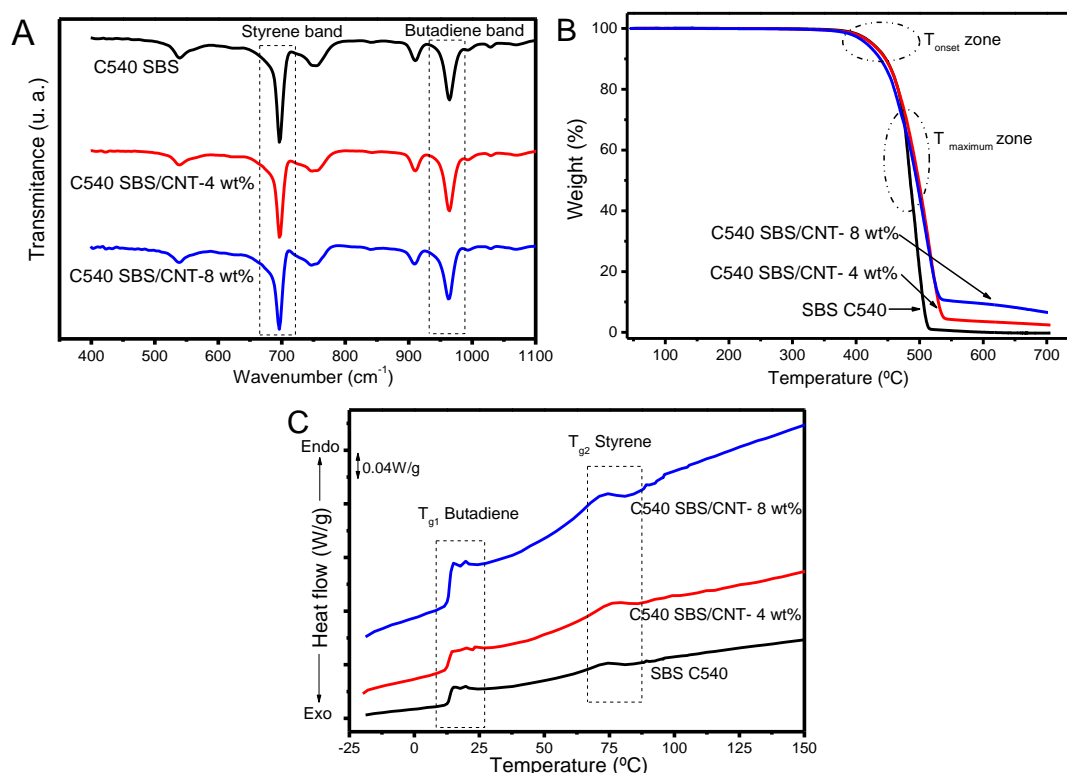


Figure 6.2- FTIR (A), TGA (B) and DSC (C) results for extruded CNT/SBS composites for C540 SBS matrix and composites with 4 and 8 wt% MWCNT.

The effect of CNT inclusions within the SBS matrix on the thermal properties of the composites was analyzed by TGA and DSC. TGA analyses (figure 6.2B) show the mass loss variation with increasing temperature. Pure SBS and the composites have similar behaviors, with initial temperature degradation (T$_{onset}$) and maximum temperature

degradation ($T_{max}$), as obtained by the derivation of the TGA graphic, DTG, around 450ºC and 500 ºC, respectively (table 6.1). The thermal degradation mechanism of SBS consists of two main processes, namely chain scission and crosslinking [27], the mechanisms not being significantly affected by the present of the fillers as indicated by the behaviors observed in Figure 6.2B. Degradation temperature of butadiene occurs at lower temperatures than styrene [28] and copolymers with larger content of styrene show larger thermal stability. $T_{onset}$ and $T_{max}$ (figure 6.2C) increase with increasing CNT content in the composites, with a slight variation for the initial degradation temperature and a larger variation in the maximum degradation temperature of ~ 20 ºC for the 8 wt% CNT filled composite sample. CNT in SBS matrix provide thermal stability, resulting from the good wetting of the carbon nanoallotropes by the polymer matrix.

Table 6.1- Initial degradation temperature ($T_{onset}$) and maximum degradation temperature ($T_{max}$), obtained from TGA experiments, and butadiene and styrene glass transition temperatures, $T_{g1}$ and $T_{g2}$ respectively, obtained from DSC, for a C540 SBS sample with butadiene/styrene ratio of 80/20 and the corresponding composites with 4 and 8 wt% filler content in extruded samples.

| SBS C540 | | | | | | | |
|---|---|---|---|---|---|---|---|
| CNT (wt%) | 0 | 4 | 8 | | 0 | 4 | 8 |
| $T_{onset}$ (ºC) | 452 | 454 | 455 | $T_{g1}$ (ºC) | 15.7 | 16.3 | 17.4 |
| $T_{max}$ (ºC) | 489 | 514 | 518 | $T_{g2}$ (ºC) | 74.3 | 77.7 | 74.4 |

Residual weight percentage at temperature higher than 600 ºC corresponds to the CNT content of the composites.

SBS shows two different glass transition temperatures (figure 6.2C), one for butadiene ($T_{g1}$) appearing around 15 ºC and one for styrene ($T_{g2}$) which appears at ~ 74 ºC.

Glass transition temperature of the composites show a slight shift to higher temperatures with increasing CNT content within the SBS matrix (table 6.1) as previously reported in literature [16]. This small shift is associated to dynamic molecular restrictions due to the interactions between the carbon nanotubes and elastomers macromolecular chains [16]. The aforementioned results are similar independently of the copolymer SBS matrix.

### 6.1.3 Mechanical Properties

The stress-strain curves of SBS C401 (figure 6.3A) and C540 (figure 6.3B) composites show that SBS C540, with larger styrene content, show a larger stress value than the samples with C401 at a given strain and CNT loading.
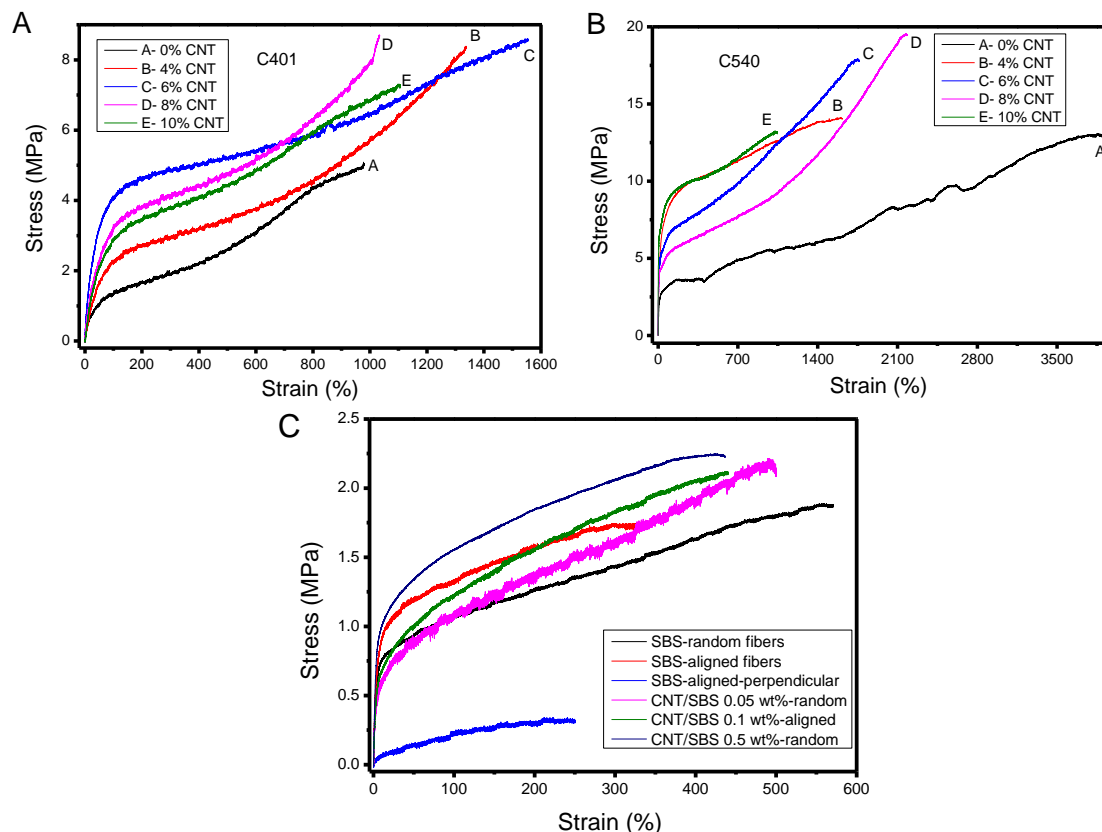


Figure 6.3- Mechanical properties of SBS C401 (A) and C540 (B) for CNT loadings up to 10 wt% for extruded samples, and C540 for CNT loadings up to 0.5 wt% for electrospun samples (C).

The maximum deformation, for extruded samples, is larger than 1000% for all composites independently of the polymer matrix and can reach 4000% for pure SBS C540. The incorporation of CNT has also a distinct effect on the deformation capabilities of both SBS matrices. For SBS C401 (higher butadiene content and radial structure), adding CNT results on larger deformations than the pure elastomer, and conversely for the SBS C540 (low % of butadiene and linear structure) where the incorporation of CNT reduces the maximum deformation reached.

Electrospun samples show mechanical properties characterized by maximum deformations between 250% and 600%, which is lower than extruded samples. Mechanical deformation on oriented fibers along the perpendicular direction shows weak properties, revealing that actually electrospun fibers are mostly aligned. The

composites show larger stress values for a given deformation with increasing CNT content in the C540 matrix.

The initial modulus of the extruded samples has distinct behavior depending on the butadiene/styrene ratio within the matrix, having SBS C401 lower initial modulus due to the higher butadiene content. Figure 6.4 shows that these values are 10 times smaller for the C401 matrix. For the C540 matrix, the initial modulus increases with increasing CNT content up to 1.5 MPa for the samples with 10 wt% loading.
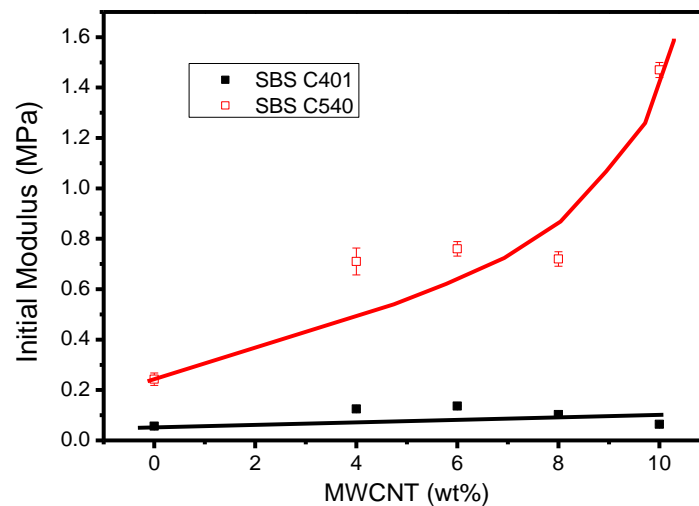


Figure 6.4 – Initial modulus for CNT/SBS composites as a function of filler content for SBS C401 and C540. Calculation of the initial modulus is until 2% of strain. The lines are for guiding the eyes.

The initial modulus for extruded samples are different for both composites (figure 6.4) being larger for the matrix with larger butadiene content (80%). The C401 matrix has the yielding strain between ~ 20% and ~ 50% for composites with CNT up to 10 wt% CNT. For the C540 matrix, with 60% of styrene, the yielding strain is lower, being between 10% and 20% for pure SBS matrix and the CNT composites. This different value is due to the relative butadiene content in SBS. For both SBS, the incorporation of CNT does not affect the yield strain values indicating that the deformation of the butadiene phase is not restricted by the presence of CNT. Extruded composites have larger yield strain than the same matrix and CNT content prepared by solvent casting or electrospinning, with yield strains around 2 to 3% [2] and 4 to 8%, respectively. The yield stress of the composites is also enhanced by adding CNT to both SBS matrices. Processing method affects the mechanical properties of SBS and their composites, with chemical dissolution decreasing yielding stress of the elastomeric materials [2]. This

fact is very relevant for the electromechanical properties and sensors applications due to the associated mechanical hysteresis.

### 6.1.4 Electrical Properties

Electrical conductivity for both SBS composites increases with increasing CNT content, with the percolation threshold being lower than 6 wt% for both matrices, C401 and C540 (figure 6.5). The inclusion of CNT leads to a strong increase of the electrical conductivity, between 7 and 9 orders of magnitude when compared to pure SBS matrices, around the percolation threshold zone, C540 matrix with 60% of butadiene shows higher values of conductivity and literature reports that MWCNT/SBS composites prepared by a casting solution technique show slightly lower electrical percolation threshold in SBS with lower butadiene contents [15], which is similar to the obtained results. Butadiene/styrene ratios have thus some influence in the electrical properties of the composites, which can be only attributed to small variations in the dispersion ability of the fillers in the softer and harder parts of the polymer matrix during the extrusion process due to the different thermo-mechanical properties of the harder and softer parts of the polymer, and therefore to variation in the CNT network topology. The variations are nevertheless small, being the electrical conductivity behavior of both matrices with increasing filler content similar and mainly dependent on the CNT content [22].

The harder copolymer matrix (C540 SBS) reinforced with CNT presents higher electrical conductivity than C401 SBS and the percolation threshold is also lower. This fact indicates, as previously referred, the importance of the polymer matrix in the electrical properties of the composite, together with the CNT type and properties [4].
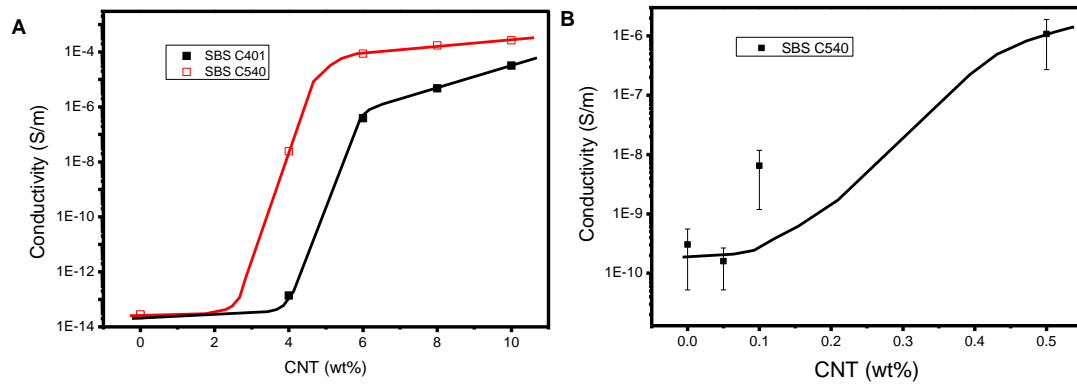
Figure 6.5 – Electrical conductivity of composites CNT/SBS. Extruded composites (A) for two SBS matrixes, C401 and C540, and electrospinning composites for C540 matrix (B) as a function of CNT content up to 10 wt% and 0.5 wt% CNT, respectively. The lines are for guiding the eyes.

Electrospinning composites show similar electrical properties that solvent casted composites, with 0.5 wt% CNT content the electrical conductivity increasing to ~$1 \times 10^{-6}$ (S/m). For extruded composites it is necessary to reach ~6 wt% CNT in order to obtain this increase. For electrospun composites it is nevertheless necessary to reach larger CNT contents in order to reach lower electrical resistance allowing electromechanical sensor applications.

### 6.1.5 Electromechanical Properties

The electromechanical properties of extruded composites were quantified through the determination of the GF (figure 6.6). Each data point of the GF presented in the following figures represents the average of 10 loading-unloading cycles (figure 6.6). All loading-unloading mechanical and corresponding electrical cycles shows good linearity.
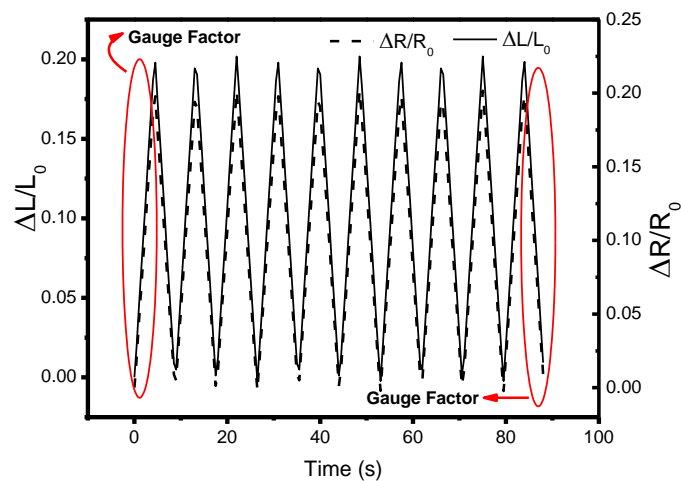


Figure 6.6- Ten loading-unloading stress-strain cycles with the corresponding electrical resistance variation used for the calculation of the GF.

Thermoplastic elastomers can support millions of cycles until failure [29] and are ideal for large deformation sensor. CNT/SBS composites from both matrixes with 8 and 10 wt% are measured for maximum strains from 1 to 5% at deformation velocities of 1mm/min (figure 6.7) and for maximum strains of 5, 10 and 20% at several deformation velocities from 1 to 50 mm/min (figure 6.9).

Near to the electrical percolation threshold the electromechanical properties are larger than in composites above the percolation threshold [30] due to the larger variation of the CNT network with strain and therefore of the changes on the electrical resistance [1, 30, 31]. The main conduction mechanism dominating the electrical response has been ascribed both to tunneling or hopping between adjacent CNT [1, 30, 31]. However, the CNT/SBS composites close to the percolation threshold cannot be appropriate for large strain sensor applications due to the large increase of their electrical resistance with applied strain to values not compatible with suitable electronic interfaces. Further, it has been shown that CNT/SBS composites prepared by solvent casting show higher GF (uniaxial measure method) for C540 SBS for deformation until 5%. In 4-point-bending experiments, GF is higher for C401 SBS [22]. It is important to prove, as it is perform in this work, the viability of producing these composites with proper characteristics for large deformation sensor applications, by solvent free and industrially scalable techniques, as well as in wire geometry.

The behavior of the gauge factor for both matrixes with 8 and 10 wt% CNT for low strains up to 5% and velocity (1mm/min) are shown in figure 6.7.
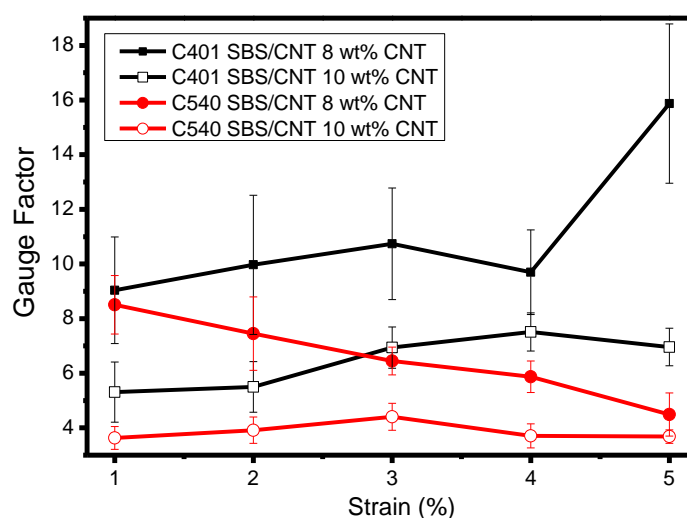


Figure 6.7- Electromechanical properties of composites for different SBS matrixes (C401 and C540) with 8 and 10 wt% of CNT. Strain varies between 1 to 5% at a velocity of 1 mm/min.

In agreement with the literature, the SBS composites near the percolation threshold (8 wt% CNT in figure 6.7) show for both matrices, larger gauge factor as function of strain. In fact, the electric sensibility of composites is larger near percolation threshold [30].

For soft composites (C401) the gauge factor slightly increases with strain unlike harder composites (C540). C401 SBS has a lower initial modulus and larger yielding strain than C540 SBS and therefore lower mechanical hysteresis, as illustrated in figure 6.8. Extruded composites show larger yield point than solvent casting composites [22]. These features allow that percolation networks of CNT present larger mobility inside the C401 matrix than in the C540 during the loading-unloading mechanical cycles. C401 SBS composites recover more efficiently during the unloading mechanical cycle and the percolation network recovers close to the near initial state whereas for the C540 the mechanical hysteresis is larger [25].
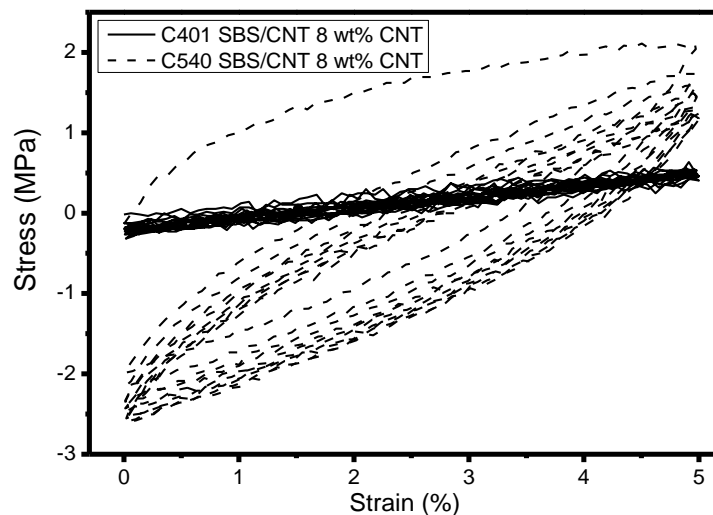


Figure 6.8- Stress-strain curves for CNT/SBS extruded composites with 8 wt% CNT for C401 and C540 matrixes at 5% of maximum strain at a velocity of 1 mm/min.

One of the goals of this work is to evaluate the electromechanical properties for larger strains in order to study the applicability of the materials for large strains applications. Figure 6.9 shows the electromechanical properties for the SBS composites at larger strains up to 20% of strain at several deformation velocities from 1 to 50 mm/min.
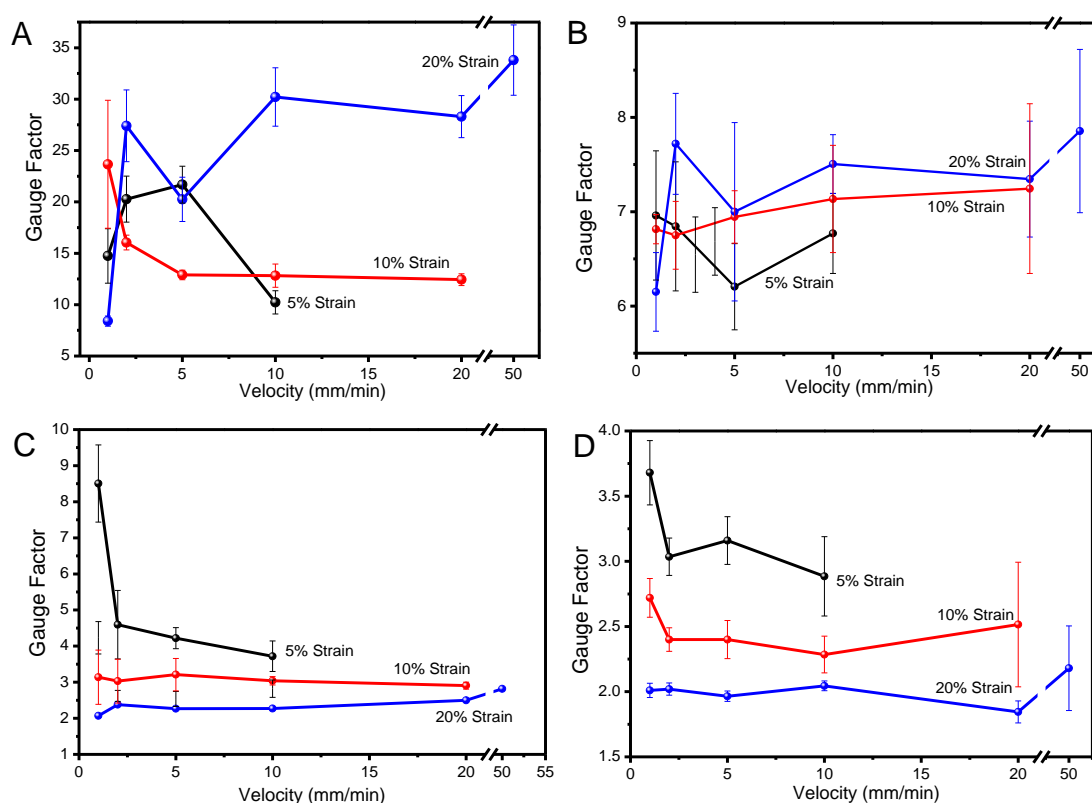
Figure 6.9- Electromechanical properties of several composites at 5, 10 and 20% of strain and test velocities range from 1 to 50 mm/min. A- C401 CNT/SBS with 8 wt% CNT. B- C401 CNT/SBS with 10 wt% CNT. C- C540 CNT/SBS with 8 wt% CNT. D- C540 CNT/SBS with 10 wt% CNT.

Composite C401 CNT/SBS with 8 wt% CNT shows higher sensibility with gauge factors from 10 to 30, close to the electromechanical properties of the composites for strains up to 5% at lower deformation velocities. Furthermore, figure 6.9 shows that the composites closer to the percolation threshold show larger gauge factors, as predicted by the percolation theory [30].

Comparing both composite matrices, the softer matrix has higher GF than the harder matrix for a given deformation. As stated previously, this behavior mainly depends on the mechanical properties of the matrix and the mobility of the CNT network within the matrix during deformation.

The composite sensibility as a function of deformation velocity for strains of 5, 10 and 20% remains practically constant from 2 to 50 mm/min. For the slower deformation of 1mm/min, the GF is generally larger due to a larger rearrangement of the CNT network along the strain direction.

An applied pre-stress in the composites can further improve the electromechanical properties. Figure 6.10 shows for the C401 CNT/SBS with 10 wt% CNT without and with 10 and 20% of pre-stress that the GF increases with increasing pre-stress.
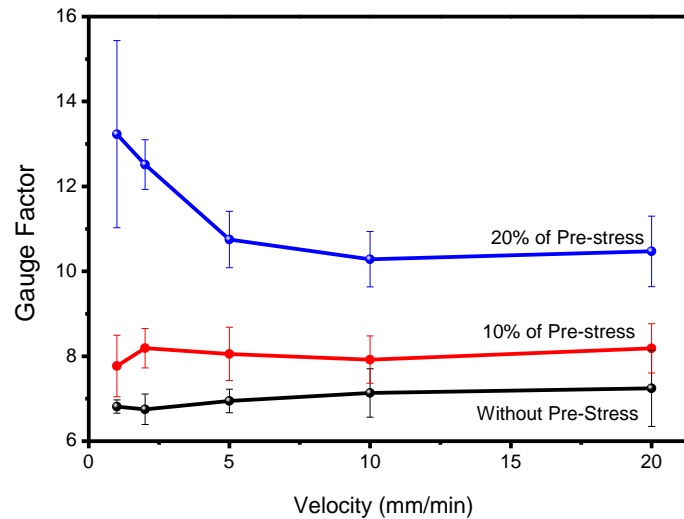
Figure 6.10- Electromechanical properties of C401 CNT/SBS with 10 wt% of CNT for 10% of strain at several velocities (1-20 mm/min) for pre-stress applied of 0, 10 and 20% of strain.

Pre-stress introduces a deformation of the composite sample and therefore of the CNT network. This initial strain increases the sensibility of the composites as further mechanical variations induce larger variations in the electrical resistance.

Pre-stress increase composites sensibility and GF usually increase with strain [2, 26]. Composites above the percolation threshold can maximize electromechanical properties using pre-stress whenever the electrical resistance remains in values compatible with the readout electronic circuits.

It has been proven that the sensitivity of the strain sensing composites strongly depends on the morphology of conductive network as well as on the interfacial stress transfer between filler and polymer matrix [30]. It the present case, differences in the stress transfer must be small for all composites due to the use of pristine CNT with no functionalization, being thus only attributed to the different styrene/butadiene ratio of the polymer matrix. In a similar way, filler network topology variations should be similar for both composites, existing just small differences in initial conductive network topology due to different levels of dispersion. On the other hand, improved stress transfer and large variations on the network topology are induced by pre-strain, being at the origin of the observed larger GF in the pre-strained samples (Figure 6.10).

## 6.2  Conclusions

Composites of SBS with CNT fillers are prepared using up-scalable, extrusion and electrospinning methods. SBS matrices with different butadiene/styrene ratios and amounts of CNT are mixed and extruded having electromechanical properties that can be used as sensor for larger strains, with a high gauge factor. Intrinsic mechanical properties of SBS almost remain unaltered by adding CNT. Large styrene contents increase the initial modulus for SBS matrix and it increases further with increasing CNT content. Electrical conductivity also increases with CNT content in the composites. Extruded composites with C540 matrix show lower electrical percolation thresholds (less than 6 wt% CNT) and larger maximum electrical conductivity when compared to the softer matrix. Percolation threshold of electrospun composites is lower than for extruded composites, but larger electrical conductivities have to be reached before the membranes can be used for electromechanical sensor applications. Composites with SBS soft matrix show larger sensibility with maximum GF ~30 for C401 CNT/SBS with 8 wt% CNT. Increasing the amount of CNT in the composites decreases the GF for both matrices. CNT/SBS prepared after conventional extrusion methods can therefore be used as sensor for larger strains up to 20% of deformation. Using pre-stress further improves the sensitivity of the composites.

## References

[1]     Rubinger C P L, Leyva M E, Soares B G, Ribeiro G M and Rubinger R M 2012 Hopping conduction on carbon black/styrene–butadiene–styrene composites *J Mater Sci* 47 860-5

[2]     Costa P, Silva J, Sencadas V, Simoes R, Viana J C and Lanceros-Méndez S 2013 Mechanical, electrical and electro-mechanical properties of thermoplastic elastomer styrene-butadiene-styrene/multiwall carbon nanotubes composites *J Mater Sci* 48 1172-9

[3]     Tang W, Liu B, Liu Z, Tang J and Yuan H 2012 Processing-dependent high impact polystyrene/styrene-butadiene-styrene tri-block copolymer/carbon black antistatic composites *Journal of Applied Polymer Science* 123 1032-9

[4]     Tsuchiya K, Sakai A, Nagaoka T, Uchida K, Furukawa T and Yajima H 2011 High electrical performance of carbon nanotubes/rubber composites with low percolation threshold prepared with a rotation–revolution mixing technique *Composites Science and Technology* 71 1098-104

[5]     Huang Z-M, Zhang Y Z, Kotaki M and Ramakrishna S 2003 A review on polymer nanofibers by electrospinning and their applications in nanocomposites *Composites Science and Technology* 63 2223-53

[6]     Norris I D, Shaker M M, Ko F K and MacDiarmid A G 2000 Electrostatic fabrication of ultrafine conducting fibers: polyaniline/polyethylene oxide blends *Synthetic Metals* 114 109-14

[7]     Senecal K J, Ziegler D P, He J, Mosurkal R, Schreuder-Gibson H and Samuelson L A 2001 Photoelectric Response from Nanofibous Membranes *MRS Online Proceedings Library* 708 null-null

[8]     Lorenz H, Fritzsche J, Das A, Stöckelhuber K W, Jurk R, Heinrich G and Klüppel M 2009 Advanced elastomer nano-composites based on CNT-hybrid filler systems *Composites Science and Technology* 69 2135-43

[9]     Breuer O and Sundararaj U 2004 Big returns from small fibers: A review of polymer/carbon nanotube composites *Polymer Composites* 25 630-45

[10]    Al-Saleh M H and Sundararaj U 2009 A review of vapor grown carbon nanofiber/polymer conductive composites *Carbon* 47 2-22

[11]    Mao Z, Wu W, Xie C, Zhang D and Jiang X 2011 Lipophilic carbon nanotubes and their phase-separation in SBS *Polymer Testing* 30 260-70

[12]    Theodosiou T C and Saravanos D A 2010 Numerical investigation of mechanisms affecting the piezoresistive properties of CNT-doped polymers using multi-scale models *Composites Science and Technology* 70 1312-20

[13]    Shih R-S, Kuo S-W and Chang F-C 2011 Thermal and mechanical properties of microcellular thermoplastic SBS/PS/SBR blend: effect of crosslinking *Polymer* 52 752-9

[14]    Munteanu S B, Brebu M and Vasile C 2005 Thermal and thermo-oxidative behaviour of butadiene-styrene copolymers with different architectures *Polymer Degradation and Stability* 89 501-12

[15]    Canto L B, Mantovani G L, deAzevedo E R, Bonagamba T J, Hage E and Pessan L A 2006 Molecular Characterization of Styrene-Butadiene-Styrene Block Copolymers (SBS) by GPC, NMR, and FTIR *Polym. Bull.* 57 513-24

[16]    De Falco A, Goyanes S, Rubiolo G H, Mondragon I and Marzocca A 2007 Carbon nanotubes as reinforcement of styrene–butadiene rubber *Applied Surface Science* 254 262-5

[17]    Das A, Stöckelhuber K W, Jurk R, Saphiannikova M, Fritzsche J, Lorenz H, Klüppel M and Heinrich G 2008 Modified and unmodified multiwalled carbon

nanotubes in high performance solution-styrene–butadiene and butadiene rubber blends *Polymer* 49 5276-83

[18] Pedroni L G, Soto-Oviedo M A, Rosolen J M, Felisberti M I and Nogueira A F 2009 Conductivity and mechanical properties of composites based on MWCNTs and styrene-butadiene-styrene block™ copolymers *Journal of Applied Polymer Science* 112 3241-8

[19] Villmow T, Kretzschmar B and Pötschke P 2010 Influence of screw configuration, residence time, and specific mechanical energy in twin-screw extrusion of polycaprolactone/multi-walled carbon nanotube composites *Composites Science and Technology* 70 2045-55

[20] Spitalsky Z, Tasis D, Papagelis K and Galiotis C 2010 Carbon nanotube–polymer composites: Chemistry, processing, mechanical and electrical properties *Progress in Polymer Science* 35 357-401

[21] Sandler J K W, Kirk J E, Kinloch I A, Shaffer M S P and Windle A H 2003 Ultra-low electrical percolation threshold in carbon-nanotube-epoxy composites *Polymer* 44 5893-9

[22] Bilotti E, Zhang H, Deng H, Zhang R, Fu Q and Peijs T 2013 Controlling the dynamic percolation of carbon nanotube based conductive polymer composites by addition of secondary nanofillers: The effect on electrical conductivity and tuneable sensing behaviour *Composites Science and Technology* 74 85-90

[23] Hapuarachchi T D, Bilotti E, Reynolds C T and Peijs T 2011 The synergistic performance of multiwalled carbon nanotubes and sepiolite nanoclays as flame retardants for unsaturated polyester *Fire and Materials* 35 157-69

[24] Peeterbroeck S, Alexandre M, Nagy J B, Pirlot C, Fonseca A, Moreau N, Philippin G, Delhalle J, Mekhalif Z, Sporken R, Beyer G and Dubois P 2004 Polymer-layered silicate–carbon nanotube nanocomposites: unique nanofiller synergistic effect *Composites Science and Technology* 64 2317-23

[25] Costa P, Ferreira A, Sencadas V, Viana J C and Lanceros-Méndez S 2013 Electro-mechanical properties of triblock copolymer styrene-butadiene-styrene / carbon nanotube composites for large deformation sensor applications *Conposites B: Engeineering,* submitted

[26] Slobodian P, Riha P and Saha P 2012 A highly-deformable composite composed of an entangled network of electrically-conductive carbon-nanotubes embedded in elastic polyurethane *Carbon* 50 3446-53

[27] Shanks R A and Spoljaric S 2012 Novel elastomer dye-functionalised POSS nanocomposites: Enhanced colourimetric, thermomechanical and thermal properties *eXPRESS Polymer Letters* 6 354-72

[28] Wu J-H, Li C-H, Wu Y-T, Leu M-T and Tsai Y 2010 Thermal resistance and dynamic damping properties of poly (styrene–butadiene–styrene)/thermoplastic polyurethane composites elastomer material *Composites Science and Technology* 70 1258-64

[29] Chen Q, Liang S and Thouas G A 2013 Elastomeric biomaterials for tissue engineering *Progress in Polymer Science* 38 584-671

[30] Hu N, Karube Y, Yan C, Masuda Z and Fukunaga H 2008 Tunneling effect in a polymer/carbon nanotube nanocomposite strain sensor *Acta Materialia* 56 2929-36

[31] Wichmann M H G, Buschhorn S T, Gehrmann J and Schulte K 2009 Piezoresistive response of epoxy composites with carbon nanoparticles under tensile load *Physical Review B* 80 245437

# Chapter 7. Implementation of styrene-butadiene-styrene/carbon nanotube composites as fingers movement sensor in a hand glove

Styrene-butadiene-styrene/carbon nanotube composites can be processed by different methods and can be used as deformation sensors. They can be incorporated into sportswear or equipment to measure, for example, movements of knees, elbows and fingers as well as deformations or impacts in sports equipment.

Electronic readout electronics and wireless communication have been implemented.

## 7.1 Hand glove application

The extruded wire composites are ideal materials to measure large deformations.

Extruded composites can measure electromechanical properties until 30% of deformation, or more (chapter 6), when CNT content is above of percolation threshold. Four wires of C540 CNT/SBS with 8 wt% CNT filler content were placed on a hand glove in order to measure finger deflection.

For integration as a part of the electromechanical sensor system for a smart glove, in order to allow measurement of the deformation and the movement of the different fingers, it is necessary to develop a readout system appropriate for this specific application.

The sensor interface should be highly configurable to allow the control system to adjust the condition circuit to the sensor to read. This is important as, although all electromechanical sensors show variation of their resistance when subjected to a deformation, the initial resistance of the various sensors is not the same and therefore the resistance variation is not identical either.

To meet these requirements the circuit structure shown in figure 7.1 was developed. This microsystem uses a total open architecture being a key feature of this circuit the use of a single readout circuit for all sensors, which enables a substantial reduction in implementation area.
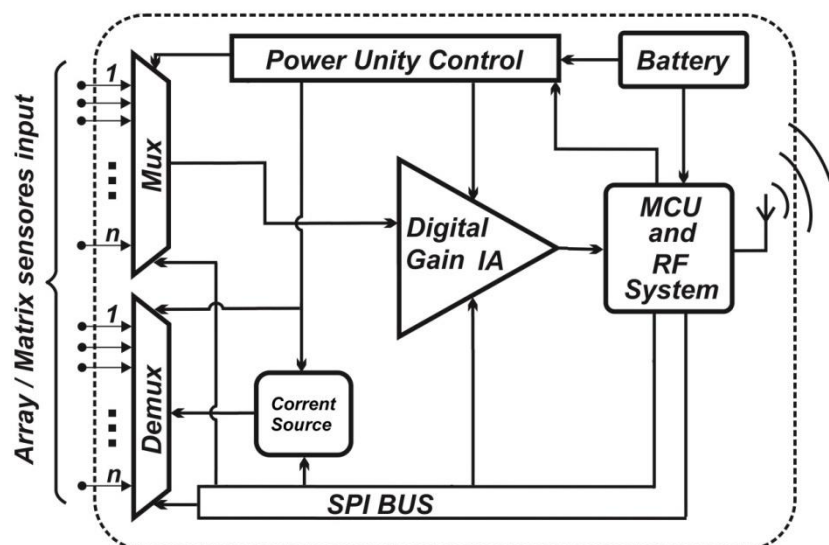


Figure 7.1- Block diagram of the piezoresistive multi-sensor interface circuit.

The various sensors are connected to a multiplexer circuit that allows addressing each sensor independently, thus ensuring that the rest are in open circuit and ensuring that they do not affect a given measurement and that there is unnecessary power consumption.

A multiplexing circuit for just eight channels has been developed, but is easily converted to a large number of channels as the readout circuit is completely independent of the number of input channels.

So one end of the sensor is connected to a controlled current source, and the other end connected to programmable gain application circuit. In this way, the source injects a constant current through the sensor, which by varying the sensor resistance causes a voltage change at the entrance of the amplifier. After signal amplification, this is measured thought an analogic digital converter incorporated internally in the microcontroller (MC).

This microcontroller is also responsible for making the activation of the measuring sensors as well as for the control of current and amplification gain for each channel. The microcontroller unit (MCU) communication with the various blocks of the readout circuit is performed using a serial peripheral interface bus which allows to control all circuit devices quickly and with a minimum of connections.

The measured data are sent via radio frequency (RF) to a remote platform responsible for data recording, allowing deformation measuring of the various sensors in real time and without requiring a physical connection.

In this way, the monitoring platform shown in figure 7.2 was implemented on a computer, which is connected to the RF receiver module with a universal serial bus connection.
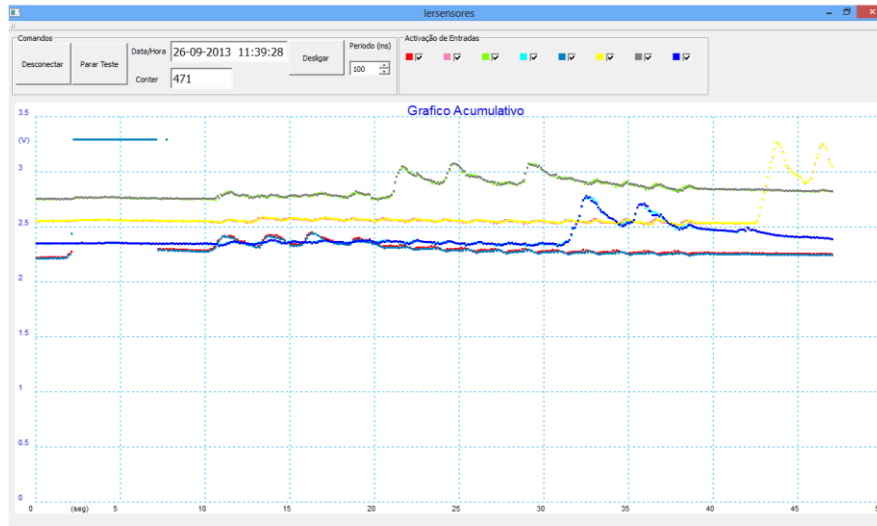
Figure 7.2- Monitoring platform for real time sensor data adquisition.

The development platform allows visualizing the response of the various sensors in real time and performs the recording of the entire measurement period to a file for a later detailed analysis.

It is important to note that the developed architecture was implemented using commercial electronic components which enable a quick transition from the architecture to the functional prototype and thus able to evaluate how the developed system meets the requirements.

The experimental procedure started by stitching the wires in the hand glove as sown in figure 7.3.



Figure 7.3- Images of the glove with the extruded composite C540 CNT/SBS with 8 wt% CNT filler content for measuring finger deformation via wireless data transmission.

After connection of the wires to the electronic platform, figure movement were monitored both by single and simultaneous finger movement experiments.

108

As electromechanical tests in chapter 6 suggest, the electrical resistance increase when the CNT/SBS composites wirer are stretched. Figure 7.4 shows that the voltage variation of the composites (at constant current) increases linearly (and therefore the resistance) when the wire is stretched.
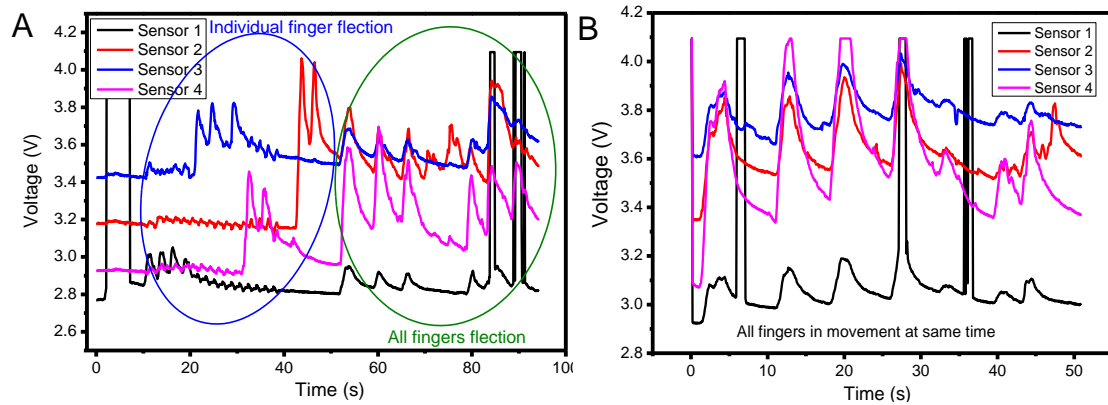


Figure 7.4- Data points of 4 sensors (extruded composites C540 CNT/SBS with 8 wt% CNT) stitched on the hand glove (figure 7.3). A) individual and all finger movement and B) all fingers in movement at the same time.

Figure 7.4 (A and B) shows that the voltage variation during the deflection of the fingers, either individual finger movements or simultaneous movements can be properly recorded.

This proof of concept shows that composite materials can be used as large deformation sensors in sportswear or equipments. With the developed electronic data acquisition is it possible to visualize in real time and to analyze the sensor measurements.

# Chapter 8.  Conclusions and future work

## 8.1 Conclusions

The main objective of this investigation was to prepare elastomeric composites suitable for the development of large strain deformation sensors. Further, it was intended to understand the main parameters affecting composite performance and characteristic, such as dispersion, mechanical, electrical, thermal and electromechanical properties.

In this way, elastomeric composites have been successfully prepared and understood with suitable and tailored properties for applications as strain sensors.

Different styrene-butadiene-styrene matrices, C401, C411, C500 and C540 with ratio butadiene/styrene of 80/20 to 60/40 and linear or radial structure show interesting electromechanical properties for specific CNT contents, depending on the processing method.

A proof of concept of the suitability of the prepared materials for applications has been achieved by using extruded composites for the development of a hand glove with the ability to measure fingers movements.

With respect to the main characteristics and specific conclusion of the developed composites:

- Thermal properties of SBS show two different Tg ascribed to polybutadiene and polystyrene domains. The polybutadiene glass transition increases with increasing butadiene in SBS matrix, from 10 to 17 ºC, with the polystyrene glass transition around 70-75 ºC. Thermal degradation of composites shows $T_{onset}$ around 450-455 ºC and $T_{max}$ between 490 and 520 ºC, increasing with amount of CNT in SBS matrices. All others thermal properties of composites CNT/SBS remain similar to SBS matrix.

- The peaks at the wave-number of 966 cm$^{-1}$ and 699 cm$^{-1}$ were selected as the most suitable ones for analysis of polybutadiene (PB) and polystyrene (PS), respectively. The butadiene/styrene ratio and structure (linear or radial) does not affect the characteristic peaks in SBS composites as well as the filler type and content did not induce any change in the SBS matrices. No new bonds attributable to CNT-matrix interactions are identified.

- Different processing methods exhibit some advantages and limitations. Mechanical properties of composites, in general, increase with increasing CNT content in the SBS matrix for all methods. Maximum deformation is larger for extruded composites (between 800 to 3500%) and electrospun composites present the

smallest maximum deformations (less than 600%). Initial modulus increases with increasing CNT and styrene content in SBS matrices, for the different processing methods. The Yield stress decreases with increasing styrene content in the SBS matrix and is the largest in extruded composites, being for the softer matrix (C401) between 20% and 50%. These values are around 10 times higher than for other processed composites, solvent casted and electrospun. Mechanical hysteresis is an important issue for large deformation electromechanical sensors. CNT/SBS composites properly recovery from large deformations and mechanical hysteresis increases with deformation and decreases with the number of stress-strain cycles. Butadiene/styrene ratio influences the mechanical behavior and softer matrices (C401) show lower hysteresis than harder matrices (C540).

- Electrical properties of CNT/SBS depend on the processing method: whereas the electrical percolation threshold is less than 1 wt% for solvent casting and electrospinning methods, increases for 4-5 wt% in extruded composites. Functionalized CNT does not show a strong increase of the electrical conductivity of the matrix until 8 wt% CNT loading. These can be explained with CNT dispersion inside SBS matrix, as functionalized CNTs show CNT dispersion and pristine CNTs show clusters of CNT dispersion. Individual CNT dispersion does not favor electrical conductivity in carbon nanoallotropes/polymer composites. Different CNT present similar electrical properties in composites, but NC7000 CNTs shows lower percolation thresholds and higher conductivity.

- Percolation theory predicts that hopping between nearest fillers is the main mechanism for the composite electrical conduction; the overall composite conductivity is explained by the existence of a weak disorder regime.

- The CNT/SBS composites show electromechanical properties in the four different matrices with appropriate CNT contents, which must be larger than the percolation threshold for the different composites and for large deformation applications. For solvent casting method the C540 SBS present higher GF up to 20% of deformation. This composite can reach a GF~120 using pre-stress in uniaxial stress-strain measurements. For uniaxial electromechanical measurements the speed of the mechanical stimulus influences the GF and is larger for deformations speeds between 10-20 mm/min, decreasing for larger speeds. The good linearity between mechanical and electrical resistance variation is also observed in 4-point-bending measurements with GF~100 for C401 CNT/SBS composites at 5 mm/min and 1 mm

of deformation. Others matrices, C411, C500 and C540, show GF<30. For uniaxial stress-strain solicitations, C150P CNT show higher GF for larger deformations, but multi walled CNT NC7000 and single walled CNT AP-SWNT shows GF between 3 and 5, which are also suitable for applications.

- Composites near the percolation threshold show higher GF than composites above the percolation threshold, but the maximum deformation is smaller for these composites, increasing with increasing filler content in the composites.

- Extruded composites under uniaxial stress-strain measurements show maximum GF for the softer matrix with 8 wt% CNT, reaching a GF~30 for 20% deformation.

- Electrospun samples results in composites with similar electrical properties as solvent casted samples and maximum deformations larger than 250%.

- The applicability of the materials has been shown by the development of an instrumented glove for measuring finger deformations.

## 8.2 Future work

The CNT/SBS composites can be used as electromechanical sensors. Several parameters can be optimized for preparing the materials for specific applications, including CNT content, initial pre-stress, butadiene/styrene ratio, among others.

The variability of processing methods also allows a large application range and industrial fabrication.

In this way, the main challenge for the future is to optimize materials already for specific applications, introducing the materials into specific devices and optimizing the upscaled production.

In this way, electrospun and extruded composites can be incorporated at different scales and, for example, cloths can be produced with these sensors already incorporated with the objectives of monitoring movement. Intelligent hand gloves are another example of the use of these electromechanical composites. Apart from the clothes, these composites can be incorporated into sport equipments.

The SBS matrices can be studied as pressure sensors. Silicone or natural rubbers are softer than SBS but present lower recovery to initial state after the applied pressure is released.

The exceptional mechanical properties of SBS make these thermoplastic elastomer excellent matrices to renewable energy sources and their properties should be explored in this field. Dielectric elastomer generators (DEG) are being developed based on the change of the capacitance of a deformable dielectric and energy is harvested through a cycle. Energy of conversion is higher for larger strains.